Dissertation zur Erlangung des Doktorgrades
der Fakultät für Chemie und Pharmazie
der Ludwig-Maximilians-Universität München

Identification of the transmembrane protein 147 (TMEM147) as a novel component of the Nicalin-NOMO membrane protein complex

Ulf Dettmer
aus
Nürnberg
2010

Erklärung

Diese Dissertation wurde im Sinne von §13 Abs. 3 der Promotionsordnung vom 29. Januar 1998 von Frau PD Dr. Konstanze Winklhofer betreut und vor der Fakultät für Chemie und Pharmazie vertreten.

Ehrenwörtliche Versicherung

Diese Dissertation wurde selbständig, ohne unerlaubte Hilfe erarbeitet.
München, am 10. Juni 2010

……...
(Ulf Dettmer)

Dissertation eingereicht am:	10. Juni 2010
1. Gutachter:	PD Dr. Konstanze Winklhofer
2. Gutachter:	Prof. Dr. Christian Haass
Mündliche Prüfung am:	26. Juli 2010

Meinen Eltern, meiner Schwester Silke und meiner Freundin Alexandra gewidmet.

One step inside doesn’t mean you understand. (title of a song by *The Notwist*)

Table of contents

Summary 6
Zusammenfassung 7
1 Introduction 8
1.1 γ-Secretase 8
1.1.1 Components of γ-secretase 10
1.1.2 Assembly and transport of γ-secretase 12
1.2 The Nicalin-NOMO complex 13
1.2.1 Components of the Nicalin-NOMO complex 16
1.2.2 Assembly of the Nicalin-NOMO complex 18
1.3 Goals of this thesis 19

2. Results 20
2.1 Transmembrane protein 147 co-purifies with the Nicalin-NOMO complex 20
2.2 TMEM147 co-localizes with Nicalin and NOMO in the ER 24
2.3 The TMEM147 topology is similar to APH-1 28
2.4 TMEM147, Nicalin, and NOMO stabilize each other 30
2.5 Nicalin controls complex levels by stabilizing excess molecules 35
2.6 TMEM147 and NOMO differ in their Nicalin binding requirements 37
2.7 The interaction of TMEM147 with Nicalin/NOMO is evolutionary conserved 40
2.8 TMEM147, like Nicalin and NOMO, is ubiquitously expressed 43
2.9 Towards the Nicalin interactome using SILAC 46

3. Discussion 51
3.1 A novel core component of the Nicalin-NOMO complex 51
3.2 Nicalin-NOMO complex and γ-secretase assembly occur stepwise 53
3.3 Nicalin is the master regulator of the Nicalin-NOMO complex 55
3.4 Analysis of the Nicalin interactome 58
3.5 The Nicalin-NOMO complex beyond Nodal signaling 61
3.6 Outlook 63

4. Materials and methods 64
4.1 Equipment 64
4.2 Chemicals 66
4.3 DNA techniques 67
4.3.1 Plasmids 67
4.3.2 Oligonucleotides 68
4.3.3 RNA isolation and cDNA synthesis 68
4.3.4 PCR 69
4.3.6 Agarose gel electrophoresis 69
4.3.9 Restriction enzyme treatment 70
4.3.10 DNA ligation 70
4.3.11 Transformation of competent bacteria 70
4.3.12 DNA isolation from bacteria 71
4.4 Cell culture 72
4.4.1 Cell lines 72
4.4.2 Cell cultivation 73
4.4.4 Cell transfection 73
4.4.5 Cell transduction, lentiviral 74
4.4.6 Cell cryoconservation 75

4.5 Protein analysis ... 76
4.5.1 Antibodies ... 76
4.5.2 Total protein lysates ... 77
4.5.3 Membrane protein lysates ... 77
4.5.4 Deglycosylation ... 78
4.5.5 Immunoprecipitation (IP) ... 78
4.5.6 Density gradient centrifugation ... 79
4.5.7 SDS-PAGE ... 80
4.5.8 Transfer of proteins to PVDF membranes ... 81
4.5.9 Immunological detection of proteins ... 81
4.6 Immunocytochemistry ... 81
4.7 Mass spectrometry ... 82
4.8 Zebrafish techniques ... 82
4.9 Bioinformatical methods ... 84

5. List of references ... 85
6. List of abbreviations ... 94
7. List of companies ... 97
8. Curriculum vitae ... 98
9. Publications and meetings ... 99
10. Acknowledgments ... 100

Summary

Nicastrin is one out of four components of γ-secretase, a membrane protein complex with a key role in the pathogenesis of Alzheimer's Disease. Its closest relative is Nicalin (Nicastrin-like protein) which, together with NOMO (Nodal modulator), is part of a novel, evolutionary conserved membrane protein complex which is involved in the regulation of the Nodal signaling pathway in developing zebrafish embryos. Since its native size (200-220 kDa) could not be satisfyingly explained by the molecular weights of monomeric Nicalin (60 kDa) and NOMO (130 kDa), the possible existence of additional components, especially in the low-molecular-weight range, was examined. Using an optimized procedure of the Nicalin affinity purification approach which had led to the isolation of NOMO, a ~22-kDa protein could be specifically enriched from membrane protein lysates of cultured human cells and identified by mass spectrometry as transmembrane protein 147 (TMEM147). TMEM147 is a novel, highly conserved polytopic membrane protein with a putative topology similar to the γ-secretase component APH-1. Its specific interaction with Nicalin was confirmed by immunoprecipitation/immunoblotting experiments and shown to be roughly stoichiometric. Immunofluorescence microscopy and density gradient centrifugation studies demonstrated a colocalization with Nicalin in the endoplasmic reticulum. mRNA *in situ* hybridization studies in zebrafish embryos revealed a ubiquitous expression during all developmental stages, in agreement with the distribution of Nicalin and NOMO. Gain-of-function and loss-of-function experiments in cultured cells demonstrated a mutual dependence in the expression levels between the three proteins further corroborating the idea that they are components of the same complex. A variety of data indicated that, like γ-secretase, the assembly of this complex is hierarchical beginning with the formation of a Nicalin-NOMO intermediate. Nicalin appears to represent the limiting factor and to regulate the assembly rate by stabilizing NOMO and TMEM147. In summary, the presented data identify TMEM147 as a novel core component of the Nicalin-NOMO complex with a structural relationship to APH-1. When the Nicalin purification procedure was combined with stable isotope labeling using amino acids in cell culture (SILAC) and a comprehensive mass spectrometry analysis, a variety of additional Nicalin interactors were identified. A few of them were confirmed by co-immunoprecipitation assays and likely represent transient binding partners which might mediate the cellular function of the Nicalin-NOMO complex. Future studies are required to analyze the relevance of these interactions in detail.

Zusammenfassung

Nicastrin ist eine von vier Komponenten der γ-Sekretase, eines Membranprotein-Komplexes mit einer Schlüsselrolle bei der Entstehung der Alzheimerschen Demenz. Sein nächster Verwandter ist Nicalin (Nicastrin-like protein), gemeinsam mit NOMO (Nodal modulator) Bestandteil eines neuartigen, evolutionär konservierten Membranproteinkomplexes, der offenbar eine Rolle im Nodal-Signalweg während der Zebrafisch-Embryonalentwicklung spielt. Da die native Größe des Komplexes (200-220 kDa) nicht hinreichend mit den Molekulargewichten der Monomere von Nicalin (60 kDa) und NOMO (130 kDa) erklärt werden konnte, wurde der Komplex auf mögliche zusätzliche Komponenten, insbesondere im niedermolekularen Bereich, hin untersucht. Durch Optimierung der Nicalin-Affinitätsreinigung, die bereits zur Isolation von NOMO geführt hatte, konnte ein ~22-kDa-Protein spezifisch in Membranproteinlysaten kultivierter humaner Zellen angereichert und mittels Massenspektrometrie als Transmembranprotein 147 (TMEM147) identifiziert werden. TMEM147 ist ein neuartiges, hochkonserviertes polytopisches Membranprotein mit einer mutmaßlichen Topologie, die der γ-Secretase-Komponente APH-1 ähnelt. Die spezifische Interaktion mit Nicalin, die in etwa in stöchiometrischen Verhältnissen erfolgt, konnte mittels Immunpräzipitations/Immunblot-Studien bestätigt werden. Immunfluoreszenz-Mikroskopie- und Dichtegradienten-Zentrifugations-Experimente legen eine Kolokalisation mit Nicalin im endoplasmatischen Retikulum nahe. mRNA-*in-situ*-Hybridisierung in Zebrafischembryonen zeigte eine ubiquitäre Expression in allen Entwicklungsstadien, im Einklang mit der Verteilung von Nicalin und NOMO. Überexpressions- und Depletionsversuche in kultivierten humanen Zellen demonstrierten eine wechselseitige Abhängigkeit der Expressionsspiegel der drei Proteine, was ihre Zugehörigkeit zu ein und demselben Proteinkomplex unterstreicht. Eine ganze Reihe von Daten legte nahe, dass - ähnlich der γ-Sekretase – der Zusammenbau dieses Komplexes ein hierarchischer Vorgang ist, der mit der Ausbildung eines Nicalin/NOMO-Intermediats beginnt. Nicalin ist offenbar der limitierende Faktor, der - indem er NOMO und TMEM147 stabilisiert - den Aufbau des Komplexes reguliert. In ihrer Gesamtheit weisen die präsentierten Daten TMEM147 als eine neue Kernkomponente des Nicalin-NOMO-Komplexes mit einer strukturellen Verwandtschaft zu APH-1 aus. Durch eine Kombination der Nicalin-Aufreinigung mit SILAC (stable isotope labeling using amino acids in cell culture) und einer umfassenden massenspektrometrischen Analyse konnte eine Reihe weiterer Interaktoren identifiziert werden. Einige von ihnen wurden durch Kopräzipitationsstudien bestätigt und stellen wahrscheinlich transiente Bindungspartner dar, die möglicherweise die zelluläre Funktion des Nicalin-NOMO-Komplexes vermitteln. Zukünftige Studien sind erforderlich, um die Relevanz dieser Interaktionen im Detail zu analysieren.

1 Introduction

1.1 γ-Secretase

Alzheimer's disease (AD) is the most common form of dementia (reviewed by Selkoe, 2001). One of its pathological hallmarks is the accumulation of amyloid plaques, large proteinaceous deposits, in certain areas of the brain (Fig. 1). They primarily consist of aggregated forms of the amyloid β-peptide (short: Aβ), a proteolytic cleavage product of the β-amyloid precursor protein (APP). Aβ exists in several forms: a major 40 amino acid form (Aβ40), and less dominant forms like Aβ42, Aβ38, and Aβ43 (Wiltfang et al., 2002). In particular the accumulation of the highly aggregation-prone Aβ42 has been shown to be central for the generation of the amyloid plaques (reviewed by Hardy and Selkoe, 2002). The plaques have been associated with pathological events like local synaptic abnormalities and breakage of neuronal processes (e.g., Tsai et al., 2004), but many studies suggest a plaque-independent pathological role of Aβ oligomers, soluble aggregates of much lower molecular weight, which for example could be shown to interfere with memory in animal models (Walsh et al., 2002; Cleary et al., 2005; Shankar et al., 2007). In patients with familial AD (FAD), an inherited form of the disease with an early age of onset, Aβ42 accumulation is accelerated due to mutations resulting in an increased Aβ42/Aβ40 ratio or overall Aβ production (reviewed by Hardy, 1997). FAD mutations have been found in *APP* and in two additional genes: *Presenilin 1 and 2*, which code for proteases involved in APP processing (see below).

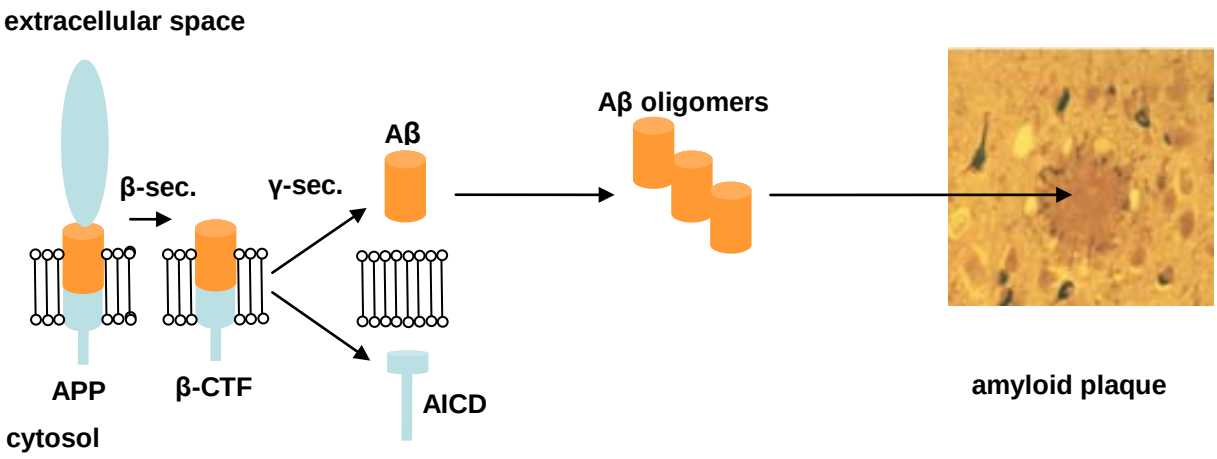

Fig. 1: Aβ generation from APP via proteolytic processing (for further details, see text). The APP ectodomain is first shedded by β-secretase (β-sec.) releasing APPsβ (not shown). The remaining membrane-bound β-C-terminal fragment (β-CTF) is then further processed by γ-secretase (γ-sec.) within the membrane, releasing Aβ to the extracellular space and the APP intracellular domain (AICD) to the cytosol. Aβ aggregates at first to oligomers, which are finally deposited in amyloid plaques. Adapted from Haass, 2004.

The APP protein, whose physiological function is only incompletely understood, is present at the surface of most cell types. It is a type-I transmembrane protein with a large amino-

terminal extracellular domain and a short carboxy-terminal cytosolic domain (Fig. 1). Its processing to generate Aβ includes two major steps, a β-cleavage and a subsequent γ-cleavage (reviewed by Steiner and Haass, 2000; Haass, 2004). The β-cleavage is performed by the β-secretase BACE (β-site APP-cleaving enzyme) causing the release of most of the extracellular domain in the form of APPsβ (APP soluble β) from the cell (reviewed by Vassar, 2004). After this so-called ectodomain shedding, the remaining membrane-bound β-C-terminal fragment (β-CTF) undergoes an unusual intramembrane cleavage, carried out by γ-secretase (reviewed by Hardy and Selkoe, 2002; Sisodia and St George-Hyslop, 2002), resulting in the generation of Aβ, which is secreted into the extracellular space, and APP intracellular domain, AICD (reviewed by Haass and Steiner, 2002).

Beyond the cleavage of APP CTFs, γ-secretase catalyzes the intramembrane proteolysis of other type-I plasma membrane proteins, which have undergone shedding, most importantly the signaling receptor Notch (reviewed by Selkoe and Kopan, 2003). In a zebrafish study (Geling et al., 2002), for example, γ-secretase inhibition by drug treatment (DAPT) was shown to phenocopy Notch pathway mutants (van Eeden et al., 1996; Jiang et al., 2000), characterized by the malformation of somites, primitive segments in the developing vertebrate embryo distributed along the two sides of the developing spinal cord (Fig. 2). The Notch signaling pathway is initiated by the binding of an extracellular ligand, Delta-like or Jagged, to the Notch receptor resulting in the shedding of the Notch extracellular domain (reviewed by Fortini, 2002). The remaining Notch fragment is then cleaved by γ-secretase generating Notch-β, the pendant of Aβ, and the Notch intracellular domain (NICD), which translocates to the nucleus and activates the transcription of Notch target genes in concert with other transcriptional regulators (reviewed by Mumm and Kopan, 2000). This pathway is highly conserved during evolution and indispensible for a variety of cell-cell communication events in multicellular organisms, especially for fundamental cell differentiation processes during embryonic development, but also in adult organisms (reviewed by Mumm and Kopan, 2000). Notch signaling is dysregulated in many cancers (www.healthvalue.net/notch.html).

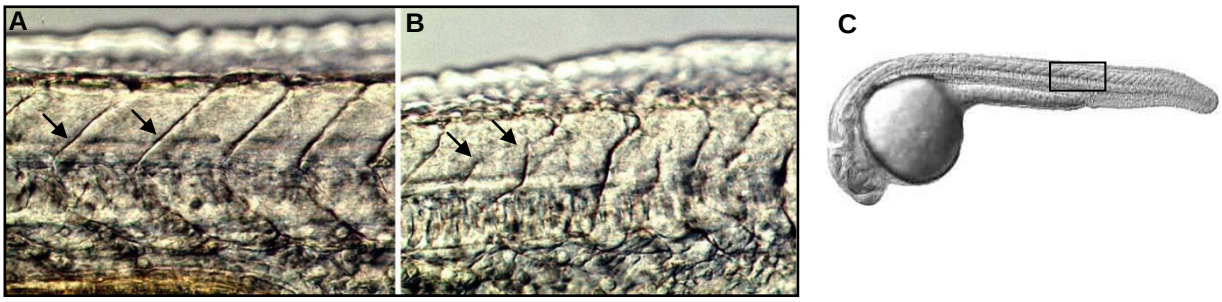

Fig. 2: Zebrafish embryos treated with the γ-secretase inhibitor DAPT show a Notch phenotype (adapted from Geling et al., 2002). Mock-treated (A) and DAPT-treated (B) embryos visualized at 24 hours post fertilization (live views, close-up views of the tail). DAPT treatment alters somitic borders [arrows in (A) and (B)]. An overview picture of a ~24 hours old embryo was added (C, source: www.zf-models.org), indicating the approximate origin of the detail pictures.

1.1.1 Components of γ-secretase

γ-Secretase is not a single protein, but rather a protein complex. It is assembled in the endoplasmic reticulum (ER) and subsequently transported to the plasma membrane (see section 1.1.2). Genetic and biochemical studies have identified four membrane proteins as γ-secretase components (Fig. 3): Nicastrin, APH-1 (Anterior Pharynx-Defective 1), PEN-2 (Presenilin-Enhancer 2) and Presenilin 1/2 (for references, see below). A 1:1:1:1 composition of the components in the high-molecular-weight protein complex, leading to a molecular weight of 200 to 250 kDa, is likely (Sato et al., 2007), but requires further investigation.

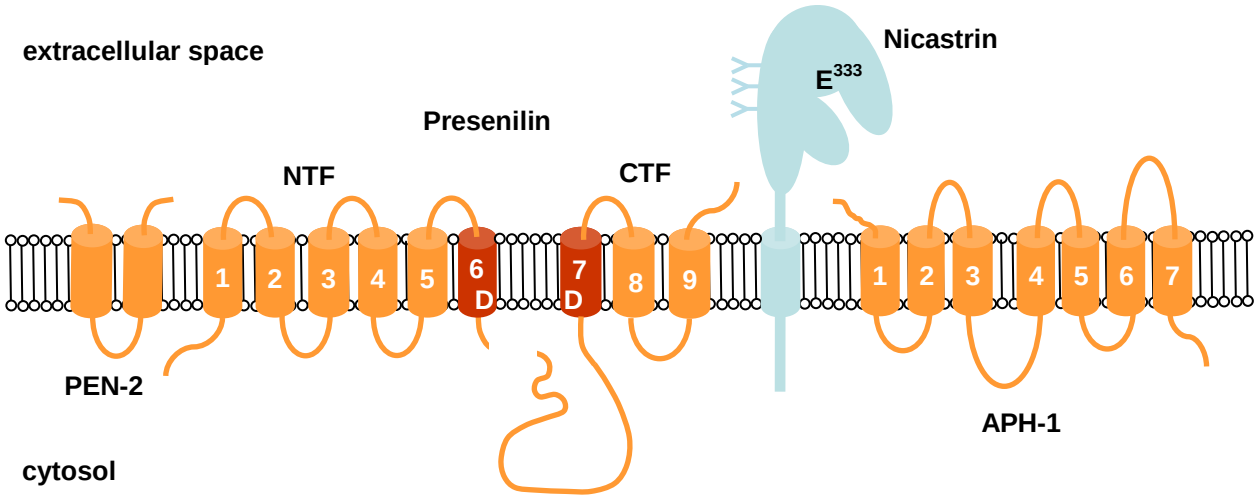

Fig. 3: The components of γ-secretase. The complex consists of the small hairpin-like PEN-2, the catalytically active Presenilin, the type-I transmembrane protein Nicastrin and the polytopic APH-1. In mature γ-secretase, PS has been autocatalytically cleaved into N-terminal fragment (NTF) and C-terminal fragment (CTF), and Nicastrin is complex glycosylated (indicated by the 'Y's). The PS transmembrane domains 6 and 7 contain two highly conserved aspartate (D) residues, critical for the catalytic activity of the complex, which represents an aspartic protease. Nicastrin may represent the substrate receptor, with a critical aspartate at amino acid position 333 in humans (E333) being involved in substrate binding.

Presenilin (PS) is the catalytic subunit of γ-secretase (see below). In mammals, the two homologs PS1 and PS2 with 63 % sequence homology exist (Yu et al., 1998). PS1 knockout mice show a strongly reduced γ-secretase activity (De Strooper et al., 1998; Naruse et al., 1998). Membrane topology studies identified PS as a polytopic 9 transmembrane domain (TMD) protein with its N-terminus and a large loop facing the cytosolic side and its C-terminus facing the extracellular/luminal side (Kaether et al., 2004; Laudon et al., 2005; Oh and Turner, 2005; Sobhanifar et al., 2010). The TMDs 6 and 7 contain two highly conserved aspartate residues leading to the idea PS might represent an aspartic protease, and indeed, the mutagenesis of the conserved aspartate residues was demonstrated to abrogate enzyme activity (Steiner et al., 1999; Wolfe et al., 1999; Kimberly et al., 2000). Moreover, aspartic protease inhibitors could be shown to inhibit γ-secretase activity (Wolfe et al., 1999; Shearman et al., 2000). Being an unusual aspartic protease, PS does not contain the classical aspartic protease motif, D(T/S)G(T/S), but rather novel active site motifs, the GxGD motif around the critical aspartate in TMD7 and a YD motif in TMD6 (Steiner et al., 2000;

reviewed by Steiner and Haass, 2000). In the mature γ-secretase complex PS exists in an N- and C-terminal fragment (Thinakaran et al., 1996), which are generated by endoproteolysis (Fukumori et al., 2010) and remain stably associated as heterodimers (Capell et al., 1998; Yu et al., 1998; Saura et al., 1999).

Nicastrin (NCT), a ~110 kDa type-I membrane protein, was identified as a PS1/2 interactor by co-immunoprecipitation studies (Yu et al., 2000). It is the largest γ-secretase component and the only one with a pronounced extracellular domain. During γ-secretase transport through the secretory pathway, NCT undergoes complex asparagine (N)-linked glycosylation leading to complex glycosylated NCT, which characterizes mature γ-secretase (Yu et al., 2000; Kaether et al., 2002; Herreman et al., 2003). NCT contains a functionally important DAP (DYIGS and peptidase) domain, an extracellular region of about 200 amino acids with a predicted structure similar to domains in aminopeptidases (Fagan et al., 2001; see Fig. 6). Mutations in the DYIGS motif reduce both PS/NCT interaction and Aβ production (Yu et al., 2000; Chen et al., 2001; Shirotani et al., 2004). Also located within the DAP domain, the carboxyl group of the glutamate at position 333 (E333; see Fig. 3) has been proposed to mediate the interaction with the free N-termini of shedded substrates (Shah et al., 2005; Dries et al., 2009). However, it has also been suggested that complex maturation rather than substrate recognition is affected when the critical glutamate is mutated (Chavez-Gutierrez et al., 2008).

PEN-2 (Presenilin enhancer 2), a 12 kDa hairpin-like membrane protein, was identified in a genetic screen for PS enhancers in a *C. elegans* strain partially deficient in the function of Sel-12, the *C. elegans* homolog of PS1 (Francis et al., 2002). Co-immunoprecipitation and RNAi studies confirmed it as a γ-secretase complex component (Steiner et al., 2002). PEN-2 was shown to bind to the TMD4 of PS1 (Kim and Sisodia, 2005; Watanabe et al., 2005) and to be required for γ-secretase complex maturation. It triggers the endoproteolysis of PS1/2 (Takasugi et al., 2003) and subsequently stabilizes the PS NTF and CTF in the complex (Hasegawa et al., 2004; Prokop et al., 2004). An involvement of PEN-2 in export of γ-secretase is discussed in section 1.1.2.

APH-1 (Anterior Pharynx-Defective 1) is a 20 kDa 7-TMD protein (Fortna et al., 2004) identified in two independent *C. elegans* screens (Francis et al., 2002; Goutte et al., 2002). It was shown to interact with NCT and PS (Lee et al., 2002). In humans, the two paralogs APH-1a and APH-1b exist, with APH-1a occuring in the two splice variants APH-1aS and APH-1aL (Francis et al., 2002; Goutte et al., 2002). APH-1 has been shown to be important for γ-secretase complex formation acting as an assembly scaffold (Gu et al., 2003; Hu and Fortini, 2003; LaVoie et al., 2003; Capell et al., 2005; see also section 1.1.2).

1.1.2 Assembly and transport of γ-secretase

Increased γ-secretase levels, accompanied by an elevated γ-secretase activity, can only be achieved by the ectopic co-expression of all four components (Edbauer et al., 2003; Hu and Fortini, 2003; Kimberly et al., 2003). This suggested that the γ-secretase assembly is tightly controled and that the expression levels of its components are balanced under wild-type conditions. Forced expression of PS alone, for example, results in a replacement of endogenous PS, i.e. the reduction of endogenous PS fragments and increased amounts of unincorporated full-length PS, which is less stable than its fragments (Thinakaran et al., 1997). It was proposed that the γ-secretase components are stabilized by complex formation and that unincorporated molecules are rapidly degraded (Thinakaran et al., 1997). This hypothesis was confirmed by a variety of loss-of-function studies, which demonstrated that downregulation of one component destabilizes at least one other component. For example, in NCT knockout embryonic fibroblasts levels of APH-1, PEN-2 and PS fragments are drastically decreased (Zhang et al., 2005), while RNAi-mediated PEN-2 downregulation in human embryonic kidney cells is associated with reduced PS levels, impaired NCT maturation and deficient γ-secretase formation (Steiner et al., 2002). In PS1 knockout embryonic fibroblasts, unincorporated immature NCT accumulates, which is less stable than the incoporated mature protein (Edbauer et al., 2002; He et al., 2007). Unincorporated PEN-2, APH-1, NCT, and full-length PS were observed to be degraded mainly by the proteasome, but also lysosomal pathways may contribute (Zhang et al., 2005; He et al., 2007).

Models for γ-secretase assembly and transport (reviewed by Kaether et al., 2006; Spasic and Annaert, 2008) agree on the initial formation of a subcomplex consisting of APH-1 and immature NCT (Hu and Fortini, 2003; LaVoie et al., 2003). In the next step, full-length PS is stabilized within the ER by binding to NCT/APH-1 in a trimeric, inactive complex (LaVoie et al., 2003; Kim et al., 2004; Capell et al., 2005). Finally, PEN-2 binds, facilitating PS endoproteolysis and γ-secretase activation (LaVoie et al., 2003; Niimura et al., 2005). The assembled complex is released from the ER, travels through the Golgi compartments, where NCT maturation occurs (Yu et al., 2000; Kaether et al., 2002; Herreman et al., 2003), and is further transported to its functional sites, plasma membrane and late secretory pathway compartments (Kaether et al., 2002; Capell et al., 2005; Chyung et al., 2005). However, little is known about the exact control of these events. None of the four components could be identified as the universal rate-limiting factor (Kimberly et al., 2002). ER-retention/retrieval signals were identified in PS and PEN-2 and their masking upon complex formation has been proposed to allow the ER exit of fully assembled γ-secretase (Kaether et al., 2004; Fassler et al., 2010). Fig. 39 in section 3.2 illustrates the assembly of γ-secretase.

1.2 The Nicalin-NOMO complex

Like γ-secretase, the Nicalin-NOMO complex is a high-molecular-weight membrane protein complex. It was identified only recently and consists of the two membrane proteins Nicalin (Nicastrin-like protein) and NOMO (Nodal modulator) (see section 1.2.1), with the former being the closest relative of the γ-secretase component Nicastrin (Haffner et al., 2004). Studies in zebrafish embryos suggest that the complex is involved in the regulation of the Nodal signaling pathway (reviewed by Haffner and Haass, 2004). Nodals are cytokines, i.e. secreted ligands for specific receptors involved in cellular growth and differentiation (reviewed by Massague, 1998). They are members of the transforming growth factor β (TGFβ) superfamily which, in addition to TGFβ itself, includes Activin/Inhibin, Bone Morphogenic Proteins (BMPs) and Lefty proteins. Nodals are especially important for patterning events during early vertebrate embryogenesis, e.g. mesoderm (and endoderm) formation, ventral midline formation, anterior-posterior patterning and anterior-posterior axis positioning (reviewed by Schier and Shen, 2000). Thus, in developing embryos their overall function consists in controling germ layer development and formation of the major body axes (reviewed by Schier, 2003). However, they have also been reported to play a role in tumorigenesis in adult organisms (reviewed by Strizzi et al., 2009), in particular a contribution to melanoma aggressiveness has been postulated (Topczewska et al., 2006).

Simultaneous ectopic expression of Nicalin and NOMO in zebrafish embryos resulted in partial cyclopia (Fig. 4; Haffner et al., 2004), a phenotype indicative of reduced Nodal signaling resulting from defective forebrain formation due to a failure in pattern formation in the axial mesoderm (Blader and Strahle, 1998). Injection of *nomo* antisense oligonucleotides in fertilized oocytes led to an increase in anterior axial mesoderm (involved in forebrain induction) - again a Nodal-specific phenotype, this time due to enhanced Nodal signaling. In addition, this effect could be prevented by overexpression of Lefty1, an established Nodal inhibitor (Fig 5). These results suggested that the Nicalin-NOMO complex acts as Nodal antagonist.

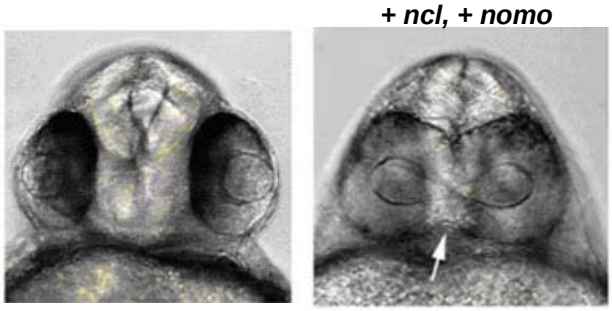

Fig. 4: Nicalin and NOMO inhibit Nodal signaling during zebrafish development. Morphology of wild-type (left) and zebrafish embryos after injection of *nicalin* and *nomo* capped mRNA (right), 36 hours post fertilization (adapted from Haffner et al., 2004). The resulting partial cyclopia is relatively specific for reduced Nodal signaling and results from defective forebrain formation due to a failure in mesoderm pattern formation.

By binding to receptors on target cells, Nodal factors initiate signaling cascades that result in the transcription of specific genes affecting cell proliferation and cell migration. Nodal ligands use a mechanism similar to that of other TGFβ superfamily members to initiate signal transduction (Fig. 5). The events taking place upon Nodal activation can be divided into four steps (reviewed by Shi and Massague, 2003):

1. A Nodal dimer binds to a heterodimer of membrane-bound type-I (ALK4 in Fig. 5) and type-II (ActRIIB in Fig. 5) serine/threonine kinase receptors. In contrast to other TGFβ superfamily members, Nodal needs a co-receptor of the Epidermal Growth Factor-Cripto-FRL1-Cryptic (EGF-CFC) protein family (Oep/Cripto in Fig. 5) for efficient binding.
2. A ligand-receptor complex forms, in which the type-II receptor kinase activates the type-I receptor by phosphorylation of its cytosolic kinase domain.
3. Activated type-I receptors phosphorylate soluble downstream effectors called Smads. The direct targets are Smad2 or Smad3 (R-Smads), which upon phosphorylation form heterocomplexes with Smad4 (Co-Smad).
4. The activated R-Smad/Co-Smad heterocomplexes translocate into the nucleus. Here they interact with other transcription factors leading to the expression of specific genes.

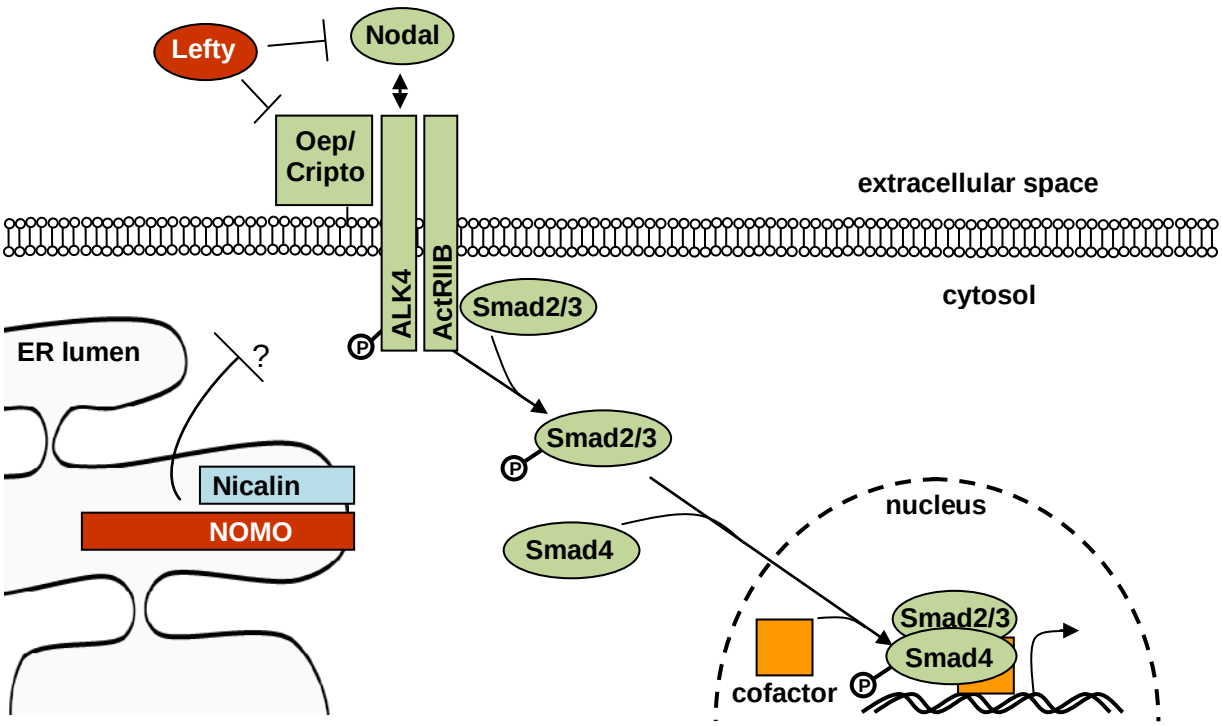

Fig. 5: The Nodal signaling pathway within the signal receiving cell (for details, see text). An inhibition of the pathway by the established inhibitor Lefty is illustrated. Furthermore, a modulation by the ER-located Nicalin and NOMO is indicated, focussing on a possible effect on extracellular and transmembrane proteins. In principle, also a Nicalin and NOMO function in the Nodal signal sending cell is possible.

Considering the critical role of Nodal signals in various aspects of vertebrate embryonic development, precise temporal and spatial control of this pathway appears necessary, involving dozens of intracellular factors (reviewed by Tian and Meng, 2006). Still, only a few antagonists have been identified so far (Tab. 1), including secreted ligands forming heterodimers with Nodal proteins (Yeo and Whitman, 2001), secreted long-range antagonists binding to both ligands and (co-)receptors (Chen and Schier, 2002; Sakuma et al., 2002; Cheng et al., 2004), specific membrane-bound competitors for binding to the EGF-CFC co-receptor (Harms and Chang, 2003), intracellular transcriptional repressors (Iratni et al., 2002; Bell et al., 2003), and mediators of the degradation of Nodal receptors (Zhang et al., 2004). The Nicalin-NOMO complex localizes to the membrane of the endoplasmic reticulum (ER) and might, therefore, inhibit Nodal signaling by modifying or trapping Nodal signaling components that are routed through the ER (Fig. 5, Tab. 1).

Factor	**Type**	**Antagonistic mechanism**
Cerberus/Dan family members	secreted proteins	binding to Nodal proteins and thus prevention of their signal transduction (Hashimoto et al., 2004)
Bmp3/Bmp7	secreted proteins	formation of heterodimers with Nodal proteins resulting in mutual inhibition (Yeo and Whitman, 2001)
Lefty proteins	secreted proteins	inhibition of Nodal signal transduction by binding to the Nodal co-receptors EGF-CFCs as well as to the Nodal ligands (Branford and Yost, 2002)
Tomoregulin-1	transmembrane proteins	binding to EGF-CFCs to prevent the Nodal signal transduction (Harms and Chang, 2003)
Dapper2	endosomal protein	promotion of the degradation of Nodal receptors (Zhang et al., 2004)
Drap1	transcriptional repressor	binding to the DNA binding domain of FoxH1 (Iratni et al., 2002)
Nicalin/NOMO	ER transmembrane proteins	possibly modifying or trapping Nodal signaling components that are routed through the ER (Haffner et al., 2004)

Tab. 1: Summary of Nodal antagonists (adapted from a review by Tian and Meng, 2006)

However, the ubiquitous expression of Nicalin and NOMO as well as their evolutionary conservation indicate that the complex may have additional functions beyond Nodal signaling. This could be involvement in other TGFβ superfamily pathways (many Nodal antagonists also inhibit other related signaling pathways) or even in unrelated events. γ-Secretase might serve as a precedent for this idea: Its manipulation in embryonic development leads to Notch-related phenotypes, but its function goes beyond Notch signaling.

1.2.1 Components of the Nicalin-NOMO complex

Nicalin was identified in 2004 as the most closely related relative of Nicastrin by a bioinformatical approach focussing on the conservation of the DYIGS and aminopeptidase (DAP) domain (see section 1.1.1) (Haffner et al., 2004). Due to its homology, which is illustrated in Fig. 6, the protein was termed Nicalin, Nicastrin-like protein. Like Nicastrin, Nicalin is catalytically inactive as, within the DAP domain, the aminoacids required for aminopeptidase activity are not conserved in either of the two proteins. Neither the DYIGS motif nor the critical glutamate residue (E333, see section 1.1.1), which are important for Nicastrin function, are conserved in Nicalin.

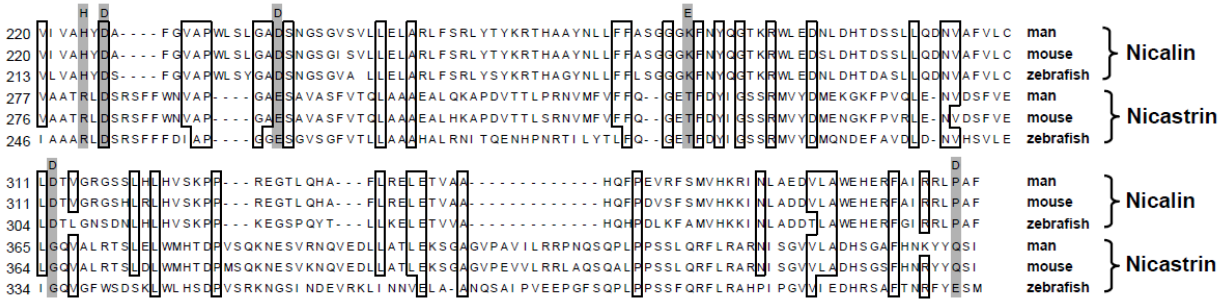

Fig. 6: Nicalin is distantly related to Nicastrin. Sequence alignment of the aminopeptidase domains of Nicalin and Nicastrin from man, mouse and zebrafish**.** Conserved residues are boxed. Residues required for catalytic activity of aminopeptidases are shown on top of the alignment and the corresponding residues in Nicalin and Nicastrin are shaded. As the required residues are only partially conserved, both Nicalin and Nicastrin are catalytically inactive. Adapted from Haffner et al., 2004

Similar to Nicastrin, Nicalin is a type-I transmembrane protein and ubiquitously expressed (Haffner et al., 2004, 2007). It contains N-linked oligosaccharides which do not undergo maturation indicating that Nicalin is not transported beyond the early secretory pathway (Haffner et al., 2004; Fig. 7). This was confirmed by immunofluorescence microscopy and subcellular fractionation showing that Nicalin localizes to the ER (Haffner et al., 2004, 2007). Charged amino acids at the Nicalin C-terminus (‘KAKTQ’, Fig. 7) could be responsible for ER retention/retrieval.

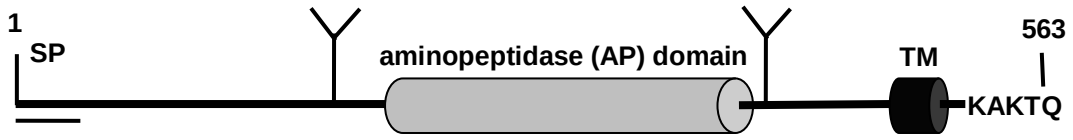

Fig. 7: Nicalin protein structure. Nicalin is a type-I transmembrane protein and contains a (catalytically inactive) aminopeptidase (AP) domain (in grey) and a transmembrane (TM) domain (in black). The observed N-glycosylation may occur at two potential sites that have been predicted (‘Y’). The immature protein has a signal peptide (SP, underlined) for translation into the ER. An amino acid sequence that is located at its C-terminus (‘KAKTQ’) may represent an ER-localization signal.

Despite the homology to Nicastrin, Nicalin cannot be co-isolated with γ-secretase and is not able to rescue the assembly of a functional γ-secretase complex in cells lacking Nicastrin, demonstrating that it is not a γ-secretase component (Haffner et al., 2004). Nevertheless,

Nicalin was found to be part of a high-molecular-weight membrane protein complex in Blue-Native PAGE (polyacrylamide gel electrophoresis) raising the possibility that Nicalin might have a function analogous to Nicastrin's role in a novel protein complex (Haffner et al., 2004). This finding triggered a search for Nicalin binding proteins which could be additional components of this novel complex. Membrane protein preparations were used for a large-scale immunoprecipitation of Nicalin and analyzed by SDS-PAGE and subsequent protein staining to identify complex partners (Haffner et al., 2004). A 130-kDa protein not present in control preparations was specifically enriched and identified by mass spectrometry as pM5, an uncharacterized protein which had been accidentally discovered in a screen for collagenase-related genes (Templeton et al., 1992). However, pM5 neither contains the conserved motif of all metalloproteases (HEXXH) nor does it show any other homology to collagenases. Based on functional data, indicating an involvement of pM5 in Nodal signaling (see section 1.2), it was given the name NOMO (Nodal modulator) (Haffner et al., 2004).

NOMO, like Nicalin a type-I transmembrane protein, has a large N-terminal domain (> 1,000 amino acids) and also localizes to the ER, as demonstrated by deglycosylation experiments, immunfluorescence microscopy and subcellular fractionation (Haffner et al., 2007). The only motifs identified by bioinformatical analyses (PFAM domain search) were a coiled-coil domain and two Cna B domains (Fig. 8). The Cna B domain is found in the collagen binding surface protein of *Staphylococcus aureus*, but does not directly participate in collagen binding (Deivanayagam et al., 2000). It is also present in a high number (88 and 13 copies, respectively) in Colossin A and B, two huge proteins (~11 and 3.7 MDa) of unknown function encoded in the genome of the social amoeba *Dictyostelium discoideum* (Eichinger et al., 2005).

In the human genome, the *nomo* gene is one of three highly similar genes (*nomo1, nomo2, nomo3*) in a region of duplication located on the short arm of chromosome 16 (Loftus et al., 1999; Martin et al., 2004). According to expression databases, all *nomo* genes are expressed and their transcripts are almost identical in sequence and length (Haffner et al., 2004; Fig. 8). Due to this similarity, the three *nomo* genes encode closely related proteins that are expected to have the same function. In this thesis, only NOMO2 was analyzed and referred to as NOMO. Two transcripts of *nomo2* differing in one exon at their 3' ends and encoding different NOMO isoforms have been described. The shorter *nomo2* transcript lacks a ~330-bp exon, which would contain a stop codon, leading to an extended coding region and a NOMO2 variant with an elongated C-terminus. This long NOMO2 isoform (NOMO2-L) appears to be a rare variant, whereas the long *nomo* transcripts (leading to the shorter NOMO proteins) represent the common species (Haffner et al., 2004, Fig. 8).

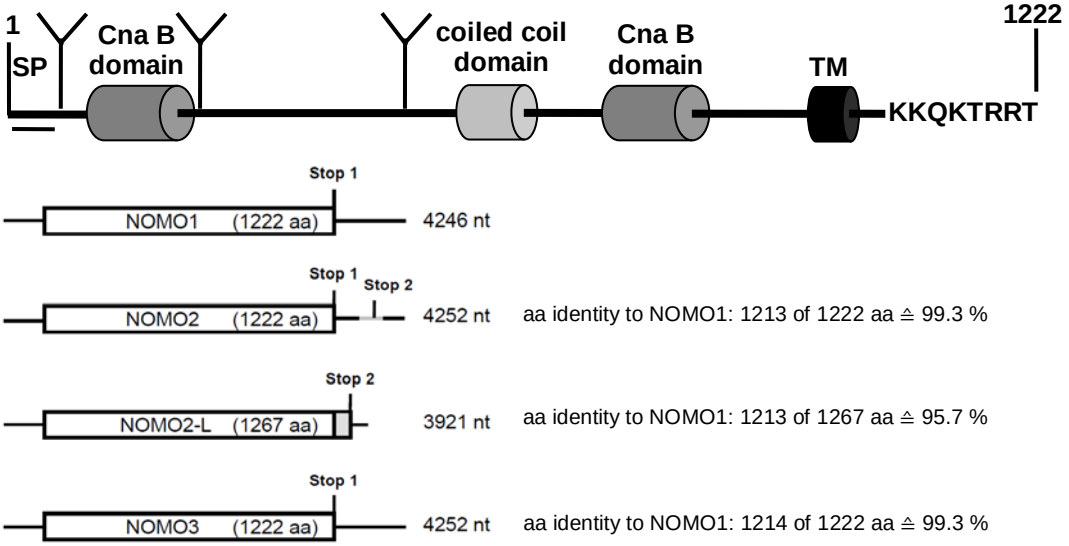

Fig. 8: NOMO protein and mRNA structure. A) Domain structure of NOMO. NOMO is a type-I transmembrane protein with a large N-terminal domain (> 1000 AS) facing the ER lumen, a transmembrane domain (TM, black), and a short cytosolic C-terminus. Three N-glycosylation sites have been predicted ('Y'). Identified domains include a coiled coil domain (light grey) and two Cna B domains (dark grey). The immature protein has a signal peptide (SP, underlined) for translocation into the ER. The longer isoform NOMO-L, generated by alternative splicing (see below), possesses an elongated C-terminus. B) The human genome contains three highly homologous *nomo* genes (adapted from Haffner et al., 2007). Schematic representation of *nomo1*, *nomo2* and *nomo3* mRNAs showing 5'-untranslated regions, coding regions (boxed) with the sizes of the encoded proteins in amino acids (aa) and stop codons, and 3'-untranslated regions. mRNA lengths in nucleotides (nt) and aa identity in comparison to NOMO1 are shown. Alternative splicing of the *nomo2* transcript results in the deletion of the exon containing stop codon 1 and the generation of an mRNA with an extended reading frame encoding the long NOMO2 isoform NOMO-L.

1.2.2 Assembly of the Nicalin-NOMO complex

First indications for a coordinate expression of Nicalin and NOMO came from RNA interference (RNAi) studies in HEK293T cells, where the knockdown of Nicalin led to a concomitant decrease of NOMO expression (Haffner et al., 2007), an effect reminiscent of the reduction of APH-1, PEN-2 and Presenilin expression in the absence of Nicastrin (Edbauer et al., 2002; Zhang et al., 2005). Likewise, a reduction of Nicalin expression was observed in NOMO knockdown cells, suggesting that both proteins, like γ-secretase components, are destabilized in the absence of complex formation. Quantitative mRNA measurements demonstrated that this destabilization takes place at the protein level. A further indication for the similarity with γ-secretase was the demonstration of Nicalin replacement: Nicalin overexpression resulted in a strong decrease of endogenous Nicalin protein, similar to a phenomenon observed for Presenilin (Thinakaran et al., 1997; see section 1.1.2). Furthermore, Nicalin overexpression in wild-type or Nicalin knockdown cells resulted in a strong increase in endogenous NOMO levels (Haffner et al., 2007), indicating that Nicalin might stabilize endogenous NOMO and thus elevate NOMO steady-state levels. In contrast, NOMO overexpression did not elevate Nicalin levels. Thus, a model was proposed in which NOMO is synthesized in excess amounts and stabilized by complex formation with Nicalin. Nicalin on the other hand has to be limited independently of NOMO.

1.3 Goals of this thesis

The Nicalin-NOMO complex and γ-secretase are high-molecular-weight complexes that contain related molecules, Nicalin and Nicastrin, respectively. Both complexes are involved in important pathways during early embryonic development, the Nicalin-NOMO complex in the Nodal signaling pathway (reviewed by Haffner and Haass, 2004; Haffner and Haass, 2006) and γ-secretase in the Notch signaling pathway (reviewed by Selkoe and Kopan, 2003). Moreover, their expression levels are tightly controled by a post-transcriptional regulation mechanism which originates from the assembly of the complexes (Thinakaran et al., 1997; Edbauer et al., 2002; Lee et al., 2002; Zhang et al., 2005; Haffner et al., 2007).

The native size of the Nicalin-NOMO complex, as determined by Blue-Native-PAGE, was shown to represent 200-220 kDa (Haffner et al., 2007), which is slightly smaller than the combined molecular weights of monomeric Nicalin (~60 kDa) and NOMO (~130 kDa). Therefore, the possibility was considered that the complex might contain unidentified components, likely in the low-molecular-weight range, similar to the γ-secretase factors APH-1 and PEN-2. In the absence of animal models suited for genetic screens and the impracticality of other protein-protein interaction technologies (e.g. the yeast-two-hybrid system) for this goal, the advancement of the Nicalin affinity purification technique used to identify NOMO (Haffner et al., 2004) appeared to represent the most promising approach. In particular, the scale of the procedure was increased and the membrane protein lysis conditions were optimized.

To rule out the missing of possible interactors because of too insensitive protein staining protocols, a proteomics approach was established in parallel. It included stable isotope labeling using amino acids in cell culture (SILAC) and subsequent mass spectrometry analysis of co-purified proteins allowing the identification of substoichiometric or transient binding partners. In addition to unidentified core complex components, this approach might yield functionally relevant transient interactors of Nicalin that could help to elucidate the molecular mechanism of the complex. The identification of such proteins could also help to shed light on the regulation and assembly mechanisms of membrane protein complexes in general.

2. Results

2.1 Transmembrane protein 147 co-purifies with the Nicalin-NOMO complex

NOMO has been identified as Nicalin-binding protein by an affinity purification approach which included the preparation of cell membranes from HEK293 cells stably overexpressing myc-tagged Nicalin, the solubilization of the membranes using 3-[(3-cholamidopropyl) dimethylammonio]-1-propanesulfonate (CHAPS) as detergent, and the purification of Nicalin-myc by anti-myc antibody-coupled agarose (Haffner et al., 2004). The Nicalin-NOMO membrane protein complex has a native size of 200-220 kDa, slightly larger than the combined molecular weights of its known components (Haffner et al., 2007). Therefore, the possibility was explored that the complex may contain unknown low-molecular-weight components which had been missed so far. The Nicalin affinity purification procedure was modified, most importantly by using higher amounts of membrane protein (up to 30 mg) and n-dodecyl-β-D-maltoside (DDM) instead of CHAPS as detergent. DDM has been used to purify γ-secretase (Winkler et al., 2009) and also allows the isolation of the Nicalin-NOMO complex. Coomassie Blue (Fig. 9) as well as silver staining (Fig. 11) methods were used to visualize potential Nicalin interacting proteins in SDS gels. Under these conditions, a 22-kDa band was specifically enriched in preparations from HEK293T/Ncl-myc cells (Fig. 9, middle panel) in addition to myc-tagged Nicalin (Ncl, ~60 kDa) and endogenous NOMO (~130 kDa).

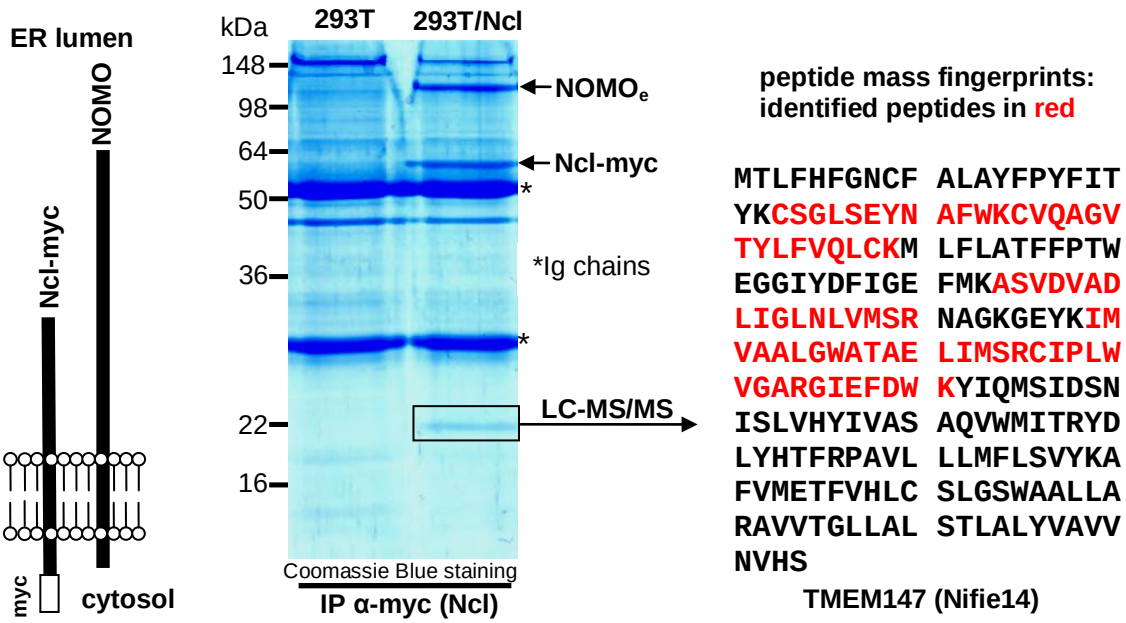

Fig. 9: TMEM147 was identified as Nicalin interacting protein by co-immunoprecipitation and mass spectrometry (LC-MS/MS) analysis. Nicalin-myc (Ncl-myc; schematically illustrated on the left) was immunoprecipitated from large-scale membrane preparations (detergent: 0.7 % DDM) using an anti (α)-myc antibody. Bound proteins were visualized by Coomassie Blue staining (middle panel). In addition to NOMO (~130 kDa; schematically illustrated on the left), a ~22-kDa band was specifically enriched in precipitates from HEK293T/Ncl-myc cells (bands denoted with * represent immunoglobulin heavy and light chains; 'e': endogenous). LC-MS/MS analysis of tryptic peptides generated from this protein identified it as TMEM147 (Nifie14). Detected peptides of the human TMEM147 sequence (from four independent experiments) are highlighted in red (right panel); note that all peptides end with arginine (R) or lysine (K) residues as the R/K-specific protease trypsin was used for their generation.

This protein band was cut out from Coomassie Blue stained gels and subjected to in-gel trypsin digestion. Peptide mass fingerprints were generated by LC-MS/MS analysis and the results were analyzed by a MASCOT database search (see section 4.7). One protein repeatedly found among the most significant hits in several independent experiments was transmembrane protein 147 (TMEM147), an uncharacterized protein of 224 amino acids also known as Nifie14. However, most likely due to its hydrophobicity (see section 2.3) only six different peptides could be identified (Fig. 9, right panel) resulting in a sequence coverage of only 34.4 % and a relatively low score in the MASCOT analysis. Still, TMEM147 was considered the most promising candidate, as its calculated molecular weight of ~24 kDa fit well to the size of the isolated band and no other protein from the hit list showed a molecular weight in this range. Moreover, TMEM147 is similarly conserved as Nicalin and NOMO (see section 2.7). It is predicted to contain seven transmembrane domains (see section 2.3) and to largely reside within the membrane. Due to the lack of a significant homology to other proteins no function could be inferred from its sequence and no functional domains were identified.

Since no anti-TMEM147 antibody was available, a monoclonal antibody (T147.11) was generated using a synthetic TMEM147 peptide as antigen (see section 4.5.1 and Fig. 31). Its specificity was demonstrated by several observations (Fig. 10): a) it recognizes a band of ~22 kDa in HEK293T wild-type cells, in good agreement with the calculated mass of TMEM147, b) this band is strongly reduced in knockdown (KD) cells overexpressing TMEM147-specific shRNAs, and c) in cells overexpressing a V5-tagged TMEM147 version (rescue) a band of ~25 kDa is labeled.

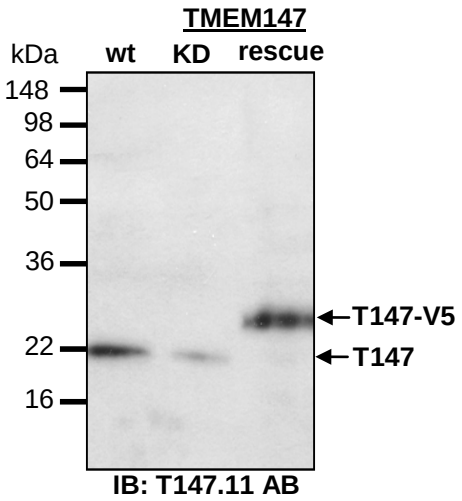

Fig. 10: The T147.11 antibody (AB) is specific for TMEM147 (T147). Immunoblot (IB) of membrane protein lysates from different HEK293T cells. A 22-kDa band is recognized in wild-type (wt) cells, which is reduced in TMEM147 knockdown (KD) cells. Reintroduction of an RNAi-insensitive V5-tagged construct (rescue cells) resulted in the labeling of a ~25-kDa band.

Using the T147.11 antibody, it could be shown that TMEM147 is indeed highly enriched in Nicalin immunoprecipitates (Fig. 11A, right panel). Unfortunately, like the Nicalin and NOMO antibodies, the T147.11 antibody did not work in co-immunoprecipitation assays. To nevertheless demonstrate the bidirectionality of the interaction between TMEM147 and Nicalin, the human TMEM147 cDNA was cloned from HEK293T cells, stably expressed in a V5-tagged version in HEK293T cells and TMEM147-V5 was precipitated from membrane protein lysates using an anti-V5-specific antibody. This specifically enriched proteins of ~60 kDa and ~130 kDa, confirmed as Nicalin and NOMO by immunoblotting (Fig. 11B).

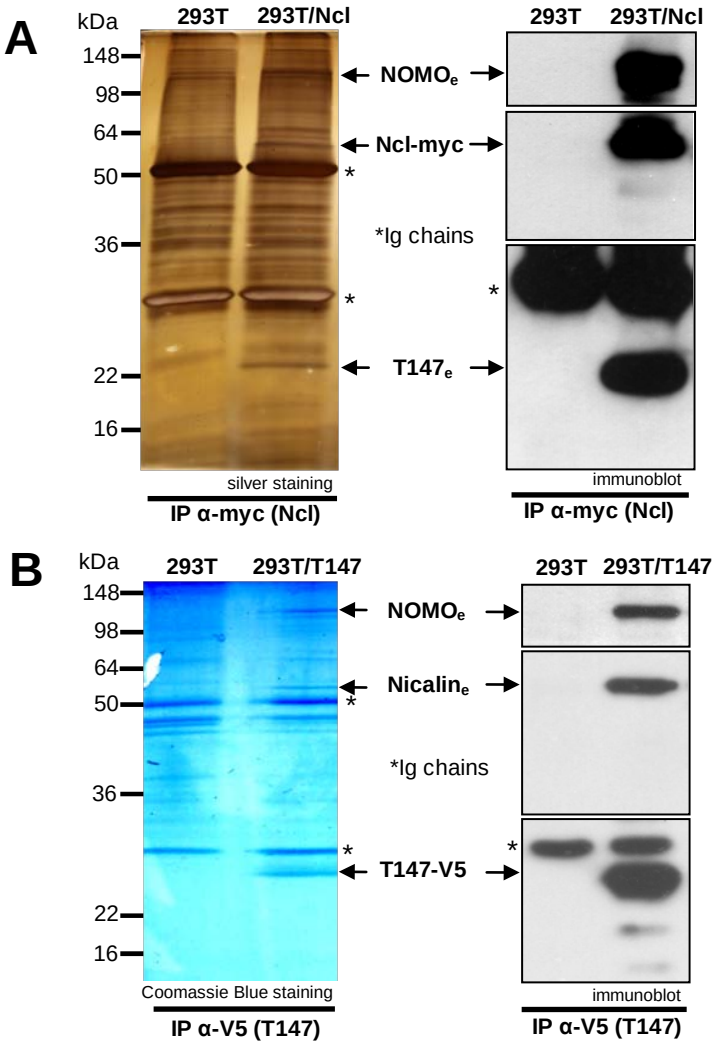

Fig. 11: Co-precipitation between Nicalin, NOMO and TMEM147. A) Nicalin-myc was immunoprecipitated from large-scale membrane preparations (detergent: 0.7 % DDM) and the bound proteins were visualized by silver staining (left panel). In addition to NOMO (~130 kDa), a ~22-kDa band, identified as TMEM147 (T147) by immunoblotting using the T147.11 antibody, was specifically enriched in precipitates from HEK293T/Ncl-myc cells. B) TMEM147-V5 was immunoprecipitated from large-scale membrane preparations (detergent: 0.7 % DDM) and the bound proteins were visualized by Coomassie Blue staining (left panel). In addition to TMEM147-V5, a ~60 and a ~130-kDa band were specifically enriched (left panel) and identified as Nicalin and NOMO by immunoblotting (right panel). (bands denoted with * represent immunoglobulin heavy and light chains; 'e': endogenous)

Moreover, a strong enrichment of all three components was observed when the extent of co-precipitation via TMEM147 (Fig. 12 A, middle lane) or Nicalin (Fig. 12 B, middle lane) was compared to input lysates (Fig. 12 A and B, respectively, left lanes). This indicated that the interaction between Nicalin, NOMO, and TMEM147 occurs in a roughly stoichiometric manner. Further support for this came from the analysis of the lysates after TMEM147 or Nicalin immunoprecipitation, where an efficient depletion of all three proteins could be demonstrated (Fig. 12 A and B, respectively, right lanes).

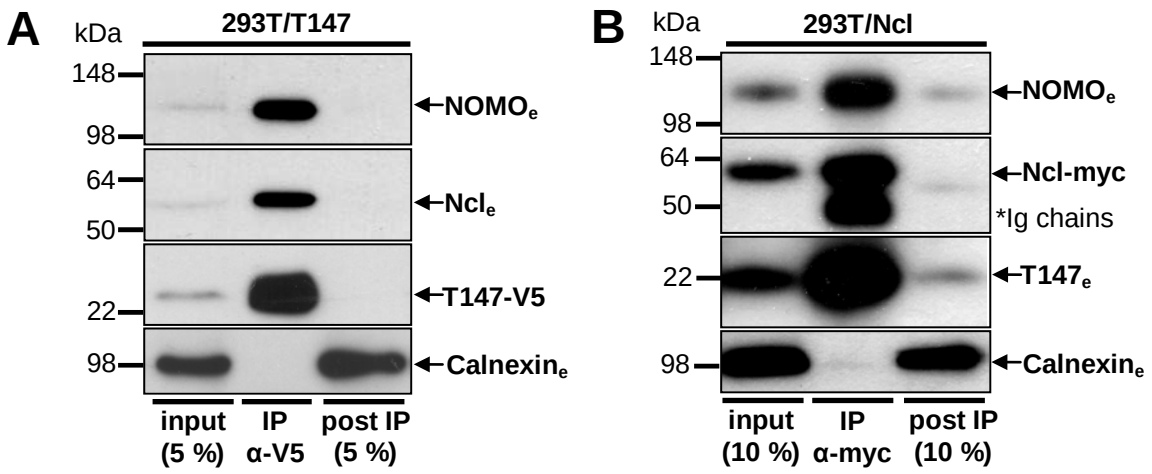

Fig. 12: TMEM147 or Nicalin precipitation leads to the depletion of all complex members. Input, bound (IP) and unbound (post-IP) material of TMEM147-V5 (A), and Nicalin-myc (B) immunoprecipitations were compared by immunoblotting. A strong enrichment of all three binding partners in TMEM147 or Nicalin-precipitates (middle lanes) as well as their depletion in the post-IP supernatants (right lanes) was observed. No significant binding or depletion of the ER membrane protein Calnexin was detectable. ('e': endogenous)

These data strongly suggested that the interaction of TMEM147 with the Nicalin-NOMO complex is highly specific and indicated that TMEM147 might indeed represent a novel component of the complex.

2.2 TMEM147 co-localizes with Nicalin and NOMO in the ER

Nicalin and NOMO have been shown to localize to the ER by various approaches including the analysis of their N-glycosylation status (Haffner et al., 2004, 2007). Many proteins of the secretory pathway receive N-linked carbohydrates during their translocation into the ER lumen (Helenius and Aebi, 2002). Preassembled sugar chains rich in mannose are attached to asparagine (N) residues residing within a certain amino acid motif (N-X-S/T, i.e. asparagine - any amino acid - serine/threonine). The carbohydrates of proteins destined for the late secretory pathway usually undergo stepwise modifications in the Golgi apparatus including removal of the majority of the mannose molecules and the addition of various other sugars. This results in the generation of complex carbohydrates, whereas glycoproteins restricted to the early secretory pathway (predominantly ER) keep their high-mannose sugars. These two types of N-linked carbohydrates can be experimentally distinguished by using sugar-cleaving enzymes and subsequently determining the molecular weight of the deglycosylated protein. Whereas this analysis confirmed the previously reported (Haffner et al., 2007) presence of high-mannose sugars on Nicalin and NOMO, no molecular weight shift was detected for TMEM147 (Fig. 13), in agreement with the absence of N-glycosylation motifs within the TMEM147 sequence (see also Fig. 18). As a consequence, this approach was not suitable to analyze the subcellular localization of TMEM147.

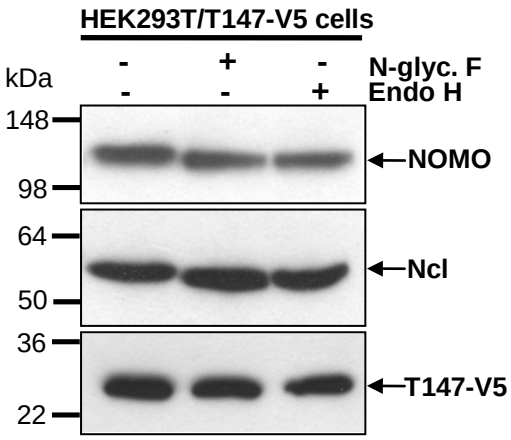

Fig. 13: Nicalin and NOMO, but not TMEM147, contain N-linked, high-mannose carbohydrates. HEK293T/T147-V5 cell lysates were treated with N-glycosidase F or endoglycosidase H and submitted to SDS-PAGE and immunoblotting. Both treatments resulted in a slight reduction in the molecular weights of Nicalin and NOMO, demonstrating the presence of high-mannose carbohydrates, while TMEM147 molecular weight was not changed, in agreement with the lack of N-glycosylation consensus sequences.

As an alternative method to analyze the subcellular localization of TMEM147, immunofluorescence microscopy was used. For overexpressed Nicalin and NOMO, an ER-like staining pattern has been demonstrated in HEK293 cells (Haffner et al., 2004) by this approach. In this thesis, the newly generated anti-Nicalin (NiNT1), anti-NOMO (NOM4A12), and anti-TMEM147 (T147.11) antibodies (see section 4.5.1) were tested in immunofluorescence experiments for their ability to detect their endogenous target proteins in human cervix carcinoma HeLa cells. Whereas staining with NiNT1 yielded a pattern very similar to that of the ER-marker Calnexin confirming the ER-localization of Nicalin (Fig. 14, top panel), endogenous NOMO and TMEM147 levels were under the detection limit of their antibodies. Therefore, TMEM147 localization had to be analyzed in cells stably overexpressing TMEM147-V5. A co-staining with NiNT1 and an anti-V5 epitope antibody showed a high degree of overlap, suggesting co-localization of Nicalin and TMEM147 (Fig. 14, bottom panel) in the ER.

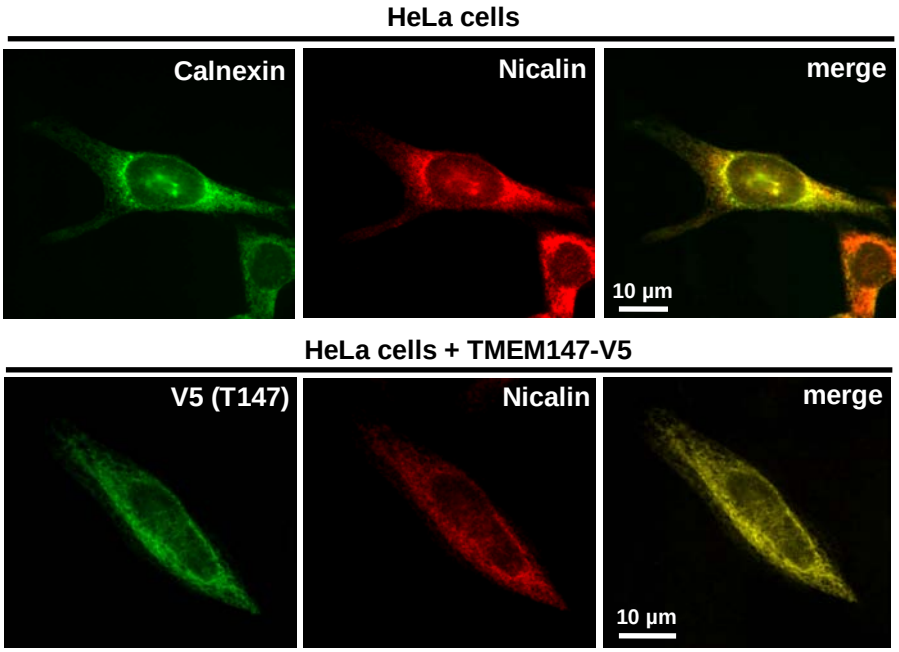

Fig. 14: TMEM147 and Nicalin co-localize within the ER. Immunofluorescence microscopy pictures of wild-type HeLa cells (top panel) and HeLa cells overexpressing V5-tagged TMEM147 (bottom panel). Nicalin co-localizes with the ER-marker Calnexin (top panel), confirming the ER-localization of endogenous Nicalin. The overlap between the TMEM147-V5 and the Nicalin staining (bottom panel) is similarly good demonstrating co-localization within the ER.

To confirm the immunoflurescence microscopy results by an independent approach and to analyze the subcellular localization of endogenous TMEM147, separation of cellular membranes by density gradient centrifugation and analysis of the obtained fractions by SDS-PAGE/immunoblotting was used. In iodixanol gradients, the buoyant density of subcellular

membranes increases in the following order: plasma membrane < early endosomes < Golgi < ER Golgi-intermediate compartment (ERGIC) < ER. As a consequence, ER membranes were found in the bottom four fractions (demonstrated by the presence of Calnexin and Nicastrin containing immature N-linked carbohydrates) when HEK293T membranes were subjected to ultracentrifugation in an iodixanol gradient (Fig. 15). The other fractions contained proteins of the later secretory pathway (e.g. Golgi) and the plasma membrane, as demonstrated by the presence of the complex glycosylated form of Nicastrin. Like Nicalin and NOMO, TMEM147 immunoreactivities could only be detected in these four fractions, suggesting that indeed none of the complex components leaves the early compartments of the secretory pathway.

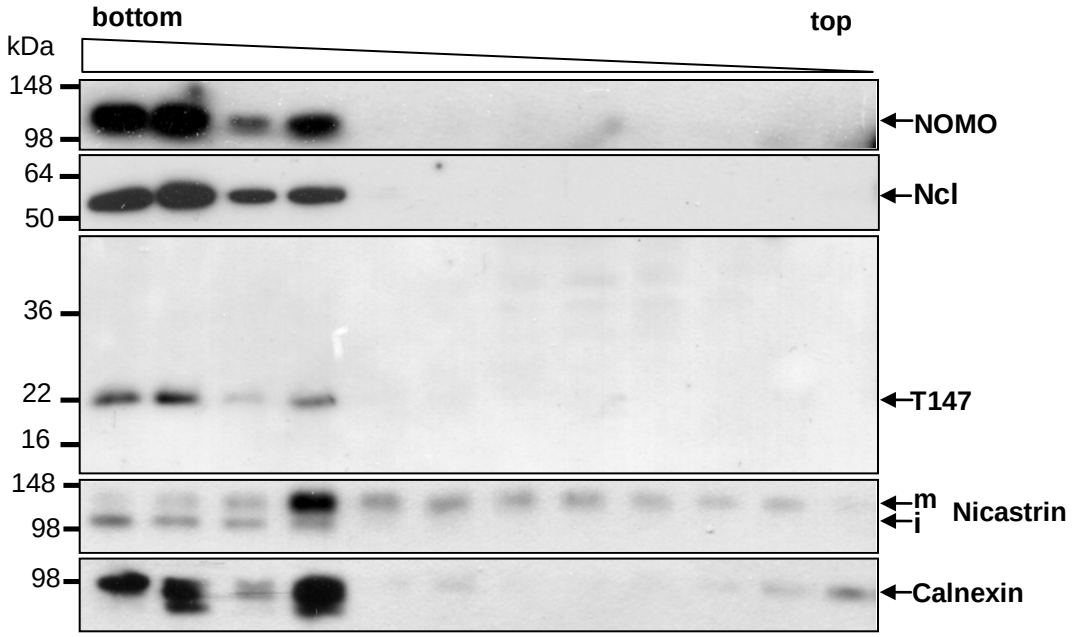

Fig. 15: TMEM147, Nicalin and NOMO cofractionate with ER membranes. Membrane protein lysates from HEK293T cells were subjected to ultracentrifugation in an iodixanol gradient. Fractions were collected and subsequently analyzed by immunoblotting. Nicalin and NOMO were detected in the four bottom fractions enriched in ER membranes, as shown by the presence of the ER-marker Calnexin, the presence of immature ('i') and the absence of mature ('m') Nicastrin (fraction 4 also contained material from the early Golgi compartment, where the maturation of Nicastrin's N-linked carbohydrates occurs). Apparently, protein concentration in fraction 3 was lower than in other fractions.

Taken together, these data demonstrated that TMEM147 co-localizes with Nicalin and NOMO in the ER further supporting the idea that TMEM147 is a genuine part of the complex.

The ER-localization of proteins is usually mediated by certain amino-acid motifs that actively promote their retention and/or retrieval. As the C-terminal motif in the cytosolic tail of Nicalin (...KAKTQ-COOH) resembles the classical KKXX-motif mediating the retrieval of transmembrane proteins to the ER (Nilsson et al., 1989; Jackson et al., 1990), it was tested whether it can function as an ER-localization signal. For that purpose, the Nicalin C-terminal sequence (YKTVQRLLVKAKTQ) was fused to the ectodomain and transmembrane domain of the cell surface protein CD4 (cluster of differentiation 4), which like Nicalin is a type-I transmembrane protein and had been used to analyze motifs in the C-termini of Nicastrin (Capell et al., 2005) and Presenilin (Kaether et al., 2004). The subcellular localization of this chimeric protein (CD4-NclC) was analyzed by immunofluorescence microscopy in transfected HeLa cells. Whereas for wild-type CD4 the expected surface-like staining was observed, the CD4-NclC chimera co-localized with Calnexin in the ER (Fig. 16) suggesting that the Nicalin C-terminus contains an ER-localization signal. However, a Nicalin deletion mutant lacking the cytosolic C-terminus (NicalinΔC, see section 2.6) still localized mainly in the ER indicating that the exact mode of ER retention/retrieval of the complex might be more complicated. Thus, this question requires further investigation.

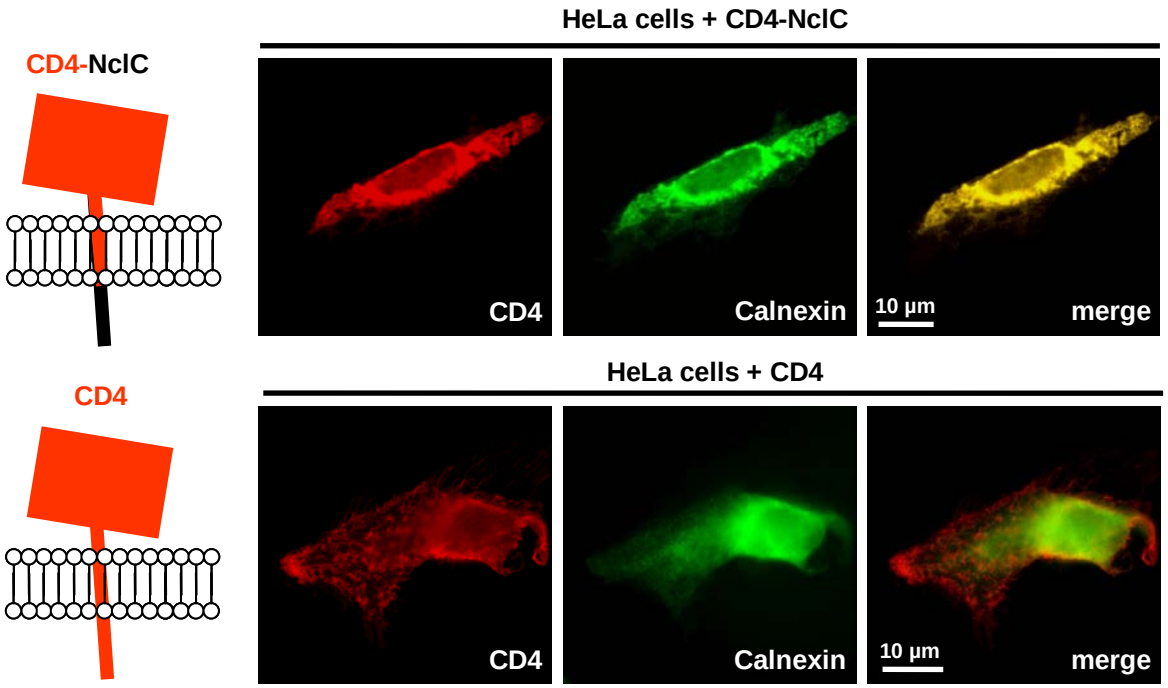

Fig. 16: The Nicalin C-terminus contains an ER-localization signal. The presumptive cytosolic C-terminus of Nicalin, YKTVQRLLVKAKTQ, was fused to the ectodomain and transmembrane domain of the cell surface protein cluster of differentiation 4 (CD4). The localization of the resulting chimeric protein CD4-Nicalin C-terminus (CD4-NclC, top panel) and of wild-type CD4 (bottom panel) were analyzed by immunofluorescence microscopy in transfected HeLa cells. As expected, the expession of wild-type CD4 only slightly overlapped with the ER-marker Calnexin, while most of the protein was found in a plasma membrane-like staining (red areas in the bottom 'merge' picture). In contrast, the chimeric CD4-NclC co-localized with the ER-marker Calnexin.

2.3 The TMEM147 topology is similar to APH-1

Human TMEM147 consists of 224 amino acids (aa), with a high percentage of hydrophobic residues like leucine (12.5 % of all aa), alanine (10.7 %) or valine (9.5 %). Thus, size and hydrophobicity of TMEM147 were reminiscent of the γ-secretase component APH-1, which consists of 247 aa in its short isoform APH-1aS and contains 12.5 % leucine, 10.9 % alanine and 9.7 % valine residues. However, global (Needleman and Wunsch, 1970) and local (Smith and Waterman, 1981) alignment by the EMBOSS program did not reveal an obvious homology between the two proteins. Nevertheless, the possibility that TMEM147 and APH-1 might share some structural similarities was further analyzed by comparing Kyte-Doolittle hydrophobicity plots using the Protscale tool (Fig. 17). For the short isoform APH-1aS seven transmembrane (TM) domains were predicted, in agreement with experimental data (Fortna et al., 2004). The plot for TMEM147 showed six to seven putative TM domains suggesting that its overall structure may be very similar to the polytopic γ-secretase component, except for a more prominent loop between TM domains three and four and a larger N-terminus in APH-1aS.

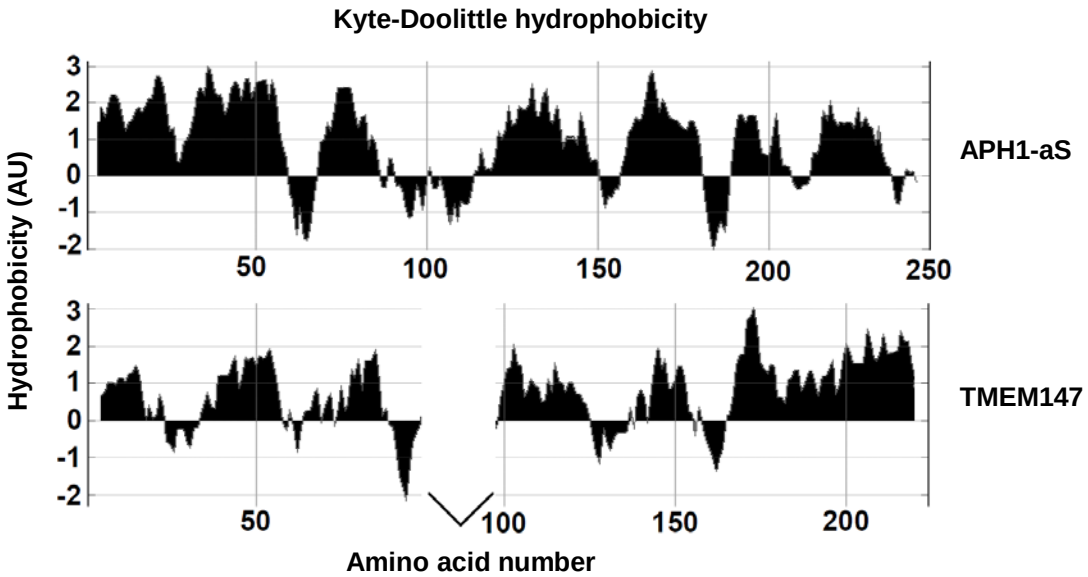

Fig. 17: Kyte-Dolittle plot of APH1-aS and TMEM147. The hydrophobicity was plotted using the Protscale tool by the Kyte-Doolittle method with a seven amino-acid window. A positive value is indicative of a transmembrane region, a negative value of a loop region. A gap was introduced into the TMEM147 plot to align transmembrane domains 4-7.

To confirm the putative TMEM147 topology especially at the C-terminus, a hidden Markov model (PRODIV-TMHMM; Viklund and Elofsson, 2004) was applied as an alternative prediction method. As for APH-1aS, the program calculated seven TM helices for TMEM147 (Fig. 18).

```
MTLFHFGNCFALAYFPYFITYKCSGLSEYNAFWKCVQAGVTYLFVQLCKM    1- 50
LFLATFFPTWEGGIYDFIGEFMKASVDVADLIGLNLVMSRNAGKGEYKIM   51-100
VAALGWATAELIMSRCIPLWVGARGIEFDWKYIQMSIDSNISLVHYIVAS  101-150
AQVWMITRYDLYHTFRPAVLLLMFLSVYKAFVMETFVHLCSLGSWAALLA  151-200
RAVVTGLLALSTLALYVAVVNVHS                            201-224
```

Fig. 18: TMEM147 is a seven transmembrane protein. Approximate localization of TM domains in TMEM147, as predicted by the PRODIV-TMHMM algorithm (Viklund and Elofsson, 2004) as a part of the TOPCONS server.

Moreover, the orientation of the TM domains within the membrane was predicted to be identical between the two proteins, with the odd-numbered loops and the C-termini facing the cytosolic side and the even-numbered loops and the N-termini facing the luminal side. A signal peptide was predicted for neither protein. The result of this analysis is illustrated in Fig. 19.

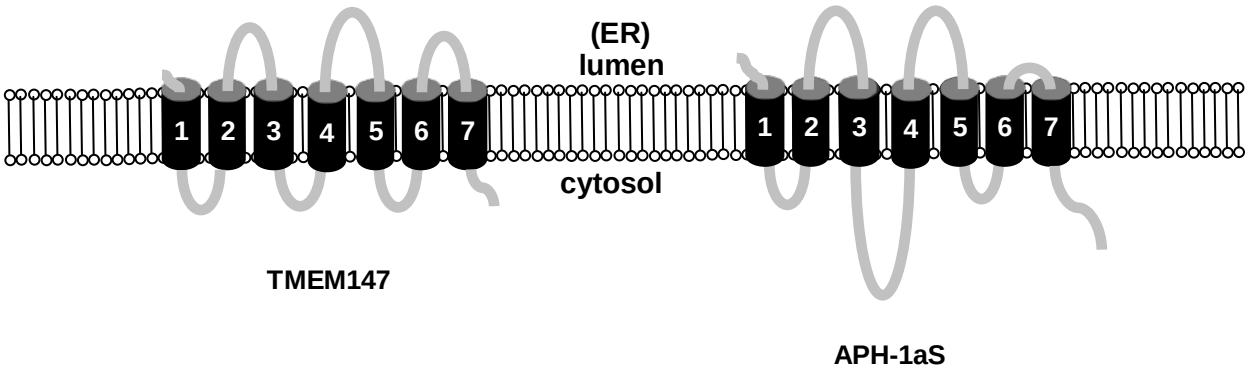

Fig. 19: TMEM147 topology is similar to APH-1aS. Comparison of topology models of human TMEM147 and human APH-1aS generated by the PRODIV-TMHMM method (Viklund and Elofsson, 2004) as a part of the TOPCONS server. The topology of APH-1 has been experimentally validated (Fortna et al., 2004) and the prediction for TMEM147 is highly similar: seven transmembrane helices, with the N-terminus residing in the ER lumen and the C-terminus facing the cytosol. Thus, the localization of the hydrophilic loops of both proteins would be identical and even their lengths similar in most cases. Transmembrane domains are numbered (white numbers) and predicted loop sizes are reflected.

However, the reliability of the bioinformatical tools used is limited and additional biochemical analyses will be necessary to validate the topology of TMEM147.

2.4 TMEM147, Nicalin, and NOMO stabilize each other

Although the precise function of APH-1 within γ-secretase is not known, it is required for the maintenance of the steady-state levels of the complex, which is based on the mutual stabilization of the individual components upon incorporation into the complex (Gu et al., 2003). One consequence of this stabilization mechanism is the so-called replacement, the reduction of the expression levels of endogenous APH-1 upon overexpression of ectopic APH-1. It is explained by the incorporation of ectopically expressed APH-1 monomers at the expense of endogenous molecules, which are likely to be degraded (although this degradation could never be formally demonstrated). Experimentally, this replacement can be analyzed by the overexpression of epitope-tagged protein versions which are separated from the endogenous proteins by their higher molecular weight. This phenomenon has not only been observed for the γ-secretase components APH-1 and Presenilin 1/2 (Thinakaran et al., 1997), but also for Nicalin. Stable overexpression of Nicalin fused to a myc/His-tag results in a strong reduction of endogenous Nicalin in HEK293T cells (Fig. 20A; Haffner et al., 2007). Thus, the replacement of endogenous proteins by their exogenously expressed counterparts appears to be a characteristic feature of both γ-secretase and the Nicalin-NOMO complex (NOMO replacement could not be shown so far, since the separation of wild-type and tagged protein is difficult in the high-molecular weight range). To examine if TMEM147 is subjected to this replacement, the effect of stable TMEM147-V5 overexpression in HEK293T cells was analyzed by immunoblotting. Strikingly, the endogenous protein was reduced below the detection limit of the T147.11 antibody (Fig. 20B) suggesting that TMEM147, like Nicalin, is controled by complex formation.

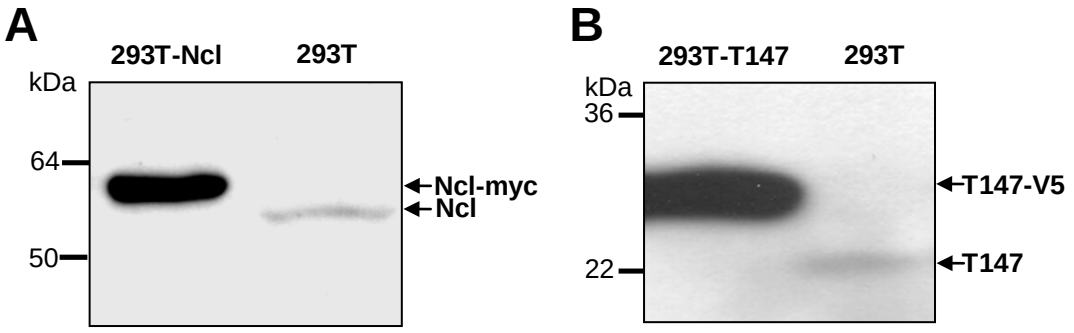

Fig. 20: Nicalin or TMEM147 overexpression leads to the replacement of the respective endogenous proteins. A) Myc-tagged Nicalin stably expressed in HEK293T cells (293T-Ncl) causes a strong reduction of the endogenous protein, which is present in wild-type HEK293T cells (293T). B) Similarly, stable TMEM147-V5 overexpression in HEK293T cells (293T-T147) leads to the replacement of endogenous TMEM147. Membrane proteins lysates were analyzed by SDS-PAGE and immunoblotting using specific antibodies.

A second consequence of the described stabilization mechanism is the instability of some (or all) complex components in the absence of one of their interaction partners. This has been shown, either in knockout cells or by RNA interference (RNAi), for the γ-secretase components Nicastrin (Edbauer et al., 2002), Presenilin (Leem et al., 2002; Edbauer et al., 2002;), APH-1 (Francis et al., 2002), and PEN-2 (Steiner et al., 2002). A similar effect has been observed for Nicalin and NOMO: The downregulation of Nicalin or NOMO expression by RNAi in HEK293T cells resulted in the reduction of the steady-state levels of the respective binding partner demonstrating a mutual dependence similar to γ-secretase components (Haffner et al., 2007; see Fig. 22A, B). Due to the long half-life of Nicalin and NOMO, the standard RNAi technique - transient transfection of siRNAs (small interfering RNAs) - was not applicable for their downregulation. Instead, stable expression of constructs encoding small hairpin RNAs (shRNAs, precursor molecules that are processed to siRNAs by the cellular machinery) was required to achieve efficient knockdowns (Haffner et al., 2007). However, this technique has some drawbacks: The selection of single-cell clones is time-consuming, involves the risk that the genetic/epigenetic background of the clone biases subsequent analyses, and does not allow analyzing the effects of acute protein depletion. Moreover, this technique is only suitable for cell lines that can be readily transfected with the existing reagents and are able to form single-cell clones. Therefore, an alternative method for the generation of stable Nicalin, NOMO, and TMEM147 knockdown cell lines was developed (1) to analyze the universality of the effects of Nicalin and NOMO downregulation and (2) to examine the consequences of TMEM147 depletion. This method was based on a lentivirus system which has been successfully used for a variety of targets (Wiznerowicz and Trono, 2003). Shortly, this approach uses a lentivirus-derived vector, which carries shRNA-coding sequences. The important regions of this vector are packaged into infective lentiviral particles by a packaging cell line. The supernatant of this cell line contains the infective particles and can be used to transduce target cells. Upon transduction, the vector regions are stably integrated into the genome and shRNAs are produced (for more details, see sections 4.3.1, 4.4.1, 4.4.5). In principle, a transduction efficiency of nearly 100 % can be achieved for all possible cells, and stable cell pools can be obtained within days and immediately be analyzed.

To test the lentiviral knockdown approach, HeLa instead of HEK293T cells were selected, which are similarly proliferative and as easy to handle as HEK293T cells, but due to their spread out morphology are superior to HEK293T cells in microscopy experiments. Thus, HeLa knockdown cells might become useful tools for microscopy-based assays in the future. In cell pools stably expressing Nicalin-, NOMO- or TMEM147-specific shRNAs knockdown efficiencies between 70 % and 90 % were reached, as quantitated on the mRNA level by

real-time PCR (Fig. 21B). In Nicalin- and NOMO-depleted cells, the mutual dependence of the expression levels of these two proteins reported in HEK293T cells (Haffner et al., 2007) could be confirmed (Fig. 21A, third and fourth lane). Strikingly, a strong reduction of TMEM147 expression was observed in both cell lines. Moreover, the knockdown of TMEM147 led to a similar reduction of Nicalin and NOMO (Fig. 21A, fifth lane) showing that TMEM147 is subjected to the same stabilization mechanism. To demonstrate the reversibility of this effect, the TMEM147 knockdown in HeLa cells was rescued by the expression of a V5-tagged version migrating at ~25 kDa (Fig. 21A, sixth lane). The TMEM147 rescue construct contained silent mutations at the siRNA targeting site conferring siRNA-resistance and was, like the shRNA constructs, transduced using a lentiviral system (see sections 4.3.1, 4.4.1 and 4.4.5). The rescue led to the restoration of Nicalin and NOMO levels and to the replacement of the residual endogenous TMEM147. An effect on the transcriptional level could be ruled out as the mRNAs of the respective non-targeted complex partners were not significantly changed, demonstrated by quantitative real-time PCR (Fig. 21B).

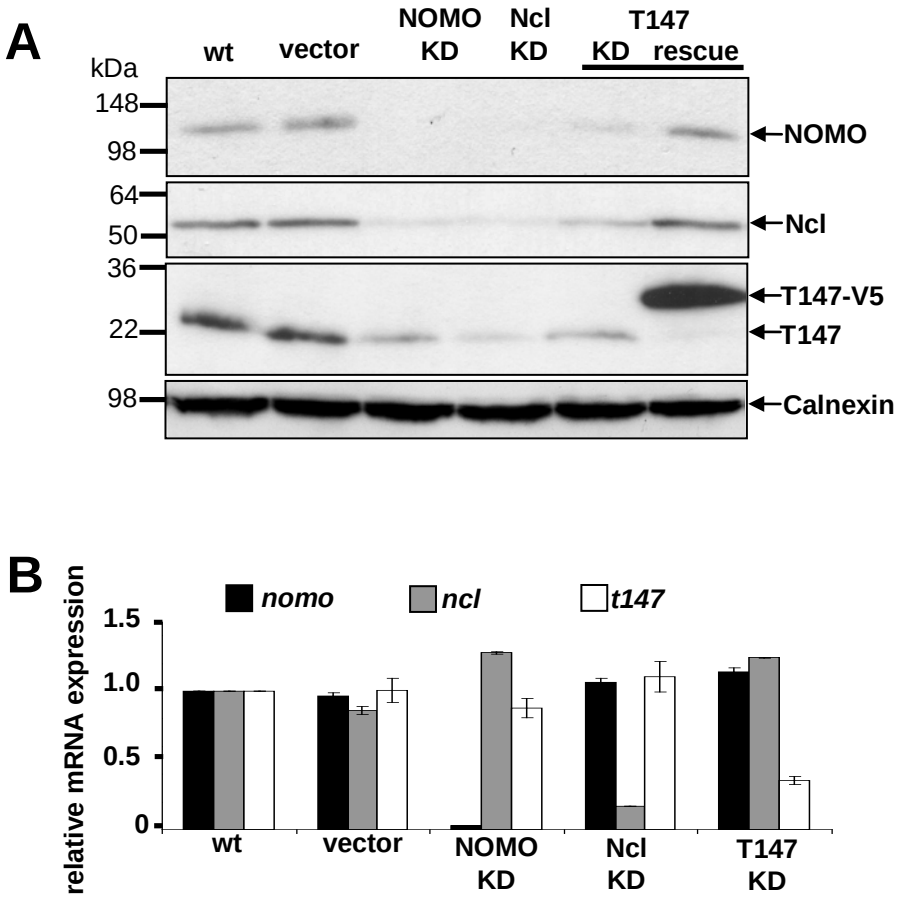

Fig. 21: Mutual dependence of Nicalin, NOMO and TMEM147 protein levels in HeLa cells. A) Stable Nicalin, NOMO, and TMEM147 knockdown (KD) cell lines were generated by transducing HeLa cells with lentiviruses encoding the respective shRNAs. Protein expression levels were detected by immunoblotting. Upon knockdown of either Nicalin, NOMO or TMEM147, a strong reduction of the respective binding partners was observed. Stable reintroduction of an RNAi-resistant TMEM147-V5 cDNA into T147 KD cells (T147 rescue) restored NOMO and Nicalin levels. B) mRNA levels in HeLa knockdown cells were analyzed by quantitative real-time PCR. Target gene expression was found to be decreased by 75-90%, while mRNA levels of the interaction partners were only marginally changed. Bars represent mean values from three experiments.

TMEM147 expression was also examined in the HEK293T Nicalin and NOMO rescue cell lines previously described (Haffner et al., 2007). The restoration of Nicalin and NOMO expression in these cell lines also resulted in a restoration of TMEM147 levels (Fig. 22A, B) strongly suggesting that the observed effects are specific. However, differences in the NOMO and Nicalin rescue cell lines became obvious: The stable expression of high levels of NOMO cDNA in NOMO KD cells restored Nicalin and TMEM147 expression levels to wt levels, but not higher (Fig. 22A). In strong contrast, a dose-dependent effect was observed in Nicalin rescue cells: The expression of roughly wild-type levels of Nicalin in a low-expressing Nicalin rescue clone (Fig. 22B, resc1) restored NOMO and TMEM147 back to roughly wild-type levels, while in a high-expressing Nicalin rescue clone (Fig. 22B, resc9) TMEM147 as well as NOMO expression exceeded wild-type levels severalfold. These results corroborated the hypothesis proposed previously that Nicalin might represent the master regulator of the complex (Haffner et al., 2007).

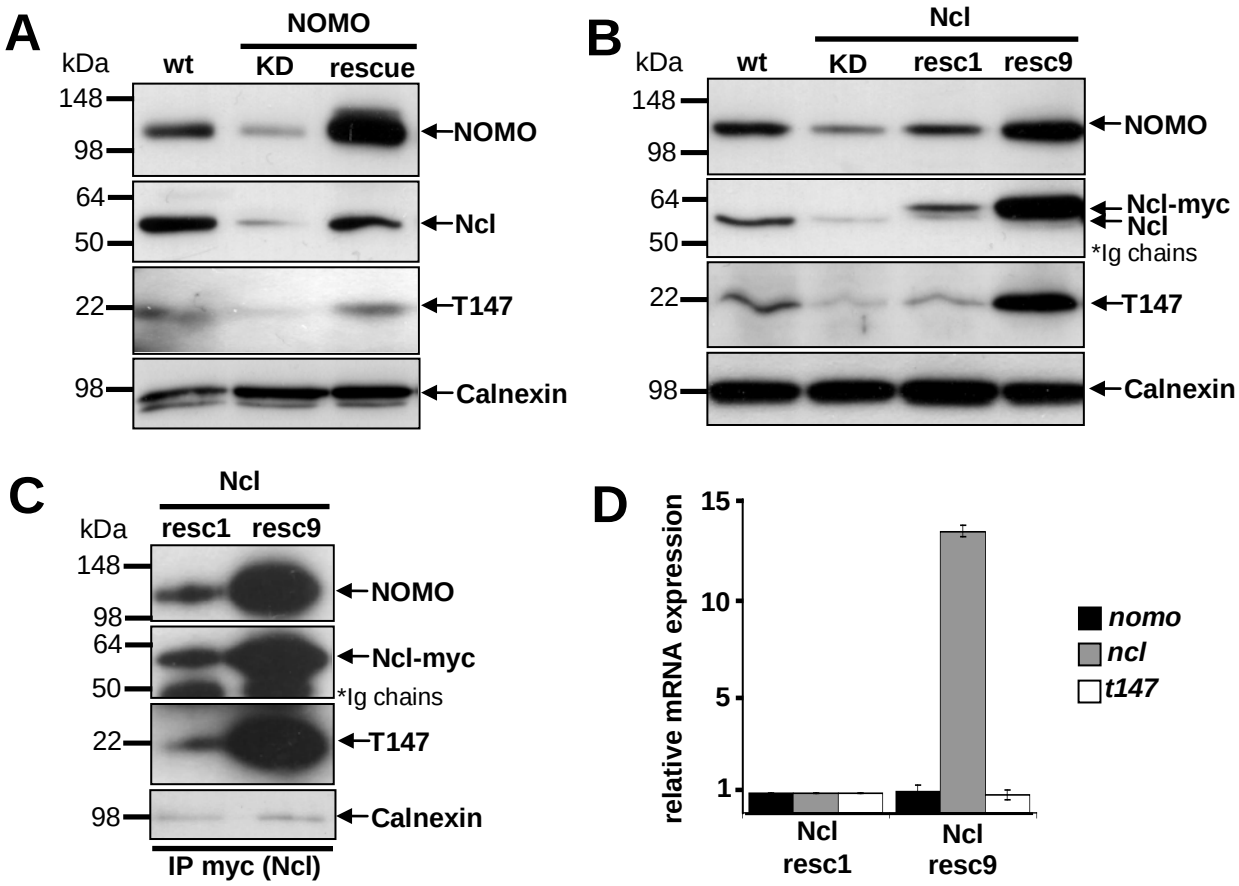

Fig. 22: Mutual dependence of Nicalin, NOMO, and TMEM147 protein levels in HEK293T cells. A) TMEM147 and Nicalin expression are reduced in NOMO knockdown (KD) cells and restored in NOMO rescue cells, i.e. KD cell lines stably expressing RNAi-insensitive *nomo* mRNA. B) TMEM147 and NOMO expression is reduced in Nicalin KD cells and restored in Nicalin rescue cells. In a high expression Ncl rescue clone (Ncl resc9), NOMO and TMEM147 expression are not only restored, but drastically increased. C) The strong increase in TMEM147 and NOMO in Ncl resc9 is accompanied by increased complex formation compared to resc1, demonstrated by a high extent of co-immunoprecipitation via Nicalin. D) The strong increase in TMEM147 and NOMO in Ncl resc9 cells is not accompanied by increased expression of *tmem147* and *nomo* mRNA as analyzed by quantitative real-time PCR (bars represent mean values from three experiments). Only *nicalin* mRNA is significantly higher in the resc9 cells (~13-fold).

Co-immunoprecipitation showed that the elevation of TMEM147 and NOMO in the high-expressing Nicalin resc9 clone is accompanied by increased complex formation compared to the low expressing resc1 clone (Fig. 22C). Quantitative mRNA measurements ruled out effects on the transcriptional level: In the high-expressing resc9 clone only *nicalin* mRNA levels were higher than in resc1 (more than ten-fold), while *nomo* and *tmem147* mRNA levels were similar (Fig. 22D).

To verify the results obtained in rescue cell lines suggesting Nicalin to represent the key regulator of the complex, overexpression experiments were repeated in HEK293T wild-type cells. Cell lines stably expressing Nicalin, NOMO, and TMEM147 cDNAs were analyzed by immunoblotting. Like in the rescue experiments, an elevation of TMEM147 and NOMO was observed upon Nicalin overexpression (Fig. 23, third lane). TMEM147 as well as NOMO overexpression, either alone or in combination, did not result in elevated Nicalin levels (Fig. 23, second, fifth and sixth lane), further confirming the data from the rescue experiments and underlining that Nicalin plays a special role in the regulation of the complex.

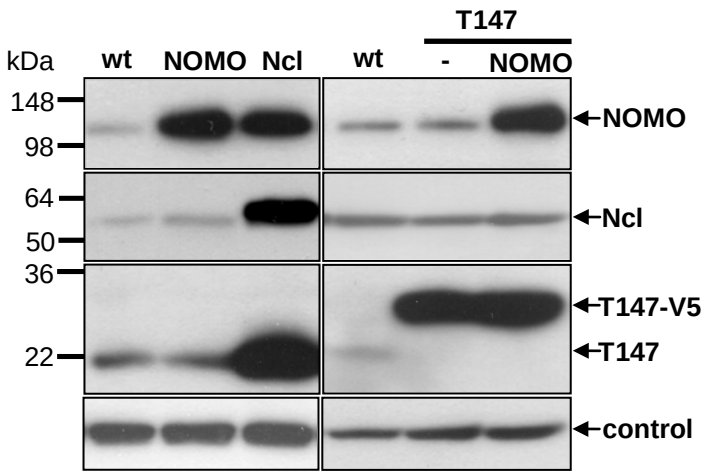

Fig. 23: Nicalin overexpression increases NOMO and TMEM147 levels, but not *vice versa*. Stable Nicalin, NOMO, and TMEM147 expression in HEK293T cells. NOMO overexpression has no effect on Nicalin or TMEM147 protein levels, whereas Nicalin overexpression leads to an increase in NOMO and TMEM147 expression. TMEM147 overexpression does not alter Nicalin or NOMO, but results in a decrease of endogenous TMEM147 below the detection limit of the T147.11 antibody (replacement; see Fig. 20). Even when TMEM147 and NOMO are simultaneously overexpressed Nicalin expression is not elevated. Controls are Calnexin (left half) and ß-Actin (right half).

In summary, the observed effects on Nicalin and NOMO upon TMEM147 downregulation as well as the changes in TMEM147 expression in response to Nicalin and NOMO depletion strongly suggest that TMEM147 is indeed a core component of the Nicalin-NOMO complex. Moreover, the key role of Nicalin in controling complex levels proposed previously was corroborated as was the posttranscriptional nature of the effects.

2.5 Nicalin controls complex levels by stabilizing excess molecules

Quantitave mRNA measurements (see Fig. 22D) had ruled out the possibility that the elevated expression of TMEM147 and NOMO upon Nicalin overexpression is due to enhanced transcription of *tmem147* and *nomo* mRNA. Moreover, co-immunoprecipitation analyses demonstrated that the elevation of NOMO and TMEM147 in Nicalin overexpressing cells is accompanied by enhanced complex formation suggesting a protein stabilization mechanism similar to that proposed for γ-secretase. If this hypothesis was true, an unstable and rapidly degraded NOMO and TMEM147 pool would be expected in wild-type cells. However, when the cellular protein synthesis was blocked for 6 hours by inhibiting the ribosome using the drug cycloheximide, the levels of all three components were not visibly changed (Fig. 24, middle lane). This finding indicated that under steady-state conditions most NOMO and TMEM147 molecules are like Nicalin present in a stable complex, while their unstable counterparts had to be extremely short-lived. To test this idea, the cellular proteasomes (one possible degradation machinery of unstable proteins) of HEK293T cells were blocked for six hours by the drug epoxomicine. Immunoblotting showed that this treatment led to an accumulation of TMEM147 and NOMO, but not Nicalin, compared to untreated cells (Fig. 24, right lane). These findings corroborated a model in which a) TMEM147 and NOMO are present in an unstable excess under steady-state conditions, b) Nicalin is not present in an excess but rather the limiting factor of the complex, and c) proteasomal pathways at least contribute to the degradation of NOMO and TMEM147 excess molecules. Thus, the elevation of NOMO and TMEM147 upon Nicalin expression can be considered a protein stabilization phenomenon.

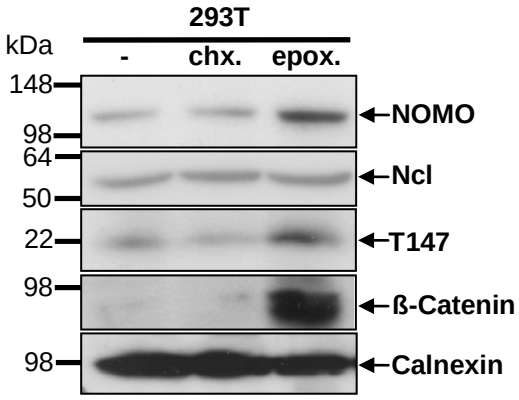

Fig. 24: TMEM147 and NOMO, but not Nicalin, are synthesized in an excess which is unstable in wild-type cells. Nicalin, NOMO and TMEM147 immunoreactivities were not visibly changed upon ribosome inhibition (chx.: cycloheximide, 6 hours) compared to untreated cells (left lane), which indicated a long half-life under steady-state conditions. Proteasome inhibition (epox.: epoxomicin, 6 hours) resulted in an increase in ß-Catenin as well as NOMO, and TMEM147 protein levels. This indicated the synthesis of excessive NOMO and TMEM147, but not Nicalin molecules.

The kinetics of the NOMO stabilization through Nicalin had been previously analyzed by using a cell line in which Nicalin expression can be induced by tetracycline (Haffner et al., 2007). In these cells, an immediate expression of high levels of Nicalin can be achieved by tetracycline treatment causing a continuous increase in NOMO protein levels over time, until NOMO has finally adapted to Nicalin levels later than 24 hours after Nicalin induction. The analysis of endogenous TMEM147 levels in these cells by immunoblotting revealed an increase with similar, but not identical kinetics (Fig. 25). Both NOMO and TMEM147 were highly increased 48 hours after Nicalin induction, but the increase in TMEM147 expression appeared to lag behind that of NOMO. NOMO levels were strongly increased already 24 hours after Nicalin induction and did not rise much further during the next 24 hours of tetracycline treatment. In contrast, only a slight increase in TMEM147 could be observed after 24 hours and most of the stabilization of TMEM147 took place between 24 and 48 hours after Nicalin induction. Nevertheless, both NOMO and TMEM147 elevation were accompanied by higher amounts bound to Nicalin, as shown by co-immunoprecipitation confirming that increased complex formation occurs. The difference in the kinetics of TMEM147 and NOMO stabilization might indicate that its assembly occurs in a stepwise manner (see sections 2.7 and 3.2).

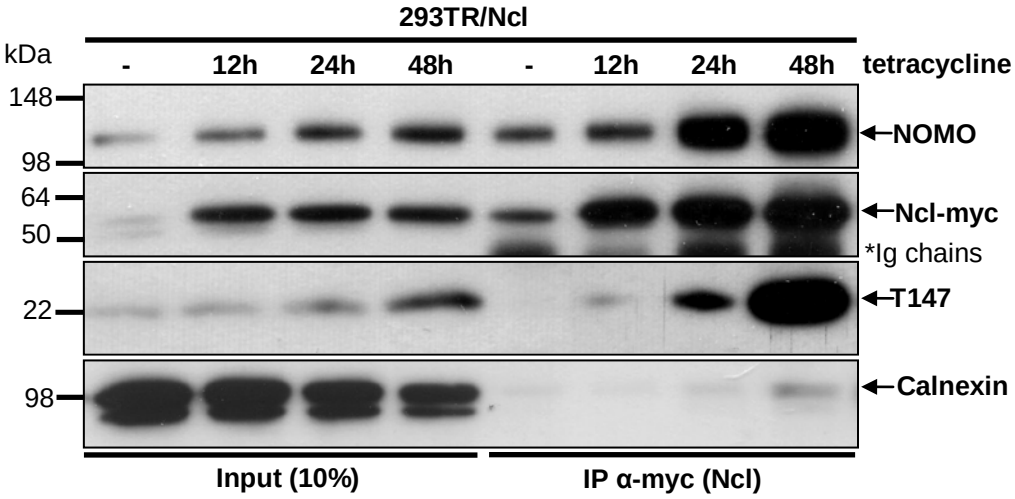

Fig. 25: Nicalin induction leads to a continuous stabilization of TMEM147 and NOMO excess molecules in the complex. Kinetics of NOMO and TMEM147 stabilization and complex formation were analyzed in cells with inducible Nicalin expression (293TR/Ncl). Expression of myc-tagged Nicalin was induced by tetracycline for the indicated times, and Nicalin, NOMO and TMEM147 levels in lysates and Nicalin immunoprecipitates were analyzed by immunoblotting. A continuous increase in TMEM147 and NOMO expression over time was observed in lysates (four left lanes), which was accompanied by enhanced co-immunoprecipitation (four right lanes). The elevation of NOMO appears to precede that of TMEM147.

2.6 TMEM147 and NOMO differ in their Nicalin binding requirements

The difference in the stabilization kinetics of TMEM147 and NOMO upon Nicalin induction (Fig. 25) indicated the possibility of distinct subcomplexes during the formation of the Nicalin-NOMO complex. In the case of γ-secretase assembly, intermediates like Nicastrin/APH-1 have been identified by using increasing concentrations of the detergent DDM for the solubilization of membrane proteins (Fraering et al., 2004). Therefore, a similar approach was applied to search for intermediates of the Nicalin-NOMO complex. A double stable cell line expressing both Nicalin-myc and TMEM147-V5 was generated and membrane protein lysates prepared under varying detergent conditions were subjected to co-immunoprecipitation studies using epitope tag-specific antibodies. The use of up to 2.5 % of DDM did not lead to clear results (data not shown), but in lysates containing 1 % Nonidet P-40 (NP-40), NOMO but not TMEM147, could be co-precipitated with Nicalin (Fig. 26, fourth lane). In agreement with this, TMEM147 immunoprecipitation from NP-40-containing lysates revealed no co-precipitation of Nicalin or NOMO (Fig. 26, sixth lane). In contrast, all three proteins could be detected in immunoprecipitates containing DDM (Fig. 26, third and fifth lane). These data supported the idea of a stable Nicalin/NOMO subcomplex.

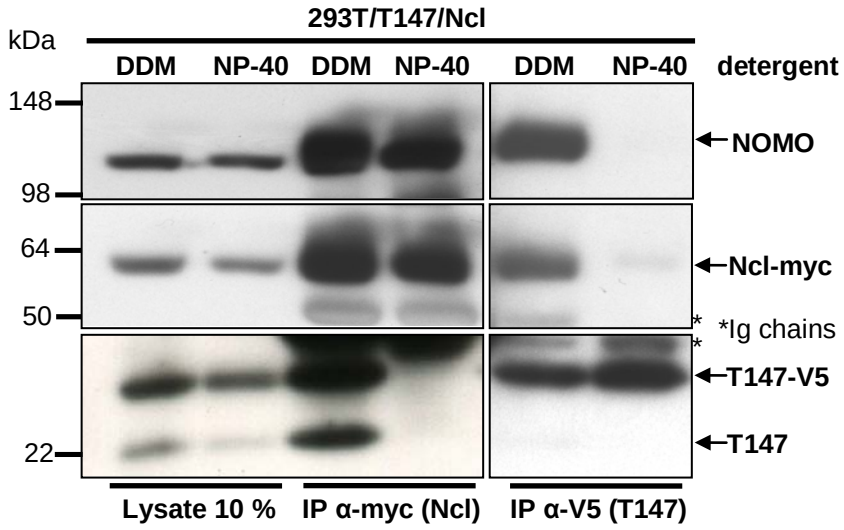

Fig. 26: TMEM147 is dispensible for Nicalin-NOMO interaction. Nonidet P-40 (NP-40) partially disrupts the complex, allowing the isolation of a subcomplex consisting of only Nicalin and NOMO. Membrane protein lysates containing either 0.7 % DDM or 1 % NP-40 were generated from 293T/TMEM147-V5/Nicalin-myc cells. Using NP-40 lysates, neither NOMO nor Nicalin could be detected in TMEM147 immunoprecipitates (right lane), but a Nicalin/NOMO subcomplex could be isolated by precipitating Nicalin (fourth lane). From DDM lysates, NOMO and TMEM147 (both V5-tagged and endogenous) were precipitated via Nicalin (third lane) and Nicalin and NOMO were precipitated via TMEM147 (fifth lane).

Interestingly, the detergent NP-40 is known to completely disrupt γ-secretase, a protein complex where the components are believed to interact mainly via transmembrane domains (LaVoie et al., 2003). Thus, the removal of TMEM147 from the Nicalin-NOMO complex in the presence of NP-40 suggested a similar type of interaction, in agreement with the predicted localization of the majority of the protein within the membrane (see Fig. 18-20). In contrast, the stability of a Nicalin/NOMO subcomplex in the presence of NP-40 raised the idea that their association might be mediated by their luminal domains. To determine the Nicalin domains required for the interaction with NOMO and TMEM147, Nicalin deletion constructs were generated, stably expressed in HEK293T cells, and their abilities to stabilize NOMO and TMEM147 levels were analyzed as an indirect measure for binding. The expression of myc-tagged Nicalin lacking the 14 amino acids of the predicted cytosolic C-terminus (NicalinΔC-myc) resulted in an increase in both NOMO and TMEM147 protein levels to a similar extent (Fig. 27), although less efficiently than the expression of myc-tagged full-length Nicalin (Nicalin-myc). In contrast, Nicalin lacking both cytosolic C-terminus and the 24 amino acids of the predicted Nicalin transmembrane domain (NicalinΔTMC, the Nicalin ectodomain) only stabilized NOMO leaving TMEM147 expression levels unchanged (Fig. 27). These findings supported the hypothesis that the Nicalin transmembrane domain is essential for TMEM147 but dispensable for NOMO interaction.

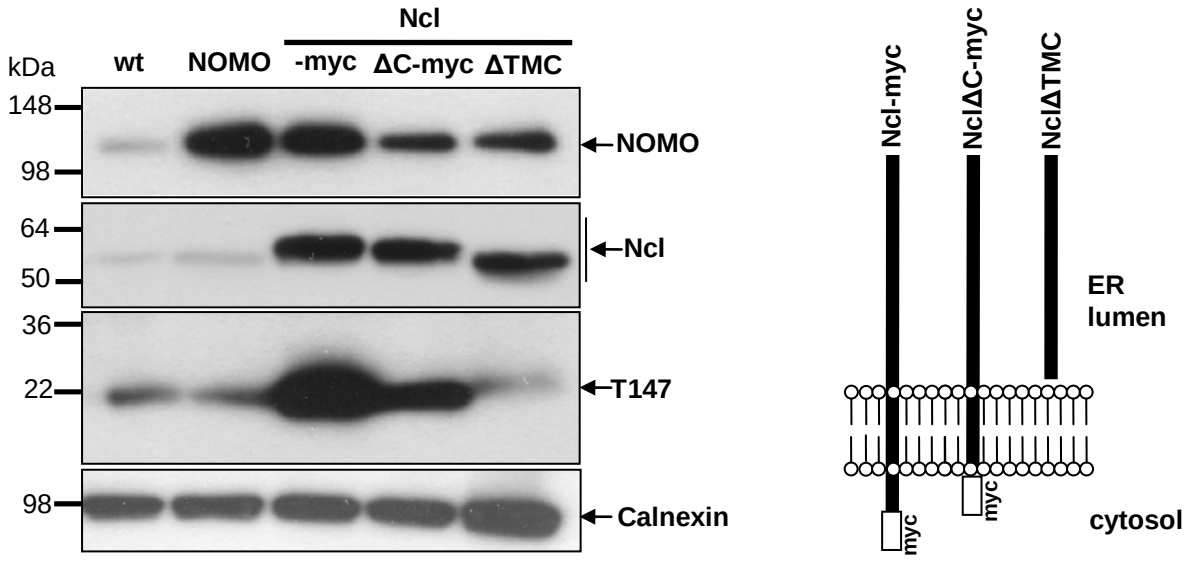

…DPEFVFYDQLKQVMNAYRVKPAVFDLLLAVGIAAYLGMAYVAVQHFSLLYKTVQRLLVKAKTQ aa 501-563

Fig. 27: The Nicalin transmembrane domain is essential for TMEM147, but dispensable for NOMO binding (I). Nicalin-myc and the deletion mutants NicalinΔC-myc and NicalinΔTMC (see schematic illustration on the right) were stably expressed in HEK293T cells. Effects on NOMO and TMEM147 levels were analyzed by immunoblotting (in comparison to wild-type and NOMO expressing cells). Whereas NicalinΔC-myc elevated both NOMO and TMEM147 (although less efficiently than Nicalin-myc), only NOMO was increased in NicalinΔTMC expressing cells. Below, the C-terminal 63 amino acids of Nicalin are shown with the predicted transmembrane domain highlighted in black.

As an alternative, independent approach for the functional analysis of the Nicalin deletion mutants, a knockdown rescue experiment was carried out (Fig. 28). RNAi-insensitive cDNAs coding for Nicalin-myc, NicalinΔC (without myc-tag), and NicalinΔTMC were stably introduced into Nicalin knockdown (Ncl KD) HEK293T cells to generate rescue cell lines (Ncl KD rescue). In a cell clone expressing high levels of NicalinΔC (untagged), NOMO and TMEM147 expression were restored to a similar extent above wild-type levels, although less efficiently than upon expression of full-length Nicalin-myc. In contrast, only low expressing clones were identified among the NicalinΔTMC rescue cells and in those NOMO expression was restored to roughly wild-type levels, while TMEM147 expression was still as low as in Nicalin knockdown cells. This confirmed the observations from the overexpression studies in wild-type cells and supported the hypothesis that Nicalin interacts with TMEM147 via Nicalin's transmembrane domain whereas the interaction with NOMO is mediated by Nicalin's luminal domain.

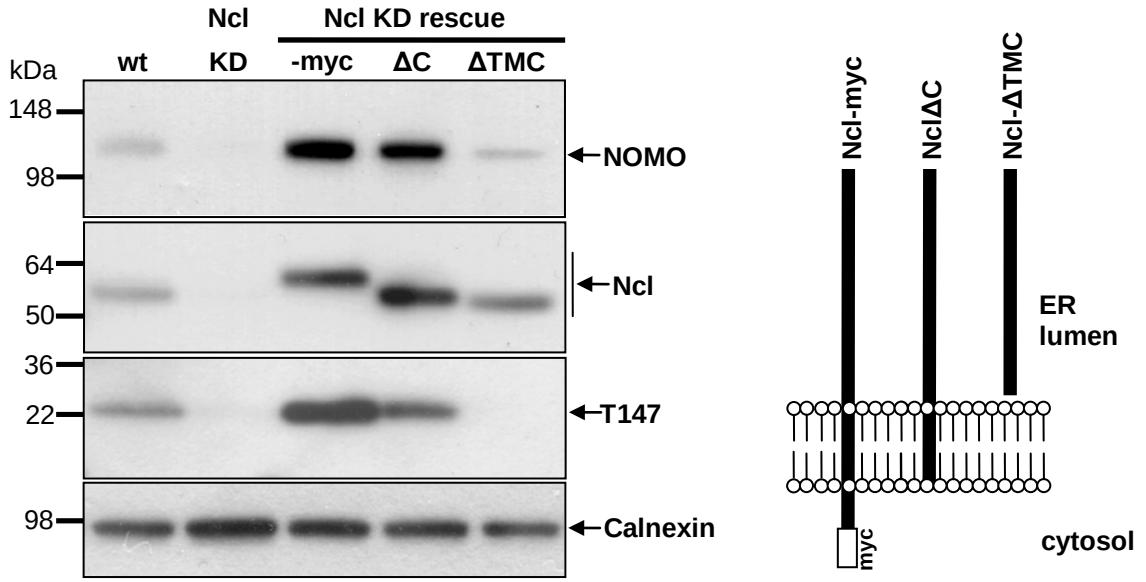

Fig. 28: The Nicalin transmembrane domain is essential for TMEM147, but dispensable for NOMO binding (II). RNAi-insensitive Nicalin-myc, NicalinΔC and NicalinΔTMC constructs (see schematic illustration on the right) were stably expressed in HEK293T/Nicalin knockdown (Ncl KD) cells, generating the respective rescue cell lines. The ability of the deletion mutants to restore NOMO and/or TMEM147 protein levels was analyzed by immunoblotting (compared to wild-type and Ncl KD cells). NicalinΔC was able to rescue both NOMO and TMEM147 expression (although the elevation of protein levels beyond wild-type levels was less efficient compared to Nicalin-myc). In contrast, NicalinΔTMC was unable to restore TMEM147 expression, but restored NOMO to wild-type levels.

To demonstrate the inability of NicalinΔTMC to interact with TMEM147 more directly, co-immunoprecipitation experiments were carried out. Since the anti-Nicalin antibody NiNT1 is not suitable for immunoprecipitation and untagged NicalinΔTMC could therefore not be specifically enriched, NicalinΔTMC was co-expressed in a stable cell line together with myc-tagged NOMO and V5-tagged TMEM147. Lysates from this triple-transfected cell line were used for co-immunoprecipitation analyses using epitope tag-specific antibodies. When

NOMO was immunoprecipitated (using an anti-myc antibody), large amounts of NicalinΔTMC were co-isolated, whereas no enrichment of TMEM147 was observed (Fig. 29, third lane). Upon TMEM147 precipitation (via an anti-V5 antibody), only minor amounts of a protein with a migration behaviour identical to endogenous Nicalin (which is not replaced by NicalinΔTMC in these cells) were observed (Fig, 29, fourth lane). This suggested that TMEM147 selectively binds to full-length Nicalin and no significant interaction with NicalinΔTMC occurs, further supporting the idea that the Nicalin TM domain is essential for TMEM147 interaction.

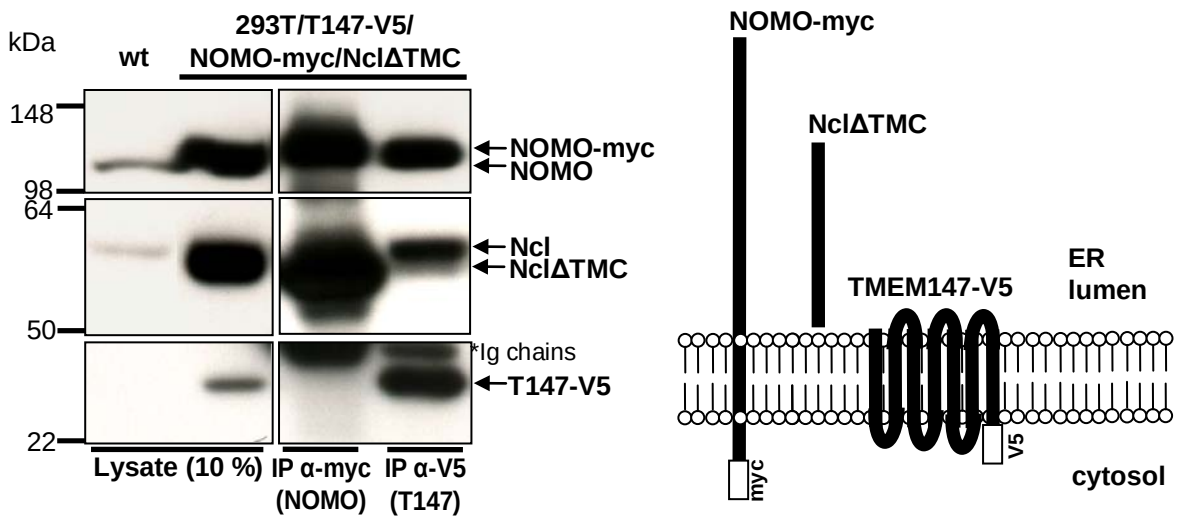

Fig. 29: NOMO, but not TMEM147, physically interacts with the Nicalin ectodomain NicalinΔTMC. Membrane protein lysates were prepared from a HEK293T cell line stably expressing V5-tagged TMEM147, myc-tagged NOMO and untagged NicalinΔTMC (see illustration on the right) and subjected to tag-specific immunoprecipitation. Precipitates were analyzed by immunoblotting (left panel, right two lanes). For comparison, input lysates and lysates from wild cells are shown (left two lanes). NicalinΔTMC could be precipitated in large quantities via NOMO. Only minor amounts of Nicalin were found in TMEM147 precipitates and the running behavior in an SDS-PAGE identified this Nicalin species as endogenous full-length Nicalin (which is not replaced by NicalinΔTMC).

The findings presented in this section led to a model of a hierarchical complex assembly, which is discussed in section 3.2.

2.7 The interaction of TMEM147 with Nicalin/NOMO is evolutionary conserved

Nicalin and NOMO orthologs have been reported to be present in all multicellular organisms (Haffner et al., 2004). Similarly, expression databases like Uniprot indicated the presence of TMEM147 orthologs in all metazoans. Fig. 30 shows the degree of amino-acid identity (generated by FASTA alignment) between the human Nicalin, NOMO, and TMEM147 proteins and the respective orthologs from common model organisms ranging from *Arabidopsis thaliana* to mouse. All three proteins are conserved to a similar extent among

vertebrates, with respect to both amino acid identity and protein lengths, (e.g., 71-78 % in the zebrafish *Danio rerio*). In distantly related species such as the fruit fly *Drosophila melanogaster*, the nematode worm *Caenorhabditis elegans* or the plant *Arabidopsis thaliana*, TMEM147 is even slightly higher conserved than Nicalin and NOMO (~40-50 % conservation compared to ~25-35 %).

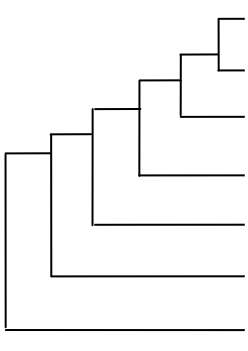

	% Identity to human			length (aa)		
	Ncl	NOMO	T147	Ncl	NOMO	T147
H.sapiens	100	100	100	563	1222	224
M.musculus	93	93	99	563	1214	224
X.laevis	81	79	78	560	1206	225
D.rerio	74	71	78	572	1208	225
D.melanogaster	35	32	49	561	1199	227
C.elegans	31	26	42	563	1121	225
A.thaliana	33	30	38	565	1227	228

Fig. 30: Nicalin, NOMO and TMEM147 sequences and protein sizes are highly conserved in multicellular organisms. Percentage of amino acid (aa) identity and lengths (number of aa) of Nicalin, NOMO and TMEM147 orthologous proteins in selected multicellular model organisms are shown. Sequences were retrieved from the Uniprot database and the percentage of amino-acid identity compared to the human proteins ('% identity') was calculated using the FASTA program. Species specific names of the orthologs are not shown; instead 'Nicalin (Ncl)', 'NOMO' and 'TMEM147' ('T147') were used for all species. Abbreviations: *H.: Homo, M.: Mus, X.: Xenopus, D.rerio: Danio rerio, D.melanogaster: Drosophila melanogaster, C.: Caenorhabditis, A.: Arabidopsis.*

In a next step, the question was addressed whether certain areas of TMEM147 and its orthologs are particularly conserved. This would be of interest, as it might help to identify amino-acid sequences that are essential for TMEM147 function. Therefore, human and model organism sequences were aligned using the clustalw2 program and the result was visualized using the Jalview software (Fig. 31). In addition, topology prediction data (see section 2.3) were integrated. Obviously, the C-terminal ~60 aa are less well conserved than the first ~165 aa, suggesting that the C-terminus might be less important for TMEM147 function. Moreover, a stretch between aa 119 and 140 is highly conserved. Interestingly, a larger ER luminal loop has been predicted for this region, namely for aa 121-136. Yet, the relevance of this stretch or other conserved regions for Nicalin/NOMO binding or additional functions will need further analysis.

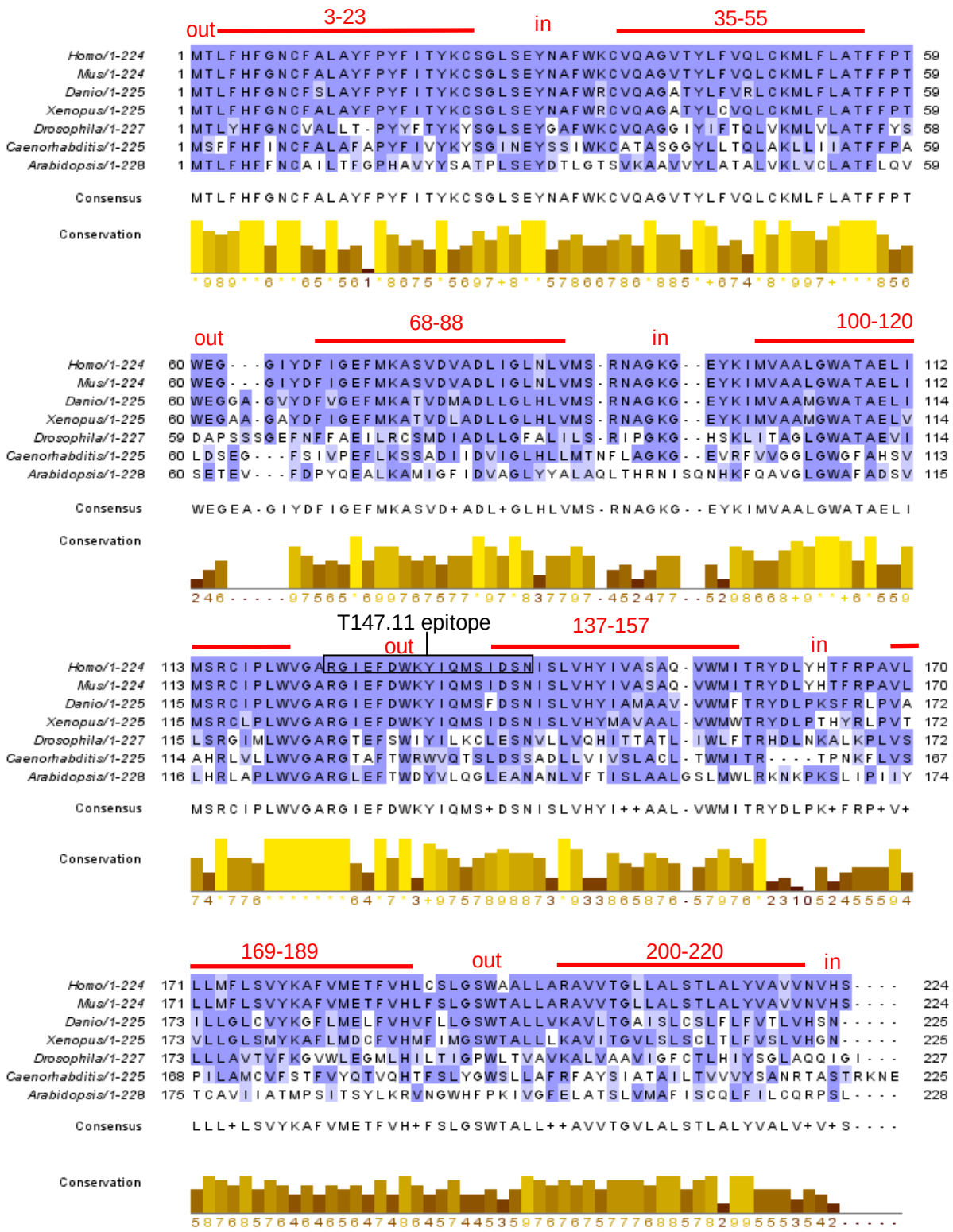

Fig. 31: Alignment of TMEM147 orthologs in multicellular organisms. TMEM147 orthologs from *Homo sapiens, Mus musculus, Xenopus laevis, Danio rerio, Drosophila melanogaster, Caenorhabditis elegans and Arabidopsis thaliana* were retrieved from the Uniprot database and aligned using the clustalw2 program. The result was visualized using Jalview, and topology prediction data (see section 2.3) were integrated. Red bars indicate the position of transmembrane domains, 'out' marks aa predicted to be ER luminal and 'in' marks aa predicted to be exposed to the cytosol. Highlighted in dark blue are aa that are identical to human TMEM147 at the respective position, highlighted in light blue are aa that are similar (e.g. hydrophobic). In addition, a consensus sequence was generated and brown/yellow bars indicate the degree of conservation at the respective position from 0 (0 %) to * = 10 (100 %). In addition, the epitope used to generate the T147.11 antibody is indicated.

The high degree of Nicalin, NOMO, and TMEM147 conservation indicated that also their interaction might be conserved. This was tested by stably expressing a myc-tagged version of zebrafish (zf) TMEM147 in human HEK293T cells followed by co-immunoprecipitation and immunoblotting studies. Indeed, zfTMEM147 precipitated endogenous human NOMO and Nicalin (Fig. 32A). In addition, stable zfNicalin expression resulted in the replacement of endogenous human Nicalin and in the stabilization of endogenous human TMEM147 as well as NOMO (Fig. 32B; note that zebrafish Nicalin runs at a higher molecular weight than its human counterpart and that the amount of overexpressed zfNicalin is underestimated due to a lower affinity of the antibody). These results strongly suggested that the interaction of TMEM147 with the Nicalin-NOMO complex is evolutionary conserved.

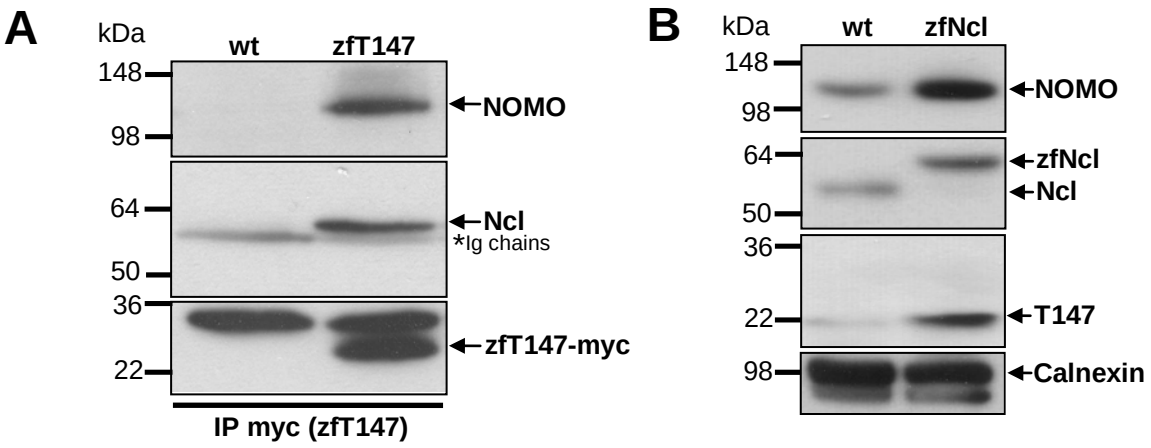

Fig. 32: Zebrafish TMEM147 (zfT147) interacts with human complex partners. A) Immunoprecipitation of myc-tagged zfTMEM147 from overexpressing HEK293T cells resulted in the specific enrichment of endogenous human Nicalin (Ncl) and NOMO. B) The stable expression of zfNicalin in HEK293T cells results in the disappearance of endogenous human Nicalin and in the elevation of NOMO and TMEM147 expression. Note that the amount of overexpressed zfNicalin is underestimated due to a lower affinity of the antibody and that zfNicalin migrates slightly higher than human Ncl (see also Fig. 33).

2.8 TMEM147, like Nicalin and NOMO, is ubiquitously expressed

Nicalin and NOMO transcripts and proteins have been found in immortalized cell lines derived from many different human tissues such as kidney, breast, skin, pancreas, liver, uterus or brain (Haffner et al. 2004, Haffner et al., 2007). For TMEM147, expression databases such as GeneNote indicated a ubiquitous expression in human tissues. Therefore, an immunoblot analysis was performed using several human and non-human cell lines originating from a variety of different tissues (Fig. 33; for details see figure legend). Similar to the widely expressed ER chaperone Calnexin (bottom panel), TMEM147, Nicalin, and NOMO immunoreactivities were found in all cell lines analyzed. Thus, a Nicalin/NOMO/TMEM147 complex is presumably present in all tissues. Between cell lines,

only minor differences in the expression levels of the complex were observed. The amounts of NOMO, Nicalin, and TMEM147 were roughly, but not absolutely, proportional supporting the idea of a coordinate expression of the three complex partners (see section 2.4). The minor discrepancies (e.g., high Nicalin, but relatively low TMEM147 and NOMO levels in MDCK cells) might be explained by cell-type specific differences in transcription and/or protein turnover rates. For an unknown reason, human Nicalin migrates faster in an SDS-PAGE than the dog (MDCK cells) or mouse (P19, 3T3, N2A cells) protein, although protein Nicalin (precursor) size is 563 aa and two predicted glycosylation sites are present in all three species. Possible explanations would be differences in the extent of glycosylation or precursor protein processing between the species. Also splice variants may occur, although this is not supported by database entries. Alternatively, a partial folding despite the denaturing conditions of the SDS-PAGE may alter the running behavior of either human or non-human Nicalin.

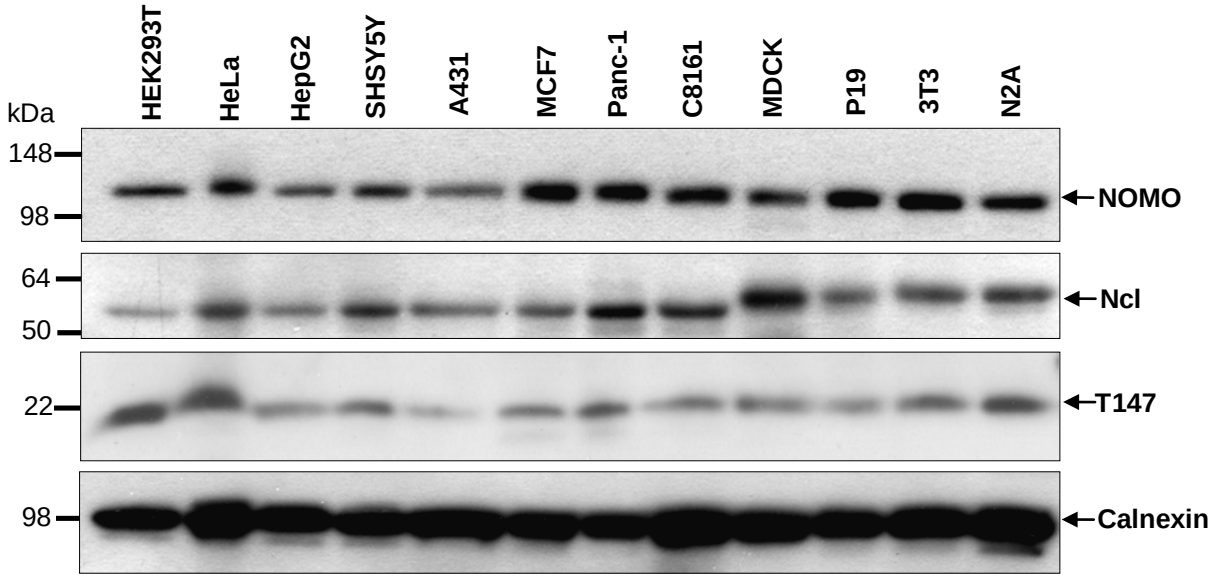

Fig. 33: TMEM147, like Nicalin and NOMO, is widely expressed in human and non-human cell lines. Membrane protein lysates were analyzed by immunoblotting using specific NOMO, Nicalin, and TMEM147 antibodies. As a control, expression levels of the ER chaperon Calnexin are shown. HEK293T, human embryonic kidney cells; HeLa, human epithelial cervical cancer cells; HepG2, human hepatocellular liver carcinoma cells; SHSY5Y, human neuroblastoma cells; A431, human epidermoid carcinoma cells; MCF7, human breast adenocarcinoma cells; Panc-1, human pancreatic carcinoma cells; C8161, human melanoma cells; MDCK, Madin-Darby canine kidney epithelial cells; P19, mouse embryonic carcinoma cells; 3T3 mouse fibroblast cells; N2A, mouse neuroblastoma cells.

During zebrafish development *nicalin* and *nomo* mRNAs are expressed maternally and throughout early embryonic stages, in agreement with their proposed role in Nodal signaling (Haffner et al., 2004). A continuous expression of Nicalin and NOMO proteins from the fertilized egg until 5 day old larvae could be confirmed by an immunoblot analysis using zebrafish total protein lysates (Fig. 34A). Unfortunately, TMEM147 levels were under the detection limit of the T147.11 antibody in these lysates. To analyze the expression pattern of

tmem147 mRNA, *in situ* hybridization was performed in fixed embryos at different stages. As representative results, the stainings for 4-cell, 64-cell, 12 hours and day 2 (48 hours) embryos are shown. The lack of a labeling with the sense probe demonstrates the specificity of the antisense probe (Fig. 34B). A maternal and zygotic expression of *tmem147* mRNA was detected. At 12 hours and 2 days post fertilization no tissue- or organ-specific but rather ubiquitous expression was observed. Similar spatiotemporal expression patterns have been shown for zfNicalin and zfNOMO (Haffner et al., 2004) further suggesting that the interaction between TMEM147 and Nicalin/NOMO is functionally relevant.

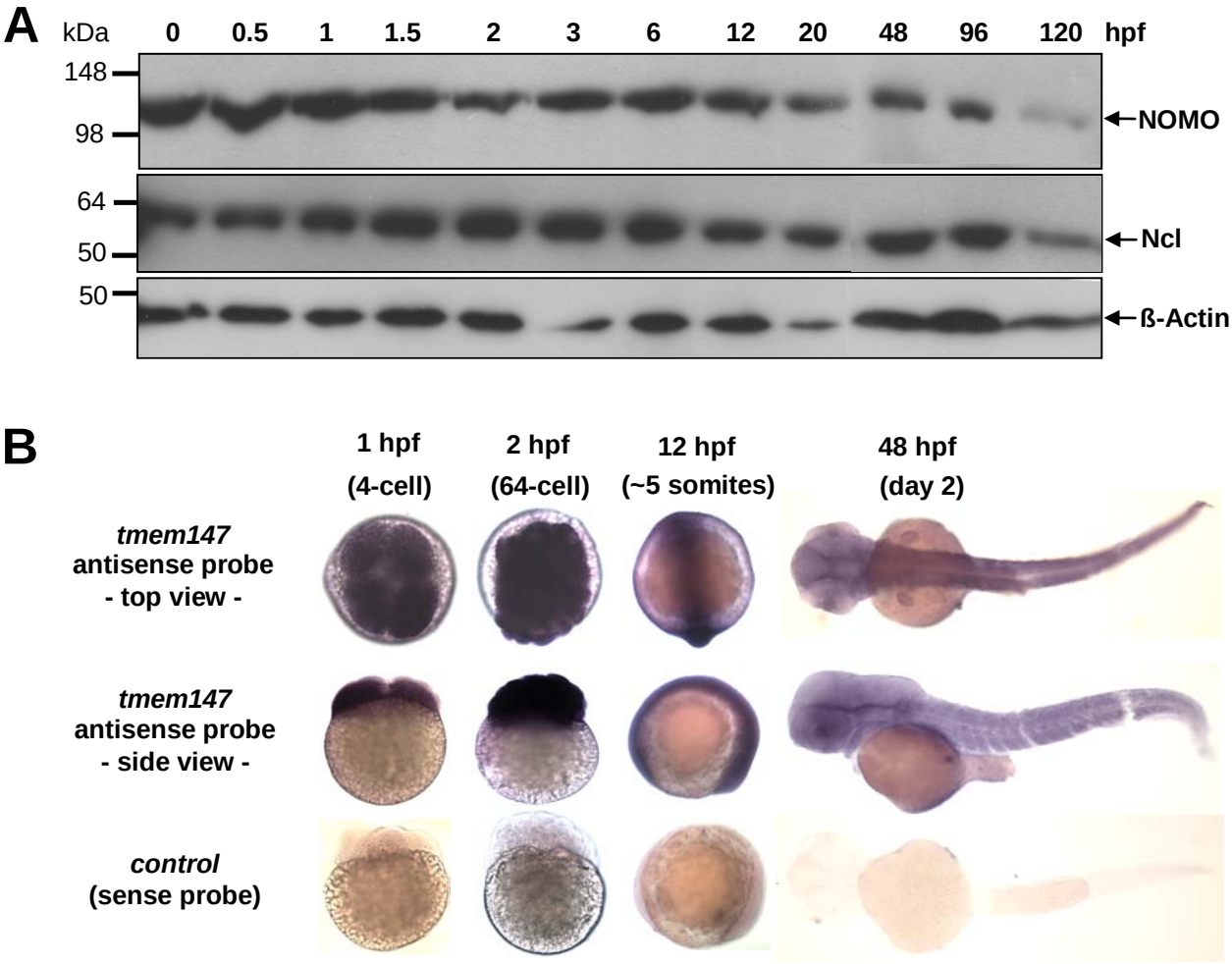

Fig. 34: Nicalin, NOMO and TMEM147 are widely expressed in zebrafish development. A) Time-course of Nicalin, NOMO and TMEM147 protein expression during zebrafish embryonic development until day 5 post fertilization, analyzed by immuboblotting. Total zebrafish protein lysates were used (see section 4.8.3). A continuous expression of Nicalin and NOMO was observed. ß-actin was used as a loading control. B) *In situ* hybridization of *tmem147* mRNA in fixed zebrafish embryos was performed at different stages, represented here by the stainings for 4-cell, 64-cell, 12 hours, and day 2 embryos. A maternal expression (4-cell stage) and ubiquitous zygotic expression of *tmem147* mRNA was revealed. The lack of a labeling with the sense probe demonstrated the specificity of the antisense probe. (hpf, hours post fertilization)

2.9 Towards the Nicalin interactome using SILAC

In the experiments described so far, TMEM147 could be identified as a novel core component of the Nicalin-NOMO complex. Although the combined molecular weight of the three proteins is in agreement with the native size of the complex (Haffner et al., 2007), the existence of additional components cannot be ruled out. Moreover, the identification of TMEM147 did not lead to a better understanding of the cellular function of the complex, which still remains elusive. Therefore, it is of high importance to identify additional binding partners, which might represent either further complex components or functionally important transient interactors. Such proteins are difficult to find because they might be very small or bind too transiently to be detected by conventional purification and staining methods. To overcome this problem, the possibility was explored to analyze the complete Nicalin interactome by a mass spectrometry approach. Due to its high sensitivity, it is the method of choice to identify even minute amounts of a protein in a sample. However, it also carries the risk of detecting a high percentage of false positives, mainly because a quantitative comparison between different measurements, e.g. sample and control, is very difficult. To avoid this problem, a technology was used which allows the analysis of two samples in a single measurement. SILAC (stable isotope labeling using amino acids in cell culture) is a technique based on the metabolic labeling of cellular proteins in cultured cells with ‘heavy’ stable isotopes which can be distinguished from their natural counterparts by their higher masses (Ong et al., 2002). This allows a quantitative comparison of the proteome from cells grown in the presence of heavy isotope-labeled amino acids with the proteome from control cells grown in the absence of heavy isotopes. Thus, the distinction between true and artificial hits becomes much more precise (Ong et al., 2002). To identify additional interactors of the Nicalin-NOMO complex, HEK293T/Ncl-myc cells were isotope-labeled for two weeks by cultivation in lysine/arginine-free medium supplemented with 5,5,6,6-D_4-lysine and $^{13}C_6$-arginine (see section 4.4.3). Control HEK293T cells were cultured in medium supplemented with unlabeled lysine and arginine. Anti-myc-immunoprecipitations from large-scale membrane protein preparations from wild-type and Nicalin-myc expressing cells were performed separately. After the binding step both samples were combined, the precipitated material eluted, separated on an SDS-gel in a single lane, and stained by Coomassie Blue. The gel lane comprising the complete molecular weight range was cut into 11 pieces, proteins digested by trypsin, extracted, and subjected to LC-MS/MS analysis (Fig. 35).

As trypsin cleaves peptide bonds after arginine or lysine, all peptides originating from Ncl-myc cells were theoretically labeled with 5,5,6,6-D_4-lysine or $^{13}C_6$-arginine. As a consequence, identified peptides with a heavy/light (H/L) ratio above a certain threshold, in this case 1.8, were considered as true hits (Tab. 2). However, one prerequisite for this

approach is a more or less complete labeling of all cellular proteins and it turned out that even after two weeks of cultivation more than one third of precipitated Nicalin was still unlabeled (~30 % of Nicalin peptides were not labeled 'heavy'). This could be explained by the stability of the Nicalin-NOMO complex, but also by a slowed metabolism of the cells in the medium which contained filtered serum. Therefore, for generating a list of the most significant hits not only the heavy/light (H/L) ratio was taken into consideration, but also by the overall intensity of the MS signals and the overall peptide coverage of the proteins detected, and weighted 1:1:1 (Table 2). As a validation of the approach, NOMO and Nicalin are found at the positions one and two and TMEM147 at position five. About 60 % of the potential interactors in the list and nine of the ten top hits are ER-associated proteins, an indication for the specificity of the approach. According to their known (or putative) function, the majority of the identified proteins can be arranged in functional groups (Tab. 2; discussed in section 3.4). Only few proteins with a destination further downstream of the early secretory pathway were found, and no factors could be specifically linked to Nodal/TGFβ signaling.

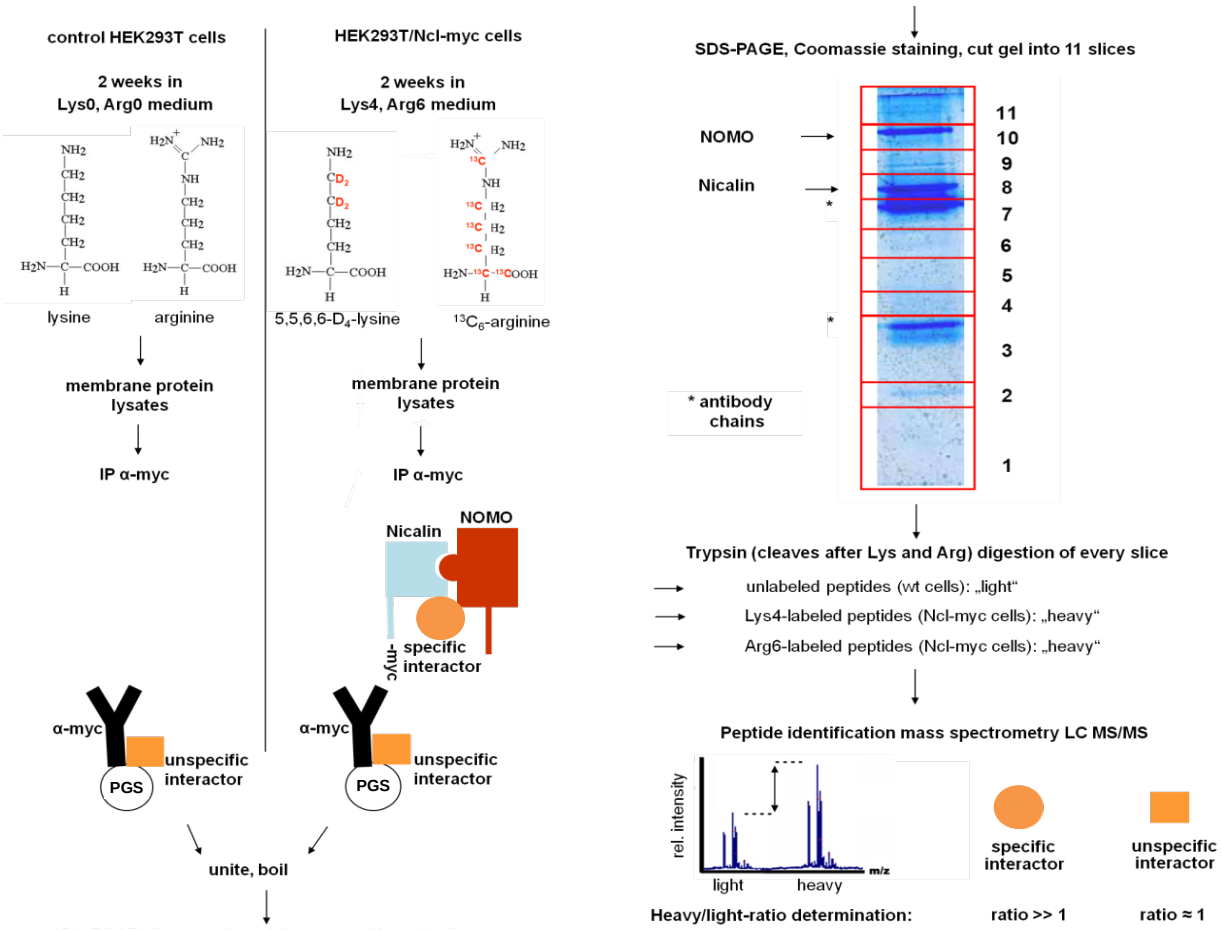

Fig. 35: Work-flow of the SILAC/Nicalin-IP/MS experiment. HEK293T/Ncl-myc and wild-type cells were grown for two weeks in 5,5,6,6-D_4-lysine/$^{13}C_6$ arginine medium and normal medium, respectively. Membrane protein lysates were subjected to an anti-myc IP. After washing, beads with precipitated material from wt and Ncl-myc cells were united and boiled. The sample was run on a NuPAGE 4%-12% Bis-Tris gel (Invitrogen) and stained with Coomassie Blue. The whole protein lane was cut into 11 pieces. Proteins within gel pieces were subjected to trypsin cleavage, extracted, and LC-MS/MS was performed. Peptides originating from Ncl-myc cells were either 5,5,6,6-D_4-lysine (Lys4) or $^{13}C_6$ arginine (Arg6) labeled. (PGS, protein G sepharose)

# Ø	Protein Name	MW [kDa]	Ratio H/L	Cover. [%]	Intensity	# Rat.	# Cov.	# Int.	Protein context
1	NOMO1/2/3	139.4	3.64	60.3	1843000000	16	2	2	ER NicNO complex
2	Nicalin	63.0	2.88	66.1	2982000000	24	1	1	ER NicNO complex
3	BNIP1	26.1	4.05	36.4	55750000	12	8	8	ER SNARE
4	Erlin1/2*	37.8	5.38	31.0	25031000	6	14	14	ER lipid raft
5	TMEM147	25.3	4.38	30.4	41647000	10	15	10	ER NicNO complex
6	p31	29.3	3.71	44.0	10610000	15	3	23	ER SNARE
7	SERCA2B*	114.8	4.42	22.0	30676000	9	24	13	ER Ca^{2+} ATPase
8	VDAC2*	36.3	2.60	31.6	71940000	32	12	5	Mitochondrium
9	Sec22b*	24.6	3.38	22.9	44307000	18	23	9	ER SNARE
10	Grp78/BiP	72.4	2.22	41.8	116560000	49	4	4	ER chaperone
11	Rap2b	20.5	3.05	31.7	9676800	20	11	27	PM (lipid raft)
12	Flotillin 1	47.4	2.69	19.7	117230000	29	28	3	PM lipid raft
13	AAA domain prot. 1	40.7	2.88	24.7	10147000	25	21	26	ATPase hexamer
14	Flotillin 2	41.7	2.11	32.7	58639000	56	10	7	PM lipid raft
15	Ddost subunit 48 kDa*	50.8	2.52	20.2	35475000	35	27	12	ER translocation
16	SRPR subunit β	29.7	2.37	39.5	9540300	42	5	28	ER translocation
17	VCP/P97*	89.2	2.70	19.1	19637000	28	30	18	ER ATPase
18	Syntaxin 18	38.7	22.56	11.6	10533000	2	54	24	ER SNARE
19	Emerin	29.0	2.91	27.6	3279300	23	17	44	Nuclear membrane
20	Rab1B	22.2	2.21	24.4	24879000	50	22	15	ER/Golgi vesicles
21	VDAC1*	30.6	2.03	27.0	70780000	64	18	6	Mitochondrium
22	60S P0	34.3	1.90	38.5	41571000	73	6	11	Ribosome
23	SPC subunit 22 kDa	20.8	3.83	21.3	2163200	14	25	52	ER translocation
24	NRas	21.2	2.96	24.9	2187000	21	20	51	Golgi/PM GTPase
25	Reticulocalbin 2	36.9	5.15	19.2	1667700	8	29	59	ER Ca^{2+} binding
26	SPC subunit 18 kDa	20.6	3.27	15.1	4438000	19	44	33	ER translocation
27	RhoA	21.8	2.10	36.3	6967500	57	9	31	GTPase cytoskelet.
28	40S S12	14.4	2.18	29.0	8617400	52	16	30	Ribosome
29	HLA I. A-3 α chain	36.9	2.38	16.9	11618000	41	37	22	HLA complex
30	NSF	82.7	2.64	15.6	9239900	31	42	29	ATPase (SNAREs)
31	Rab35	23.0	2.56	12.9	19236000	33	50	19	GTPase PM
32	Sec61 subunit β	9.8	2.50	37.9	1226900	36	7	63	ER translocation
33	Rab9A	22.8	1.97	25.4	18397000	68	19	20	GTPase ubiquitous
34	Peroxisom. Prot. 11A	28.4	22.61	8.1	2693200	1	64	47	Peroxisome
35	TM protein 70	29.0	2.40	15.8	4370000	40	40	34	Mitochondrium
36	Sec61 subunit α1	52.3	2.34	12.6	12884000	44	51	21	ER translocation

Tab. 2: **Potential interactors identified by the SILAC experiment**. Hits were listed according to their heavy/light (H/L) peptide ratio, the degree of protein sequence coverage by the detected peptides (Cover. [%]), and the overall intensity of the signals obtained from the particular protein (Intensity), weighted 1:1:1. In addition, a ratio of 1.8 was used as a cut-off to exclude unspecific interactions. For each criterium, a ranking (#) was obtained, eventually the overall position of the hits was calculated as an average (# Ø). Abbreviations: MW, molecular weight; BNIP1, BCL2/adenovirus E1B 19kDa interacting protein 1; Erlin1/2, ER-lipid enriched protein 1/2; SERCA2B, sarcoplasmic/endoplasmic reticulum calcium channel 2B; VDAC1/2, voltage-dependent ion channel 1/2; Grp78, glucose-related protein; BiP, binding protein; Rap2b, Ras-associated protein 2b; AAA domain prot. 1, AAA domain containing protein 1; Ddost, dolichyl-diphosphooligosaccharide-protein-glycosyltransferase; SRPR, signal recognition particle receptor; VCP, valosine-containing protein; Rab1B, Ras associated binding protein; 60S P0, 60S ribosomal protein 0; SPC, signal peptidase complex; NRas, neuroblastoma RAS viral oncogene homolog; RhoA, Ras homolog A; HLA I, human leukocyte antigen I; NSF, N-ethylmaleimide-sensitive fusion protein; Rab 35/9A, Ras associated binding protein 35/9A; Peroxisom. Prot. 11A, peroxisomal protein 11A, TM protein 70, transmembrane protein 70s; NicNO, Nicalin-NOMO; SNARE, soluble NSF attachment receptor; PM, plasma membrane. Proteins denoted with * were also identified by a recent analysis of the γ-secretase interactome (Wakabayashi et al., 2009), indicating that they might be common contaminations and/or general interactors of ER membrane protein complexes.

Four members of the SNARE (soluble NSF attachment receptor) family of vesicle fusion factors (Syntaxin 18, BNIP1, Sec22b and p31) were identified as potential Nicalin interactors with a high ratio, coverage and intensity. They have been shown to localize to the ER and to form a complete SNARE complex (Aoki et al., 2008). This Syntaxin 18 complex has been proposed to be involved in homotypic and heterotypic membrane fusion events regulating ER homeostasis as well as vesicle trafficking between the ER and downstream compartments of the secretory pathway (Okumura et al., 2006; Hatsuzawa et al., 2009; Iinuma et al., 2009). It is regulated by the vesicle-fusing ATPase NSF (N-ethylmaleimide-sensitive factor), which is also present in the hit list. The interaction was confirmed by immunoprecipitation of Nicalin, NicalinΔC, NOMO and subsequent immunoblotting (Fig. 36). Syntaxin 18, BNIP1, Sec22b and p31 were all detected in the precipitated material, but the amount was considerably less when compared to NOMO indicating a substoichiometric ratio. In addition, the expression of none of these proteins was elevated in Nicalin-myc cells (Fig. 36, input lanes) further suggesting a transient interaction.

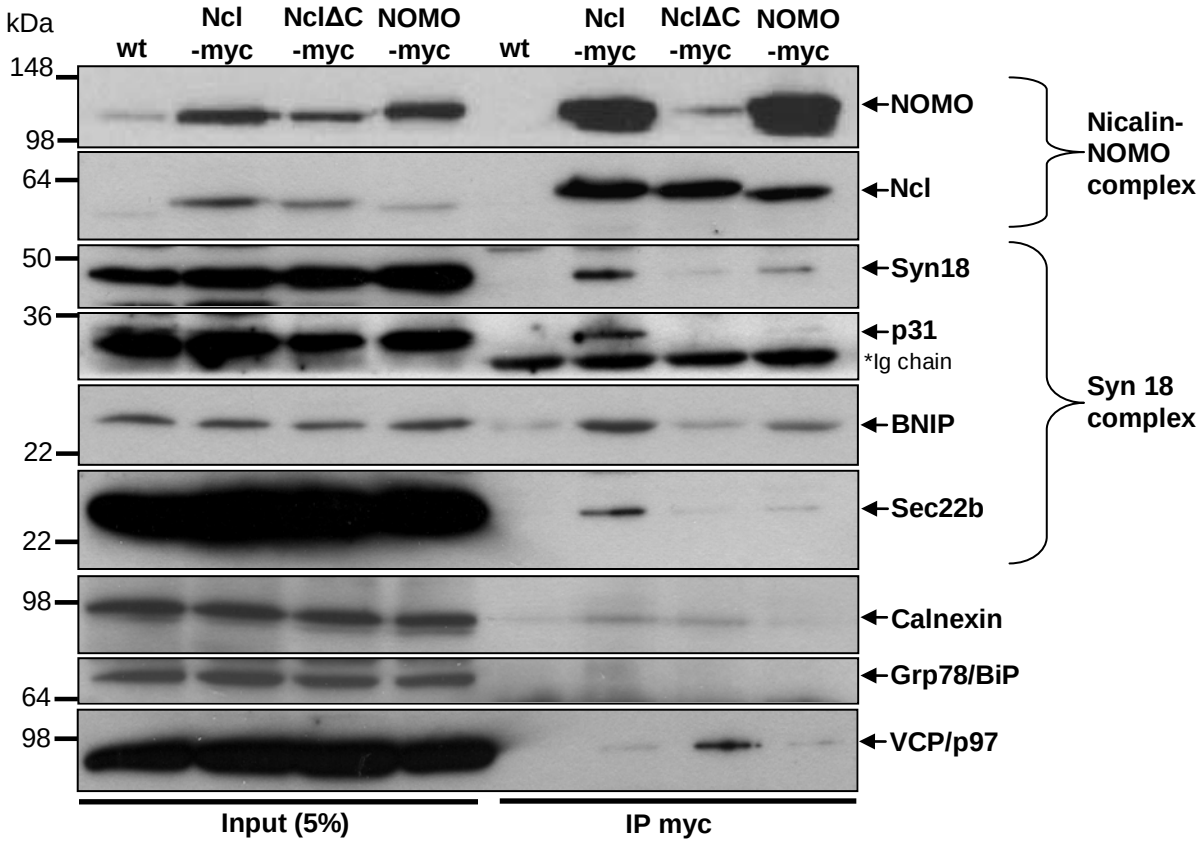

Fig. 36: Co-IP/immunoblotting indicates an interaction between the Nicalin-NOMO complex and ER SNAREs. Anti-myc IPs were performed from membrane protein lysates of wild-type (wt) and stably transfected HEK293T cells. Co-isolation of the ER-SNAREs is proportional to the amount of Nicalin-NOMO complex precipitated. While complex levels are elevated by Nicalin (Ncl) overexpression, NOMO-overexpressing cells only contain wild-type complex levels. C-terminally truncated Ncl-ΔC apparently is partially deficient in NOMO and ER-SNARE binding. Calnexin, Grp78/BiP and VCP/p97 specific antibodies were used as controls.

Two observations strongly support the idea that this interaction is specific and occurs between the entire complexes: (1) in NOMO-myc cells, which contain only wild-type levels of the Nicalin-NOMO complex, the amount of SNARE proteins detected in the immunoprecipitate was strongly reduced, (2) in Nicalin-ΔC cells no specific interaction could be detected, in agreement with our finding that this truncated protein is at least partially defective in complex formation (reduced NOMO binding, see Fig. 36; reduced NOMO and TMEM147 stabilization, see Fig. 27 and 28).

To corroborate the binding results, the subcellular localization of Nicalin, Syntaxin 18 and BNIP1 was compared to that of Nicalin in HeLa cells by immunofluorescence microscopy. Syntaxin 18 with an N-terminal FLAG-epitope tag and BNIP1 with a C-terminal V5-epitope tag were expressed and co-staining was performed with endogenous Nicalin (Fig. 37). Overexpression of Syntaxin 18 and BNIP1 leads to large aggregates at the endoplasmic reticulum, likely as a result of an increased fusion activity of ER membranes (Hatsuzawa et al., 2000; Nakajima et al., 2004). This observation was confirmed in the HeLa cells Fig. 37, indicated by arrows) and endogenous Nicalin almost perfectly co-localized with Syntaxin 18 and BNIP1 within the aggregates as well as in other regions of the cell. A potential physiological role of the interaction is discussed in section 3.4.

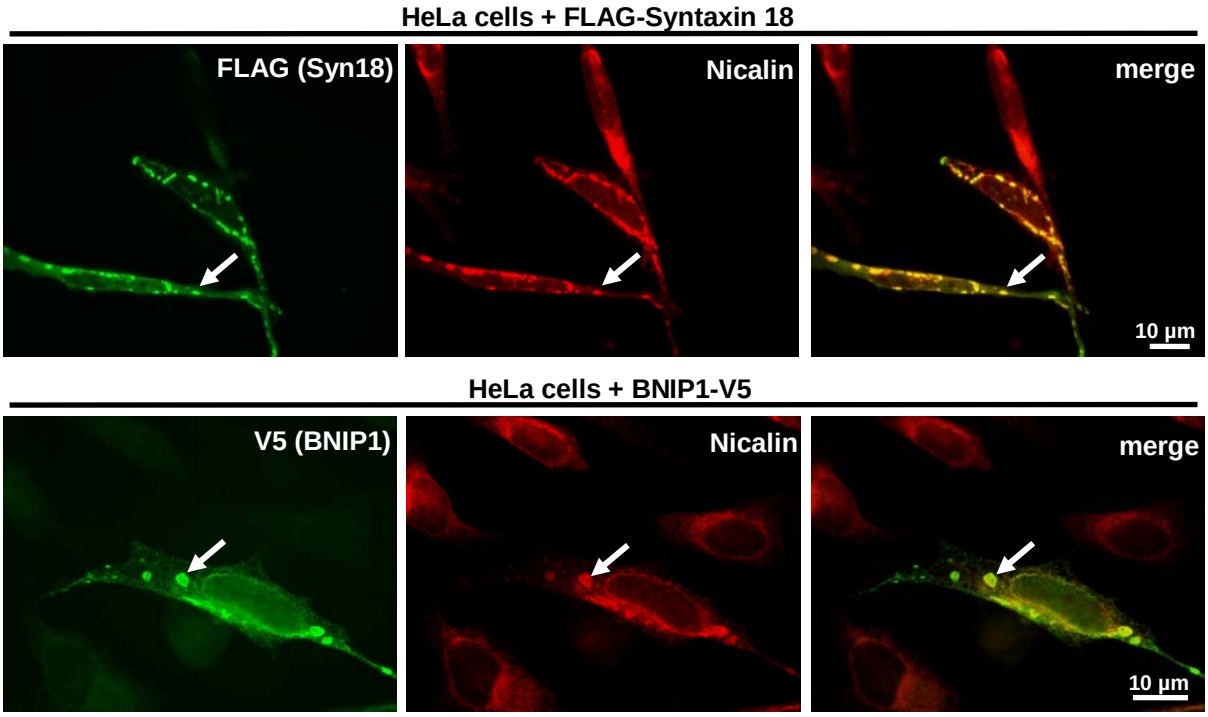

Fig. 37: Nicalin and ER SNAREs co-localize. Immunofluorescence microscopy of transfected HeLa cells stained with anti-tag antibodies recognizing the transfected SNARE proteins and with a monoclonal anti-Nicalin antibody. Overexpression of Syntaxin18 and BNIP1 leads to aggregation of ER membranes (indicated by arrows), as reported by Hatsuzawa et al. (2000) and Nakajima et al. (2004). Endogenous Nicalin co-localizes with both proteins in these structures as well as in normal ER. Costaining was also observed between Nicalin and Sec22b or p31 (not shown).

3. Discussion

3.1 A novel core component of the Nicalin-NOMO complex

In the present work the possibility was explored that the Nicalin-NOMO membrane protein complex, whose composition and molecular function is only poorly understood, may contain additional protein components, preferably in the low-molecular-weight range. Previously, a Nicalin affinity purification approach had led to the identification of NOMO and the use of a modified procedure now allowed the isolation of a ~22-kDa protein from human HEK293T cells, which could be identified as TMEM147 by mass spectrometry analysis. TMEM147 is a novel and uncharacterized polytopic membrane protein predicted to be largely embedded within the membrane. A variety of data are presented which leave little doubt about the hypothesis that TMEM147 is a genuine component of the Nicalin-NOMO complex:

1. The co-immunoprecipitation analysis revealed a roughly stoichiometric interaction between Nicalin, NOMO, and TMEM147.
2. All three proteins are conserved in multi-cellular organisms to a similar extent and zebrafish and human proteins interact in cell culture.
3. Similar to Nicalin and NOMO, TMEM147 appears to be ubiquitously expressed as indicated by immunoblot analysis of different cell lines and mRNA *in situ* hybridization in zebrafish embryos.
4. No transport of TMEM147 beyond the early secretory pathway was observed by immunofluorescence microscopy or density gradient centrifugation, in agreement with the intracellular localization of Nicalin and NOMO.
5. Similar to Nicalin, the overexpression of TMEM147 leads to the replacement of the endogenous protein demonstrating that the TMEM147 steady-state levels are tightly regulated.
6. The RNAi-mediated downregulation of TMEM147 results in the reduction of Nicalin and NOMO expression and *vice versa* strongly suggesting that all three factors stabilize each other within the complex (see also section 3.3).
7. Nicalin controls the expression levels of both TMEM147 and NOMO by a post-transcriptional mechanism (see also section 3.3).

Although no other major Nicalin interactor was found and the combined molecular weights of Nicalin (~60 kDa), NOMO (~130 kDa), and TMEM147 (~22 kDa) are in good agreement with the native size of the complex (200-220 kDa), the existence of additional complex

components, which might be of low molecular weight or not elevated in Nicalin-overexpressing cells, cannot completely be ruled out.

TMEM147 shows no significant homology to any other known protein nor were functional domains detected. Thus, a possible function could not be inferred from its amino-acid sequence. According to topology prediction programs, TMEM147 contains seven transmembrane domains and is largely embedded within the hydrophobic environment of the membrane. Its N-terminus is predicted to reside within the ER lumen and its C-terminus to face the cytosolic side of the membrane. Thus, size and topology are highly reminiscent of the γ-secretase component APH-1 and a variety of data presented in this thesis suggest that TMEM147 and APH-1 might play at least partially similar roles in the assembly of their respective complexes. In any case, one consequence of the identification of TMEM147 as a third component of the complex is that the Nicalin-NOMO complex does not, as previously thought, comprise only two transmembrane domains, but a total of nine (Fig. 38). Thus, a contribution of the transmembrane regions of the complex in addition to the prominent Nicalin and NOMO luminal domains to the function of the complex now appears more likely.

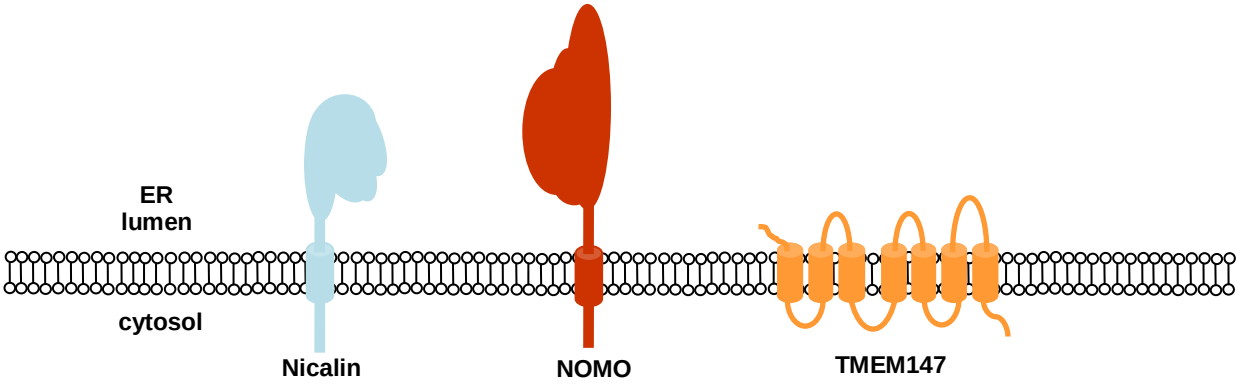

Fig. 38: Schematic illustration of the components of the Nicalin-NOMO complex. Nicalin and NOMO are type-I transmembrane proteins. The 7 transmembrane topology of TMEM147 was predicted by the PRODIV-TMHMM algorithm as a part of the TOPCONS server and is reminiscent of the γ-secretase component APH-1.

3.2 Nicalin-NOMO complex and γ-secretase assembly occur stepwise

For γ-secretase, a stepwise mode of complex assembly and subsequent transport has been proposed (reviewed by Kaether et al., 2006; Spasic and Annaert, 2008). Different studies agree on the initial formation of a Nicastrin (NCT)/APH-1 subcomplex (Hu and Fortini, 2003; LaVoie et al., 2003), which is stable even in the absence of Presenilin (PS) and PEN-2 (Shirotani et al., 2004) and more resistant to detergent dissociation than other subcomplexes (Fraering et al., 2004). In the prevailing scenario for the following steps, the nascent PS holoprotein is stabilized in a high-molecular-weight inactive PS/NCT/APH-1 complex, until PEN-2 triggers endoproteolysis of PS and ER export of the complex (Kim et al., 2004; Capell et al., 2005). The assembled γ-secretase continues its way through the secretory pathway and reaches its final destinations, the plasma membrane and the late secretory pathway compartments (Kaether et al., 2002; Capell et al., 2005; Chyung et al., 2005).
In contrast to γ-secretase, no transport of the Nicalin-NOMO complex beyond the early secretory pathway could be observed. Therefore, the assembly mode of the Nicalin-NOMO complex does not reflect the need to regulate the ER export of the complex, as it may be the case for γ-secretase. Nevertheless, a hierarchical assembly of the complex is indicated by the following observations:

1. Upon induced expression of Nicalin the stabilization of NOMO appears to precede that of TMEM147.
2. A subcomplex consisting only of Nicalin and NOMO can be immunoisolated from cell lysates when Nonidet P-40 is used as a detergent.
3. Whereas the interaction between Nicalin and NOMO is most likely mediated by their ectodomains, TMEM147 appears to bind to Nicalin's transmembrane domain.

These findings fit into a model where the formation of a Nicalin-NOMO subcomplex, mediated by their luminal domains, initiates complex assembly, followed by the addition of TMEM147 (Fig. 39). Apparently, the Nicalin transmembrane domain is essential for TMEM147 binding, but further analysis is needed to test if it is also sufficient. In any case, this mode of TMEM147 binding is analogous to APH-1 in γ-secretase, where the NCT transmembrane domain has been demonstrated to be absolutely required for the NCT/APH-1 interaction (Capell et al., 2003). However, TMEM147 differs from APH-1 in being dispensable for the formation of the Nicalin-NOMO subcomplex, whereas APH-1 is considered a scaffold protein for the assembly of γ-secretase. Another difference is the stability of the Nicalin-NOMO subcomplex in the presence of the detergent NP-40. NP-40 is known to completely disrupt γ-secretase, which is believed to be held together mainly by

interactions between transmembrane domains (LaVoie et al., 2003). This difference can be explained by the two large ER luminal ectodomains mediating the interaction between Nicalin and NOMO. In contrast, NCT is the only component with a prominent luminal domain in γ-secretase.

Because of the different subcellular localizations of mature γ-secretase and the Nicalin-NOMO complex, they use different targeting mechanisms. During complex assembly, immature γ-secretase is kept in the ER by retention signals which might be located in the transmembrane domain 1 of PEN-2 (Fassler et al., 2010), in the ER-luminal Presenilin C-terminus close to or even embedded within the membrane (Kaether et al., 2004) and in the Presenilin transmembrane domain 4 (Fassler et al., 2010). After completion of the assembly, these signals are believed to be masked allowing the transport of fully assembled γ-secretase to the plasma membrane (Kaether et al., 2004; Kaether et al., 2006; Fassler et al., 2010). In contrast, the Nicalin-NOMO complex is kept within the ER even in its fully assembled form. The Nicalin C-terminus, which contains a motif resembling a classical ER retention signal, was shown to be sufficient to mediate the ER retention/retrieval of a plasma membrane protein. However, NicalinΔC lacking this motif still localizes to the ER demonstrating that the *in vivo* situation might be more complex.

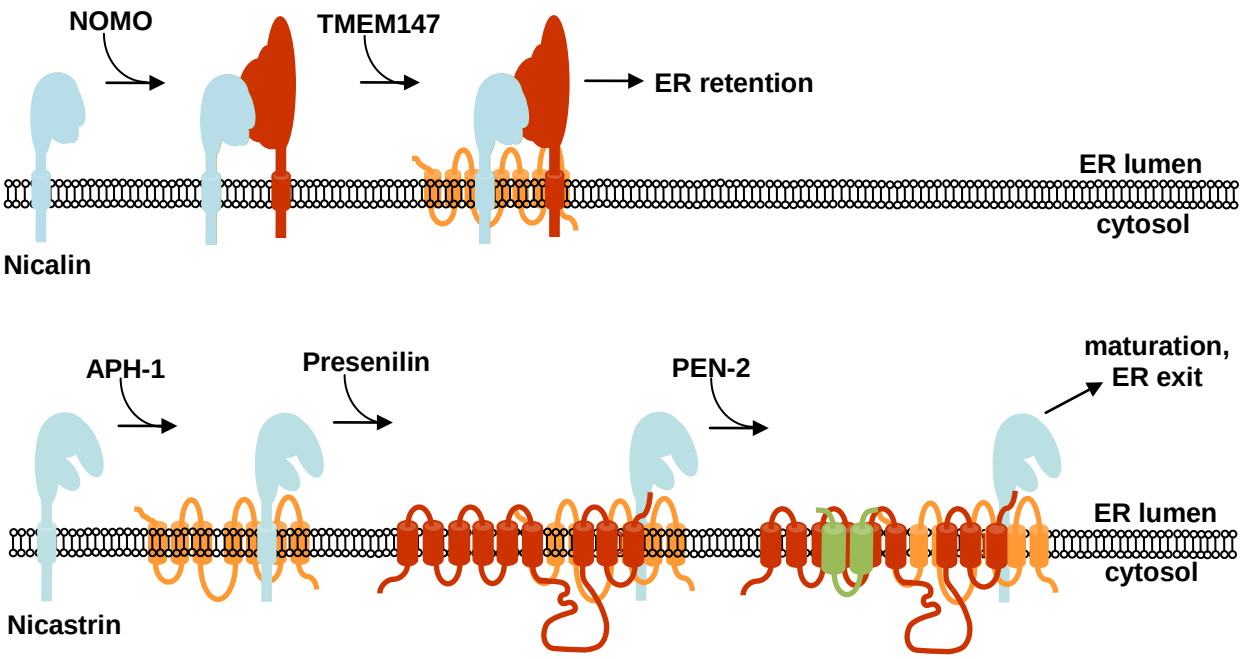

Fig. 39: Stepwise assembly of Nicalin-NOMO complex and γ-secretase. A simplified model. The assembly of the Nicalin-NOMO complex (top) appears to be triggered by the binding of NOMO to Nicalin, likely mediated by their luminal domains, followed by the addition of TMEM147 in the transmembrane region. The heterotrimeric complex is retained in the ER by an unknown mechanism (the illustrated interactions between TMEM147 transmembrane domains and Nicalin/NOMO are just an example for a possible interaction). γ-secretase assembly (bottom) is initiated by the formation of a Nicastrin/APH-1 intermediate, which incorporates the Presenilin holoprotein. Finally, the binding of PEN-2 triggers the ER exit of the whole complex. On its way through the secretory pathway, γ-secretase undergoes maturation, e.g. Presenilin autoproteolysis and complex glycosylation of Nicastrin. The γ-secretase illustration integrated knowledge about the exact molecular interactions within the complex (adapted from Kaether et al. 2006). In this simplified model neither all interactions in the complex nor details about the three dimensional structure of γ-secretase are reflected.

3.3 Nicalin is the master regulator of the Nicalin-NOMO complex

For the assembly of γ-secretase, a concept was proposed in which individual components are stabilized by complex formation and excess molecules are rapidly degraded (Thinakaran et al., 1997). This hypothesis was confirmed by a variety of studies which demonstrated that downregulation of one complex component results in the destabilization of other components (see section 1.1.2). However, only the co-expression of all four components leads to an increase in catalytic activity (Edbauer et al., 2003; Hu and Fortini, 2003; Kimberly et al., 2003) indicating that under wild-type conditions they are not produced in significant excess. Thus, there appears to be no general rate-limiting factor of the γ-secretase complex and it has been proposed that the least abundant complex member may vary by cell type (Kimberly et al., 2002).

A mutual stabilization mechanism has also been demonstrated for Nicalin and NOMO (Haffner et al., 2007) and now been extended to TMEM147 (this thesis). TMEM147 is unstable in the absence of one of its complex partners and its own downregulation results in the reduction of Nicalin and NOMO protein levels. In contrast to γ-secretase, this mutual stabilization has been suggested to function as specific regulatory mechanism in the case of the Nicalin-NOMO complex (Haffner et al., 2007). The synthesis of Nicalin, like that of all γ-secretase components, appears to be strictly regulated, whereas NOMO is produced in excess. The data presented in this thesis show that this is also the case for TMEM147. The enhanced expression of Nicalin is sufficient to increase the cellular levels of both NOMO and TMEM147 by a post-transcriptional mechanism. In contrast, overexpression of TMEM147 and NOMO, either alone or in combination, does not elevate endogenous Nicalin levels nor the levels of the respective other complex partner. The existence of a pool of excess NOMO and TMEM147 molecules under exogenous conditions is directly shown by proteasome inhibition in wild-type cells leading to an increase in NOMO and TMEM147, but not Nicalin expression. This result in addition indicates that excess complex components are degraded by the proteasome.

Thus, a special role can be assigned to Nicalin, which has never been observed for Nicastrin or any other γ-secretase component: No matter how high Nicalin was overexpressed, the other complex components were always found to adapt via stabilization of excess monomers. Nicalin can be considered the rate-limiting factor which binds other complex components and thus triggers complex assembly (Fig. 40).

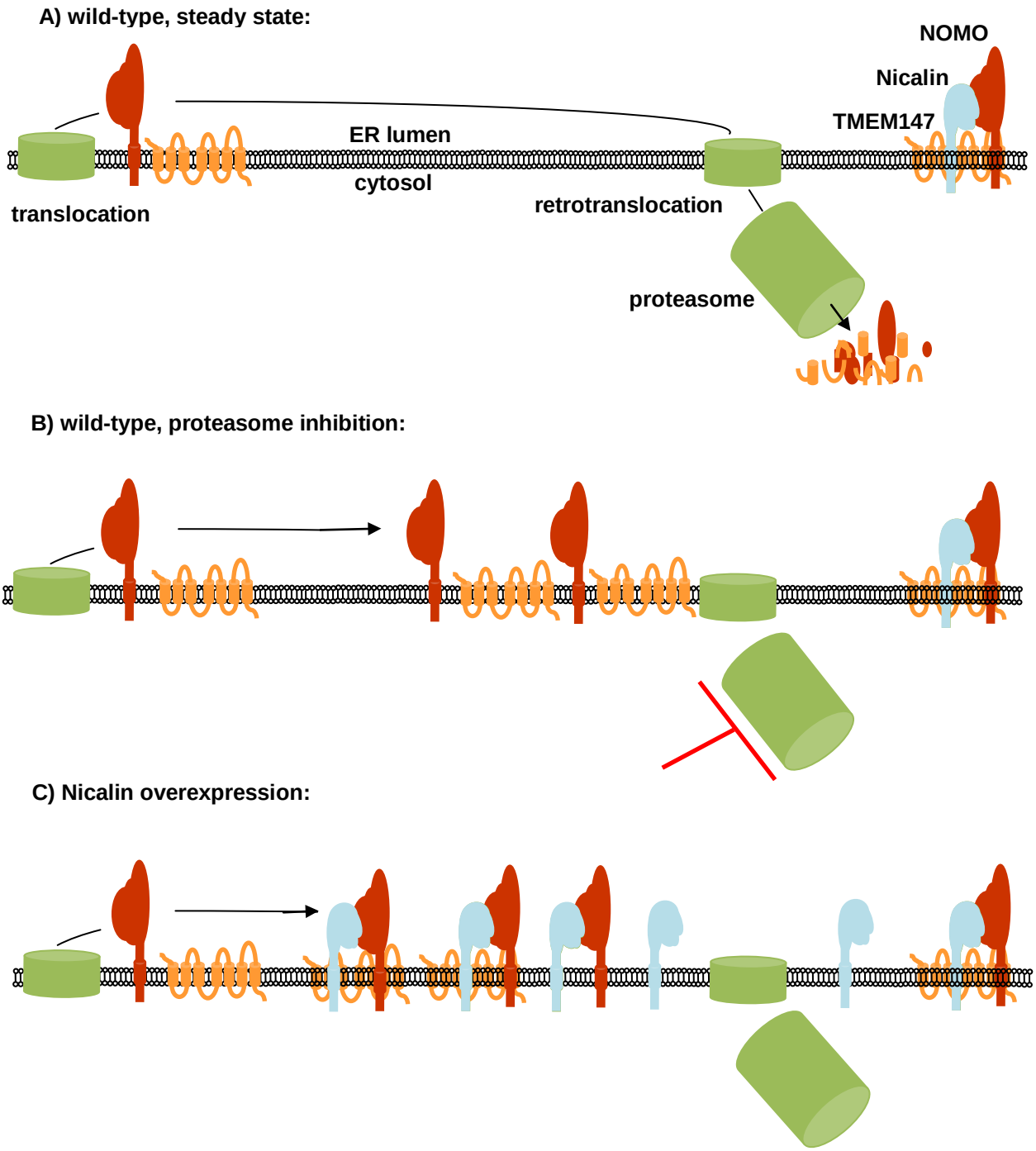

Fig. 40: Nicalin regulates NOMO and TMEM147 expression. A) Under steady-state conditions in wild-type cells, TMEM147 and NOMO excess molecules which do not 'encounter' a Nicalin molecule are rapidly degraded involving retrotranslocation and cytosolic proteasomes (ER associated degradation). B) Upon proteasome inhibition, excess TMEM147 and NOMO monomers are stabilized. C) Nicalin overexpression stabilizes TMEM147 and NOMO by complex formation, thereby preventing their degradation.

This situation offers the cell a potent mode to regulate complex levels solely via Nicalin, which in turn raises the question if there is a transcriptional and/or translational control of Nicalin expression. The possibility that Nicalin and the complex might fulfill a chaperone function in the ER, gave rise to the idea that Nicalin levels may be elevated after ER stress

like the ER ‘heat shock’ chaperones Grp78/BiP and Grp94 (reviewed by Wegele et al., 2004). However, in this work different forms of ER stress conditions failed to induce Nicalin expression. This was in agreement with the inability to identify binding sites for transcription factors that regulate the induction of certain proteins upon ER stress, such as the activating transcription factors 4 or 6 (reviewed by Ye and Koumenis, 2009), in association with the *nicalin* gene (using the PROMO 8.3 program). Instead, a recent study (Myslinski et al., 2006) reported the presence of six binding sites of the transcription factor STAF/ZNF143 in the Nicalin promoter (Fig. 41A), but STAF/ZNF143 binding sites are associated with a variety of human genes without overlapping function (Fig. 41B) and no context for Nicalin-NOMO function could be deduced from this observation. Nevertheless, the finding may be worth further analysis, as the sites are evolutionary conserved (Fig. 41A) and no other human gene possesses such a high number of STAF/ZNF143 binding sites in its promoter region.

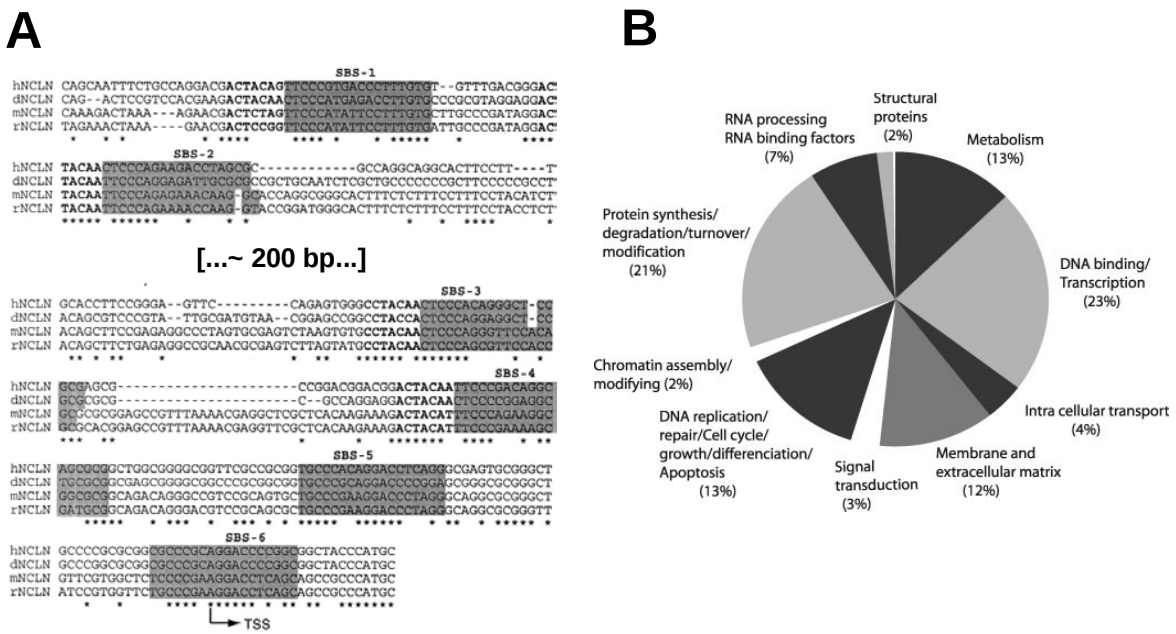

Fig. 41: Cross-species conservation of six STAF/ZNF143 binding sites in Nicalin. A) Multiple sequence alignment of human (*h*), dog (*d*), mouse (*m*), and rat (*r*) *Nicalin* promoter regions performed with ClustalW. Identical nucleotides are denoted with *. The putative STAF/ZNF143 binding sites 1-6 have been highlighted in gray. In addition, an ACTACAN (nucleotide code; N, any nucleotide) submotif, associated with STAF/ZNF143 binding sites 1-4, is in boldface. The transcriptional start site is indicated by an arrow. A gap was introduced, so that ~ 200 bp characterized by low homology are not shown. B) Categorization of the hStaf/ZNF143 target genes. Genes targeted by hStaf/ZNF143, whose function was known or could be inferred, were classified according to the function of the encoded protein. Adapted from Myslinski et al., 2006.

3.4 Analysis of the Nicalin interactome

The Nicalin-NOMO complex has been shown to be involved in the Nodal signaling pathway in zebrafish embryos (Haffner et al., 2004), but the molecular mechanism mediating this effect is unknown. Based on the ER-localization of the complex, two modes of action were conceivable: an influence on the secretion of the ligand Nodal or a regulation of the trafficking of Nodal receptors or co-receptors. However, co-isolation and co-regulation studies using these molecules did not lead to clear results and made an unbiased approach necessary to identify possible interactors which could provide a link between the complex and the Nodal pathway. The approach used to identify NOMO and TMEM147 - Nicalin affinity purification with subsequent protein staining - proved not sensitive enough for the detection of transient interactors. Therefore, the purification was combined with mass spectrometry analysis to identify co-purified proteins. To minimize the detection of false positives, a common problem in mass spectrometry approaches, stable isotope labeling using amino acids in cell culture (SILAC) was used and only hits with a heavy/light ratio above 1.8 were considered true interactors resulting in a list of 36 proteins. To identify the most promising interactors, signal intensity and protein coverage data were included in the analysis in addition to the heavy/light ratio (see Tab. 2). NOMO as well as TMEM147 were among the top hits confirming the suitability of this approach. Its specificity was demonstrated by the fact that nine of the ten top hits were ER-associated proteins. However, none of the potential interactors represented an obvious link to the observed phenotypes from animal studies, i.e. Nodal signaling or nAChR assembly (see sections 1.2 and 3.5).

The most interesting group of proteins on the hit list were four SNARE proteins - Syntaxin 18, BNIP1, Sec22b and p31 - previously shown to form the Syntaxin 18 complex involved in the retrieval of proteins from the Golgi apparatus back to the ER (Hatsuzawa et al., 2000). The interaction between Nicalin and all four members of the SNARE complex was confirmed by co-isolation/immunoblotting and co-localization was demonstrated by immunofluorescence microscopy. An effect on the function of this complex by the Nicalin-NOMO complex could result in alterations in the trafficking of molecules involved in Nodal signaling. Alternatively, the Syntaxin 18 complex might also be responsible for the ER retrieval of the Nicalin-NOMO complex. However, SNARE proteins mediate the fusion of vesicles to target membranes, but are usually not involved in the recruitment and binding of cargo proteins in the respective vesicles (reviewed by Wickner and Schekman, 2008). Adapter proteins, on the other hand, that mediate this recruitment, were not among the hits. In addition, the Syntaxin 18 complex has been attributed other important functions such as ER subdomain organization (Iinuma et al., 2009). Thus, the relevance of this interaction will need further investigation.

Another interesting group among the potential Nicalin interactors were ER-residual proteins implicated in protein translocation through the ER membrane, such as Grp78/Bip, Ddost (dolichyl-diphosphooligosaccharide-protein glycosyltransferase) 48 kDa subunit, SRPR (signal-recognition particle receptor) subunit β, SPC (signal-peptidase complex) 22 kDa subunit, SPC (signal-peptidase complex) 18 kDa subunit, the translocon subunits Sec61 α and Sec61 β and ribosomal proteins. These interactions could not be explained by the precipitation of nascent Nicalin interacting with translocation factors, as the precipitated Nicalin was tagged C-terminally. Interestingly, a recent proteomics study (Gilchrist et al., 2006), which analyzed the secretory pathway by the isolation of its compartments and subsequent mass spectrometry, indicated an enrichment of Nicalin and NOMO in the rough ER, where translocation occurs. Moreover, the distribution of Nicalin and NOMO between rough ER, smooth ER and Golgi apparatus observed in that study was very similar to that of the translocon component Sec61 α (Fig. 42).

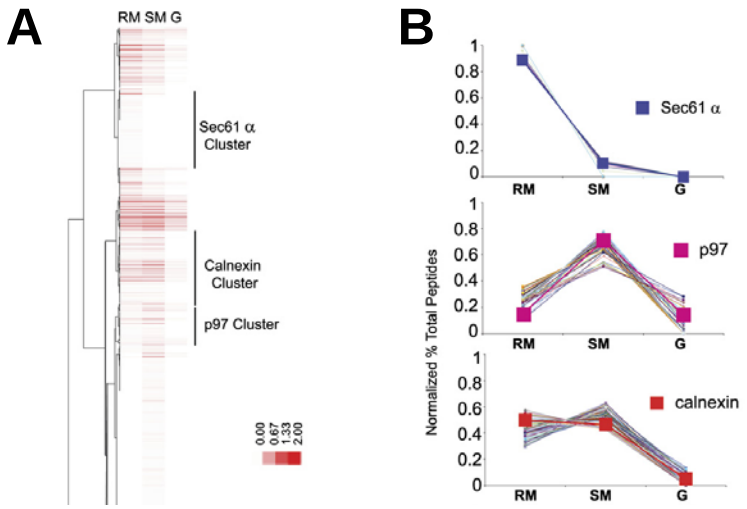

Fig. 42: 'Co-clustering' of proteins of the early secretory pathway. A) Rough ER membrane (RM), smooth ER membrane (SM), and Golgi (G) data (n = 3) were averaged and a heat map was generated. Clusters containing Sec61, p97 and Calnexin as markers were selected (Pearson correlation coefficient > 0.90). B) Mean values for proteins in each of these three clusters were plotted individually (normalized % total peptides). Both Nicalin and NOMO showed a similar RM/SM/G distribution as the translocon subunit Sec61 α, indicating a functional relationship. Adapted from Gilchrist et al., 2006.

Following the rationale of the study (Gilchrist et al., 2006), this 'co-clustering' is an indication for a function of the Nicalin-NOMO complex in the context of protein translocation into the ER. Indeed, the proteins enriched in the 'Sec61 α cluster' comprised translocation factors such as Ddost subunits, translocon subunits and ribosomal proteins. On the other hand, it also contained proteins unrelated to translocation such as enzymes involved in ER lipid metabolism, while proteins involved in translocation such as signal peptidase were found in different clusters. Thus, further (biochemical) data are needed to proof or disproof a functional relationship between Nicalin and the translocation machinery. Yet, further support for an involvement of the Nicalin-NOMO complex in translation/ER quality control came from

a study that analyzed the interactions of the secreted human hepatic lipase (HL) during its maturation in chinese hamster ovary (CHO) cells by tandem-affinity purification (TAP) and mass spectrometry (Doolittle et al., 2009; Fig. 43). 16 interacting ER proteins were identified, including NOMO (but not Nicalin) and components of the two major ER chaperone systems, the BiP/Grp94 and the Calnexin/Calreticulin system. However, NOMO was only found to interact when cells were stressed using dithiothreitol, a reducing agent that causes protein unfolding, indicating that the interaction is only triggered under enhanced stress conditions, which might lead to artificial interactions.

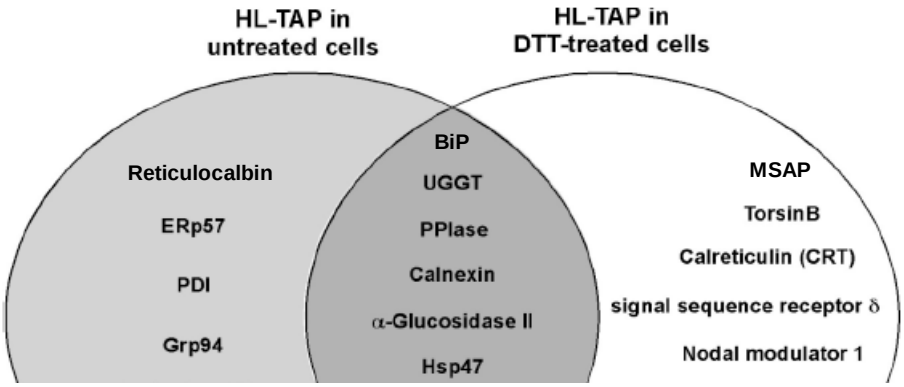

Fig. 43: Hepatic lipase may interact with NOMO during maturation. Diagram comparing ER proteins co-purifying with TAP-tagged hepatic lipase (HL-TAP) in untreated CHO cells or cells treated with dithiotreitole (DTT), a reducing agent that causes protein unfolding. The shaded areas represent proteins that are the strongest candidates for roles in HL maturation and/or degradation. (Nodal modulator 1, NOMO1). Adapted from Doolittle et al., 2009

Some of the potential Nicalin interactors were identical to γ-secretase interactors identified recently by a study based on a tandem-affinity purification (TAP)/mass spectrometry approach (Wakabayashi et al., 2009). Among these proteins were voltage dependent ion channel (VDAC), ER lipid raft enriched (Erlin) proteins, sarcoplasmic/endoplasmic reticulum calcium ATPase (SERCA), dolichyl-diphosphooligosaccharide-protein-glycosyltransferase (Ddost) subunits and Sec22b, indicating that these factors may be common contaminations of (ER) membrane affinity purifications and/or (maybe less likely) they generally interact with (ER) membrane protein complexes.

In summary, the combination of SILAC, co-isolation and mass spectrometry presented in this work is a promising approach for the identification of novel Nicalin interactors. However, subsequent studies will have to analyze the identified interactions in more detail. The described analysis needs to be repeated in wild-type cells with endogenous Nicalin to avoid overexpression artifacts. To that end, an anti-Nicalin antibody has to be generated which allows the precipitation of the intact complex. Alternatively, another purification approach could be developed to purify the endogenous complex, as has been achieved for the γ-secretase complex (Winkler et al., 2009).

3.5 The Nicalin-NOMO complex beyond Nodal signaling

The Nicalin-NOMO complex has been reported to have an antagonistic effect on Nodal signaling in zebrafish (Haffner et al., 2004). *In situ* hybridization experiments revealed similar spatiotemporal expression patterns of TMEM147 (this work), Nicalin and NOMO (Haffner et al., 2004) during zebrafish development underlining the functional relevance of their interaction. However, the lack of information about the cellular function of TMEM147 prevented the further elucidation of the molecular role of the Nicalin-NOMO complex. Moreover, no factor with a known role in Nodal signaling was identified in the Nicalin interactome. Nodal function is believed to be mainly restricted to processes during and before gastrulation stages of chordate development (reviewed by Shen, 2007), but all complex components were also detected at later stages. In addition, they are widely expressed in various cell lines (Haffner et al., 2004, 2007; this work) and orthologs are present in invertebrates which lack Nodal signaling indicating that the complex might fulfill additional functions. In agreement with this, an involvement in invertebrate nicotinic acetylcholine receptor (nAChR) assembly has been proposed (Gottschalk et al., 2005; Almedom et al., 2009). nAChRs are homo- or heteropentameric ligand-gated ion channels involved in excitatory neurotransmission and muscle activation. They consist of α- and non-α-subunits, each contributing 4 transmembrane domains (TMDs), leading to a total of 20 TMDs in the assembled pentamer (reviewed by Albuquerque et al., 2009). The agonist, physiologically acetylcholine (ACh), binds at the interface between an α- and either another α- or a non-α- subunit (Chiara and Cohen, 1997). The binding of two or three ACh molecules is needed for maximal activation (Karlin, 2002; Cleary et al., 2005; Rayes et al., 2007). Thus, nAChR properties are affected by the number of α-subunits and the presence of certain subunits in the complex. In vertebrate muscle, α-, β-, γ-, δ- and ε-subunits exist, and nAChRs are of $\alpha_2\beta\gamma\delta$ or $\alpha_2\beta\delta\varepsilon$ composition, depending on the developmental stage (Mishina, 1986). In vertebrate neurons, 9 α- and 3 β-subunits form an α_5- or an $\alpha_2\beta_3$-type receptor. In *Caenorhabditis elegans* (*C. elegans),* the nAChR subunit repertoire is even more complex, with 29 confirmed nAChR subunits (Jones et al., 2007). In 2005, a tandem-affinity-purification approach of *C. elegans* (ce) nAChRs led to the co-isolation of ceNicalin and ceNOMO (Gottschalk et al., 2005). A subsequent study (Almedom et al., 2009) demonstrated the existence of a Nicalin-NOMO complex and its ER-localization in *C. elegans*, and further showed that mutant animals lacking ceNicalin or ceNOMO proteins exhibited moderate, but specific, resistance to AChR agonists such as levamisole and nicotine. These cholinergic deficits were confirmed by whole-cell voltage-clamp analyses, where sensitivities towards the agonists were reduced (while the effects of the physiological ligand ACh were less clear). It

was further shown that in the absence of ceNicalin or ceNOMO the neuromuscular junction (connecting the axon terminal of a motoneuron with the motor end plate, i.e. the highly excitable region of the muscle fiber plasma membrane) contained nAChRs of different subunit composition, or altered relative amounts of different nAChRs with specific subunit compositions (particularly the subunits UNC-38 and UNC-29 were enriched, while ACR-8 incorporation was reduced). Based on their findings, the authors proposed a model in which the Nicalin-NOMO complex acts as a 'nucleation centre' for nAChR assembly regulating the inclusion of particular subunits during pentamer assembly (Fig. 44, more details in legend).

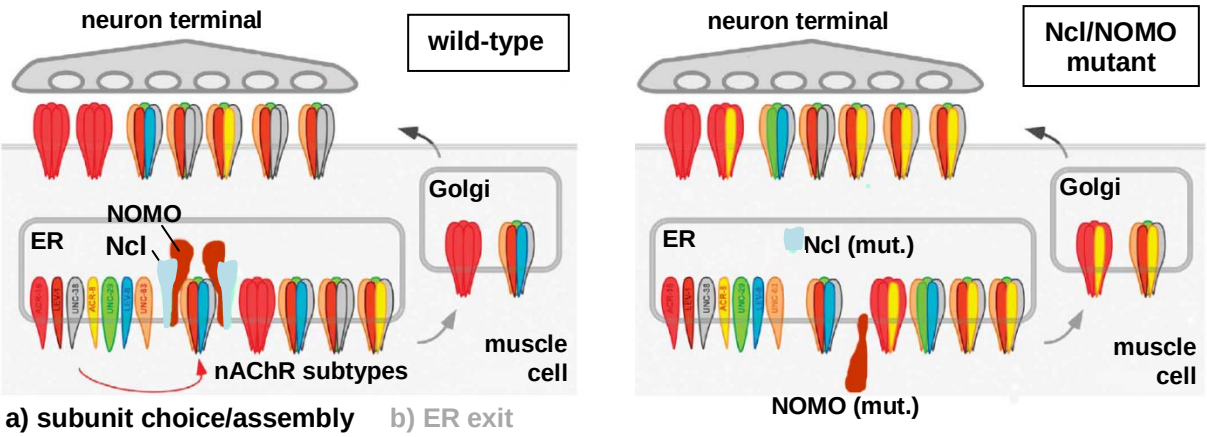

Fig. 44: Model of ceNicalin/ceNOMO function. Left, ceNicalin (Ncl)/ceNOMO influence either a) choice/assembly of particular subunits (indicated by different colors) of the pentameric nAChRs, or b) these proteins determine to which extent pentamers of a certain subunit composition are allowed to leave the ER (less favored, as no obvious accumulation of ceNicalin was observed at ER exit sites). Right, in the ceNicalin or ceNOMO mutants, nAChRs of other composition are found, for example, containing ACR-8 or UNC-29 subunits more often. Adapted from Almedom et al., 2009.

Although most knockout animals tested were likely to be complete loss of function mutants, the phenotypes described were rather subtle, suggesting that a functional Nicalin-NOMO complex is not essential for survival, at least in nematodes. Interestingly, ceNicalin mutant phenotypes could be partially rescued by expression of the human homolog, indicating a possible conservation of the effect on nAChrR assembly. However, due to differences between vertebrate and invertebrate nAChR subunit composition (Jones et al., 2007) the relevance of the findings for the vertebrate system are unclear. Corresponding knockout models in vertebrates will have to be generated to elucidate the precise function of the Nicalin-NOMO complex in higher organisms.

Of note, ceTMEM147 was not identified in the *C. elegans* study, which can be interpreted in two ways: either it is not required for the function of the Nicalin-NOMO complex in *C. elegans* or it was missed in the purification procedure. Based on the difficulties to identify TMEM147 in the less complex purification scenario presented in this work, the latter possibility is favored and TMEM147 is expected to be a genuine complex component in all species.

3.6 Outlook

Although the existence of additional small components cannot completely be ruled out, it appears likely that all components of the Nicalin-NOMO complex have now been identified. Thus, the next challenge will be the characterization of its precise cellular/molecular function. From none of the three components - Nicalin, NOMO, and TMEM147 - a function could be inferred, as no enzymatic or other known motif could be identified in any of them. A general involvement of the complex in translocation and/or ER quality control has been suggested by preliminary data from this work and other studies. Indeed, such a role could explain the wide-spread expression of the complex and its apparent involvement in two unrelated cellular processes, acetylcholine receptor assembly and Nodal signaling. Still, other possible functions of the Nicalin-NOMO have to be kept in mind, one being based on the observed interaction with a SNARE protein complex which is involved in ER homeostasis. In any case, the high degree of conservation of Nicalin, NOMO, and TMEM147 clearly points to an important function in multicellular organisms. For future analyses, the generation of further tools is required. In this work, a combination of SILAC, co-isolation and mass spectrometry was shown to offer a promising approach for the identification of novel Nicalin interactors, but the success may depend on the generation of an antibody which allows the precipitation of the intact complex from wild-type cells. Most importantly, loss-of-function animal models, especially in vertebrates, are needed. This work suggests that it is sufficient to target only one of the three genes to eliminate the complex. Likewise, a gain-of-function should be achieved solely by increasing Nicalin expression. These studies will not only contribute to the understanding of the function of the Nicalin-NOMO complex, but might also help to elucidate general mechanisms involved in the assembly of membrane protein complexes. One general conclusion from this work might be that the presence of small polytopic proteins in membrane protein complexes, like TMEM147 in the Nicalin-NOMO complex and APH-1 in γ-secretase, could be an overlooked phenomenon, as their identification can be very demanding.

4. Materials and methods

4.1 Equipment

37 °C incubator (Function line)	Heraeus
37 °C shaker (Certomat BS-1)	B. Braun Biotech International
Autoclave (Tuttnauer 3850 EL)	Systec
Bunsen burner (Vulcan)	Heraeus
Cell lifter	Costar
Centrifuge for large disposable tubes (Megafuge 1.0)	Heraeus, Kendro
Centrifuge for disposable tubes (Biofuge pico)	Heraeus, Kendro
Centrifuge for disposable tubes / 4 °C (Biofuge fresco)	Heraeus, Kendro
Centrifuge / 4 °C / swing rotor (Megafuge 1.0R)	Heraeus, Kendro
Centrifuge / 4 °C / swing rotor (Multifuge 3 L-R)	Heraeus, Kendro
Clean bench (Hera Safe HS12)	Heraeus, Kendro
CO_2 incubator (Hera cell)	Heraeus, Kendro
Disposable culture dishes (60 x 15 mm, 100 x 17 mm, 24 well, 12 well)	Nunc
Disposable cuvette (10 x 11x 45 mm)	Sarstedt
Disposable pipets (25 mL, 10 mL, 5 mL)	Sarstedt
Disposable tubes (50 mL, 15 mL, 2 mL, 1.5 mL, 0.5 mL, 0.2 mL)	Sarstedt
Electrophoresis chamber (Model B1; Model B2)	Owl Separation Systems
Electrophoresis cell (Mini-PROTEAN 3)	BioRad
Film developer (Curix 60)	Agfa
Films (Super RX)	Fuji
Freezer -80 °C (HFU 80)	Heraeus
Freezer -20 °C	Electrolux
Freezing tubes (Qualifreeze)	Qualilab
Gas burner (Vulcan)	Heraeus, Kendro
Glass pipet for gel loading	Hamilton
Heatblock	Liebisch
Incubator 37 °C (Function line)	Heraeus
Magnet stirrer (IKAMAG RCT basic and KMO2 basic)	IKA Labortechnik
Microscope (Wiloverts 10 x 4/10/20)	Hund
Microscope slides	Menzelgläser
Microwave	Bosch
N_2 tank (Chronos)	Messer Griesheim
Needle (0.7, 0.9 mm diameter)	Braun
Pasteur pipets	Sarstedt
PCR machine (Mastercycler personal)	Eppendorf
pH-Electrode (Blueline 23 pH)	Schott
pH-Meter (Inolab pH Level 1)	WTW

Photometer (SmartSpecTM 3000)	Bio-Rad
Pipet controler (Accu-Jet)	Brand
Power supply (Power Pac 300)	BioRad
Pipet tips (1 mL, 200 µL, 20 µL, 2 µL)	Sarstedt
Quarz cuvette (10 x 10 x 45 mm, Quartz Spectrofotometer Cell)	BioRad
Pipets with disposable tips (2 µL, 20 µL, 200 µL, 1,000 µL)	Gilson
Rotator (Roto-shake Genie)	Scientific Industries
Shaker (KM2)	Edmund Bühler
Scale (Analytical+ 200 g - 0,0001 g)	Ohaus
Scale (Standard 2000 g - 0,01 g)	Ohaus
Syringe	Terumo
Table ultracentrifuge (Optima ultracentrifuge)	Beckman
TLA-55 rotor	Beckman
MLA-80 rotor	Beckman
Transfer membrane (PVDF-Immobilon)	Millipore
Transfer chamber (Mini Trans-Blot Cell)	BioRad
Ultracentrifuge (L7-55)	Beckman
Ti 50 rotor	Beckman
UV lamp (White/ Ultraviolet Transilluminator)	UVP
Vortex (Vortex Genie 2)	Scientific Industries
Whatman paper	Schleicher + Schuell
Water deionizing machine (Milli-Q academic)	Millipore
Water bath (Typ 1002 ; Typ 1003)	GFL

4.2 Chemicals

Acetic acid	Roth
Agar	Becton Dickinson
Agarose	Amersham
Ampicillin	Roth
APS (ammoniumperoxidisulfate)	Sigma
Bromophenol blue	Fluka
DDM (N-dodecyl-β-D-maltoside)	Calbiochem/Applichem
DMSO (dimethylsulfoxide)	Roth
EDTA (ethylendiaminetetra-acetic acid)	Merck
Ethanol	Merck
Ethidiumbromide	Sigma
Formamide	Merck
Glycerol	Roth
Glycine	Applichem
H_2O_{dest}	generated by water deionizing machine
H_2O_{dest} for PCR	H_2O_{dest} at 120 °C, 1.2 bar, 20 min autoclaved
H_2O_2 (30 %)	Merck
Heparin	Sigma
I-Block blocking reagent	Applied Biosystems
KH_2PO_4	Merck
Methanol	Merck
2-Mercaptoethanol (β-Mercaptoethanol)	Roth
Mowiol 4-88	Roth
NaCl	Roth
Na_2HPO_4	Merck
NP-40/Igepal	Sigma
Paraformaldehyde	Sigma
Poly-L-lysine	Sigma
Ponceau-S (3-Hydroxy-4-[2-sulfo-4-(4-sulfo-phenylazo)-phenylazo]-2,7-naphthalene disulfonic acid)	Sigma
2-Propanol (Isopropanol)	Merck
SDS (sodium dodecyl sulfate)	Serva
TEMED (N,N,N',N'-tetramethylethylendiamine)	Roth
Tetracycline	Clontech
Tris (Tris-(hydroxymethyl)-aminomethane)	Applichem
Triton X-100	Merck
Xylene cyanol FF	J. T. Baker

Usually, chemicals were of purity grade p.a. (*pro analysi*). Chemicals not listed were purchased from Merck, Sigma or Roth in p.a. grade.

4.3 DNA techniques

4.3.1 Plasmids

Tab. 3 lists plasmids that were used in this thesis, while Tab. 4 gives details about those plasmids that were generated in this thesis.

Name	Description of plasmid	Ref.
pcDNA3.1(-)	mammalian protein expression vector	(1)
pcDNA3.1 Hygro(+)	mammalian protein expression vector (abbreviation: pcDNA3.1)	(1)
pcDNA4/TO/myc-His A	mammalian protein expression vector (abbreviation: pcDNA4)	(1)
pcDNA6/V5-His A	mammalian protein expression vector (abbreviation: pcDNA6)	(1)
pcS2+	multipurpose protein expression vector	(2)
pLVTHM	lentiviral shRNA expression vector (see section 4.4.5)	(3)
FUΔZeo	lentiviral protein expression vector (see section 4.4.5)	(4)
pcDNA4/Ncl-myc	encodes human Nicalin C-terminally fused to a myc/His-tag	(5)
pcDNA4/NclΔC-myc	encodes human Nicalin w/o C-terminus (CT), fused to a myc/His-tag	Tab. 4
pcDNA4/NclΔTMC	encodes human Nicalin w/o CT and transmembrane domain (TMD)	Tab. 4
pcS2+/zfNcl	encodes *Danio rerio* Nicalin	(5)
pcDNA6/Nclmut-myc	encodes RNAi-resistant human Nicalin C-terminally fused to a myc/His-tag	(5)
pcDNA6/Ncl-mutΔC	encodes RNAi-resistant human Nicalin w/o CT	Tab. 4
pcDNA6/Ncl-mutΔTMC	encodes RNAi-resistant human Nicalin w/o CT and TMD	Tab. 4
pcDNA4/NOMO-myc	encodes human NOMO C-terminally fused to a myc/His-tag	(5)
pcDNA6/T147-V5	encodes human TMEM147 C-terminally fused to a V5/His-tag	Tab. 4
pcDNA4/zfT147-myc	encodes *Danio rerio* TMEM147 C-terminally fused to a myc/His-tag	Tab. 4
pcS2+/zfT147	encodes *Danio rerio* TMEM147	Tab. 4
FUΔZeo-T147mut-V5	encodes RNAi-resistant human TMEM147 C-terminally fused to V5/His-tag	Tab. 4
pcDNA3.1/CD4	encodes human CD4	(6)
pcDNA3.1/CD4NC	encodes human CD4, C-terminus exchanged for Nicalin C-terminus (NC)	Tab. 4
psPAX2	encodes lentiviral packaging proteins (gag, pol, pro; see section 4.4.5)	(7)
pcDNA3.1(-)-VSV-G	encodes vesicular stomatitis virus G glycoprotein (see section 4.4.5)	(8)
pLVTHM-T147	encodes shRNA targeting human TMEM147	Tab. 4
pLVTHM-Ncl	encodes shRNA targeting human Nicalin	Tab. 4
pLVTHM-NOMO	encodes shRNA targeting human NOMO	Tab. 4

Tab. 3: List of plasmids. Descriptions of vectors and their inserts as well as sources/references (Ref.) are given. References: (1) Invitrogen; (2) Rupp et al., 1994; (3) provided by Dr Peer-Hendrik Kuhn (LMU, Munich, Germany), generated from pLVTHM (Wiznerowicz and Trono, 2003) by modification of the ClaI site to a XmaI site; (4) provided by Dr Peer-Hendrik Kuhn, generated from FUGW (Lois et al., 2002) by exchanging GFP for a multiple cloning site and removing zeocin resistance (5) Haffner et al., 2004; (6) Kaether et al., 2004; (7) provided by Dr Peer-Hendrik Kuhn, Addgene Plasmid 12260 (http://www.addgene.org); (8) provided by Dr Peer-Hendrik Kuhn, generated from pCMV-VSV-G (Addgene Plasmid 8454);

Name	Primers or Inserts	Template	Restriction
pcDNA6/T147-V5	T147F and T147R	cDNA HEK293T cells	EcoRI/XhoI
pcDNA4/zfT147-myc	zfT147F and zfT147R	cDNA day 1 zf embryos	EcoRI/XhoI
pcS2+/zfT147	zfT147F and zfT147R	cDNA day 1 zf embryos	EcoRI/XhoI
FUΔZeo/T147mut-V5	pcDNA31F and T147mutR; T147mutF and T147R-Not1	pcDNA6/TMEM147-V5	BamHI/NotI
pcDNA4/NclΔC-myc	NclF and Ncl-ΔC	pcDNA4/Ncl-myc	EcoRI/XbaI
pcDNA4/NclΔTMC	NclF and Ncl-ΔTMC	pcDNA4/Ncl-myc	EcoRI/XbaI
pcDNA6/Ncl-mutΔC	NclF and Ncl-ΔCStop	pcDNA6/Nclmut-myc	EcoRI/XbaI
pcDNA6/Ncl-mutΔTMC	NclF and Ncl-ΔTMC	pcDNA6/Nclmut-myc	EcoRI/XbaI
pcDNA3/CD4NC	CD4F and Ncl-CD4; CD4-Ncl and NclR-Not	pcDNA3/CD4 pcDNA4/Ncl-myc	NheI/NotI
pLVTHM-T147	T147.2v-F and T147.2v-R	-	MluI/XmaI
pLVTHM-Ncl	Ncl1531v-F and Ncl1531v-R	-	MluI/XmaI
pLVTHM-NOMO	NOMO2v-F and NOMO2v-R	-	MluI/XmaI

Tab. 4: Details about DNA constructs generated in this thesis. The first nine entries are cDNA expression constructs. Primers, templates and restriction sites that were used for their generation are indicated. FUΔZeo-T147mut-V5 and pcDNA3/CD4NC were created by site-directed mutagenesis PCR: In a first step, 5'- and 3'-part of the insert were generated separately and a subsequent PCR was carried out using 5'- and 3'-parts together with the outer primers. The following three entries are pLVTHM-based shRNA expression constructs, which were generated by annealing denatured oligonucleotides in H_2O_{dest} for 15 min at 37 °C and cloning them into pLVTHM using MluI/XmaI restriction sites.

4.3.2 Oligonucleotides

Tab. 5 lists the oligonucleotides that were used as PCR primers or annealed to generate the inserts of shRNA expression constructs.

Name	Sequence
T147F	5' GCGAATTCGGCATCATGACCCTGTTT-3'
T147R	5'-GCCTCGAGATAGGAGTGCACATTGACAAC-3'
zfT147F	5'-GCGAATTCACCATGACTCTTTTTCA-3'
zfT147R	5'-GCCTCGAGGTTGCTGTGGACGA-3'
pcDNA31fw	5'-CTCTGGCTAACTAGAGAAC-3'
T147mutR	5'-GTAGGCCAGGGCAAAACAATTCCCGAAGTGAAACAGGGTCATG-3'
T147R-Not1	5'-GATCGCGGCCGCTCAATGGTGATGGTGATG-3'
T147mutF	5'-GGAATTGTTTTGCCCTGGCCTACTTCCCCTACTTCATCACCTAC-3'
pcDNA31F	5'-CTCTGGCTAACTAGAGAAC-3'
Nicalin1531v-F	5'-CGCGACCCCGCAAGTGATGAATGCGTACTTCAAGAG AGTACGCATTCATCACTTGCTTTTTGGAAA-3'
Nicalin1531v-R	5'-CCGGTTTCCAAAAAGCAAGTGATGAATGCGTACTCTC TTGAAGTACGCATTCATCACTTGCGGGGT-3'
NOMO2v-F	5'-CGCGACCCCGTCGGACGTGGAGATCAACTTCAAGAG AGTTGATCTCCACGTCCGACTTTTTGGAAA-3';
NOMO2v-R	5'-CCGGTTTCCAAAAAGTCGGACGTGGAGATCAACTCTC TTGAAGTTGATCTCCACGTCCGACGGGGT-3'
T147.2v-F	5'-CGCGACCCCCTGCTTCGCTCTTGCCTACTTCAAGAGA GTAGGCAAGAGCGAAGCAGTTTTTGGAAA-3'
T147.2v-R	5'-CCGGTTTCCAAAAACTGCTTCGCTCTTGCCTACTCTC TTGAAGTAGGCAAGAGCGAAGCAGGGGGT-3'
T147R	5'-GCCTCGAGATAGGAGTGCACATTGACAAC-3'
T147F	5'-GCGAATTCGGCATCATGACCCTGTTT-3'
Ncl-qPCR-F	5'-ACCACCTGAGCCGCTACCTGAA-3'
Ncl-qPCR-R	5'-GACGGCCGGCTTGACTCTGT-3'
NOMO-qPCR-F	5'-AGCGGTGGGCCAGAACGACT-3'
NOMO-qPCR-R	5'-ACATCCCGGCAGCAATCCAC-3'
bAct-qPCR-F	5'-CTGGGACGACATGGAGAAAA-3'
bAct-qPCR-R	5'-AAGGAAGGCTGGAAGAGTGC-3'
CD4F	5'-GGTGCTAGCTTTCCAGAAGGCCTCCAGCATAGTC-3'
NclC-CD4	5'-TAGAGGAGGCTGAATGCTGGACACAGAAGAAGATGCC-3'
CD4-NclC	5'-GGCATCTTCTTCTGTGTCCAGCACTTCAGCCTCCTCTA-3'
NclR-Not	5'-GCGCGGCCGCTACTGTGTCTTGGCCTTCACGAG-3'
NclΔC	5'-GCTCTAGAGAGGAGGCTGAAGTGCTGGACAG-3'
NclΔCStop	5'-GCTCTAGACTAGAGGAGGCTGAAGTGCTGGACAG-3'
NclΔTMC	5'-GCTCTAGACTAGTCAAAGACGGCCGGCTTGA-3'
NclF	5'-GCGAATTCGGCCAGGATGCTGGAGGAA-3'

Tab. 5: List of oligonucleotides (all oligonucleotides were purchased from Thermo Electron, Ulm, Germany)

4.3.3 RNA isolation and cDNA synthesis

Total RNA from cultured human cell lines or day 1 zebrafish embryos were isolated using the RNeasy Kit (Qiagen). 4 µg of mRNA were used for the synthesis of cDNA using oligo(dT) primers and the SuperScript III First-Strand Synthesis SuperMix (Invitrogen).

4.3.4 PCR

A typical polymerase chain reaction (PCR) contained the following components.

Component	Volume
dNTP-Mix	1 µL
forward primer (10 µM)	1 µL
reverse primer (10 µM)	1 µL
template (50 nM)	1 µL
Pfu polymerase buffer 10x (Stratagene)	5 µL
Pfu polymerase (Stratagene)	1 µL
H_2O_{dest} for PCR (see 4.2.1)	ad 50 µL

Tab. 6: typical PCR reaction mixture

PCR reaction mixtures were pipetted on ice and performed in a thermocycler using the following program.

Temperature	Periode
95 °C	3 min
30 cycles:	
95 °C	30 sec
52 °C	60 sec/1,000 bp
70 °C	30 sec
70 °C	10 min
4 °C	∞

Tab. 7: PCR program

4.3.5 Quantitative real-time PCR

4 µg total RNA were used for the synthesis of cDNA using the SuperScript III First-Strand Synthesis SuperMix (Invitrogen) and oligo(dT) primers. 2.5 % of the cDNA were used for a SYBR Green (Bio-Rad) real-time PCR reaction (40 cycles with 15 s at 95 °C and 60 s at 65 °C) on a Bio-Rad IQ5 machine. Primers for Nicalin (Ncl-qPCR-R and -F), NOMO (NOMO-qPCR-R and -F), and TMEM147 (T147-R and -F) were used (see Tab. 5). Reactions were performed in triplets. The obtained CT values were normalized to β-actin expression (primers bAct-F and -R) by the comparative CT method (Livak and Schmittgen, 2001).

4.3.6 Agarose gel electrophoresis

Agarose gels:
0.8 - 1.5 % agarose in TAE-buffer, ~3 min heated in the microwave (max. temperature), 0.2 µg/mL (final concentration) ethidiumbromide

DNA loading buffer (6x):
30 % Glycerin, 0.25 % Bromphenol blue, 0.25 % Xylencyanol FF in H_2O_{dest}

TAE buffer 1x:
242 g Tris, 57.1 mL acetic acid, 100 mL 0.5 M EDTA, H_2O_{dest} ad 1

Depending on the size of the DNA to be separated, 0.8 to 1.5 % (w/v) agarose gels were applied using electrophoresis chambers from Owl Separation Systems (Models B1 and B2)

Electrophoresis was done in TAE buffer using a constant voltage of 120 volt. As a molecular marker, a 1 kb DNA ladder (Invitrogen) was used. If required, separated DNA fragments were extracted and purified using the Nucleo Spin Extract Kit (Macherey-Nagel).

4.3.9 Restriction enzyme treatment

Restriction enzymes (10 U/µL ; Fermentas):
XhoI, EcoRI, BamHI, NotI, MluI, XmaI

Restriction emzyme buffer (Fermentas):
Y+ (Yello Tango) buffer

Analytical restriction enzyme treatment for plasmid analyses was performed as follows.

Component	Volume
Restriction enzyme (10 U/µL)	0.3 µL each
Restriction enzyme buffer	1 µL or 2 µL
DNA	500 ng
H_2O_{dest}	ad 10 µL

Tab. 8: Analytical restriction enzyme treatment

Preparative restriction enzyme treatment for subsequent ligation was performed as follows.

Component	Volume
Restriction enzyme (10 U/µL)	1 µL each
Restriction enzyme buffer	8 µL
DNA	4 µg
H_2O_{dest}	ad 40 µL

Tab. 9: Preparative restriction enzyme treatment

Mixtures were incubated 1 h at 37 °C. After the reaction, cDNA fragments were isolated by agarose gel electrophoresis and purified using the Nucleo Spin Extract kit (Macherey-Nagel).

4.3.10 DNA ligation

100-300 ng vector, 0.3-1 µg cDNA fragment, 5 U T4 DNA ligase (5 U/µl) (Roche) and 2 µL T4 DNA ligase buffer (Roche) were mixed with H_2O_{dest} at a final volume of 20 µL. The ligation mixture was incubated for 20 min at room temperature. 10 µL of the ligation mixture was used for transformation of competent bacteria (*E.coli* DH5α).

4.3.11 Transformation of competent bacteria

LB medium (Low Salt Luria-Bertani medium):
1 % Trypton (Becton Dickinson), 0.5 % yeast extrakt (Becton Dickinson), 0.5 % Nacl, pH = 7.0, at 120 °C and 1.2 bar for 20 min autoclaved

LB_{AMP} medium:
LB medium, 100 µg/mL ampicillin (Roth)

LB_{AMP} agar plates:
LB medium, 15 g/l agar (Becton-Dickinson) was added and at 120 °C and 1.2 bar for 2 min autoclaved. After chilling down to ~50 °C, ampicillin was added at a final concentration of 100 µg/mL.

50 µL of competent bacteria (*E.coli* DH5α, present in the laboratory) were added to ligation mixtures (or other DNA constructs to be amplified) and incubated for 30 min on ice. Subsequent heat shock treatment was done at 42 °C for 90 sec. Then the mixture was kept several minutes on ice. 450 µL of fresh LB-medium were added, followed by a regeneration step at 37 °C for 30 min while shaking. 100 µL were plated onto LB-agar plates containing 100 µg/mL ampicillin (LB_{AMP} agar plate), the rest was centrifuged at 7,000 rpm for one minute at RT, 300 µL of the supernatant were substracted, the pellet was resuspended in the residual liquid and plated onto another LB_{AMP} agar plate. After o/n incubation at 37 °C, colonies were picked, inoculated into 3.5 mL of fresh LB_{AMP} medium containing and incubated o/n at 37 °C. 3 mL of the culture were used for small scale DNA isolation.

4.3.12 DNA isolation from bacteria

3 mL of transformed *E.coli* DH5α o/n culture were used for small-scale DNA isolation using the Nucleospin Plasmid Kit (Macherey-Nagel). DNA concentration was measured by photometer. Correctness of the inserts was analyzed by restriction enzyme treatment and agarose gel electrophoresis. DNA was sent away for DNA-sequencing to GATC Biotech AG (Konstanz, Germany). For large-scale DNA isolation, small amounts of transformed *E.coli* bacteria were inoculated into 200 mL of LB medium containing 100 µg/mL ampicillin, and cultured o/n at 37 °C while shaking. Plasmid cDNA was isolated and purified from the o/n culture using the Nucleobond AX 500 Kit (Macherey-Nagel). DNA was resolved in H_2O and the DNA concentration was measured by photometer.

4.4 Cell culture

4.4.1 Cell lines

Tab. 10 and 11 list wild-type and transgenic cell lines, respectively, which were used in this thesis.

Cell line	Description
HEK293T	human embryonic kidney cells
HeLa	human epithelial cervical cancer cells
HepG2	human hepatocellular liver carcinoma cells
A431	human epidermoid carcinoma cells
SHSY5Y	human neuroblastoma cells
MCF7	human breast adenocarcinoma cells
Panc-1	human pancreatic carcinoma cells
C8161	human melanoma cells
MDCK	Madin-Darby canine kidney epithelial cells
P19	mouse embryonic carcinoma cells
3T3	mouse fibroblast cells
N2A	mouse neuroblastoma cells

Tab. 10 List of wild-type cell lines. All cell lines were obtained from the laboratory's cell line collection.

Cell line	Expression construct	Resistance	Source/Reference
T-Rex-293 (293TR)			Invitrogen
293T/Ncl-myc	pcDNA4/Ncl-myc	zeocin	(Haffner et al., 2004)
293T/zfNcl	pcS2+/zfNcl pcDNA6	blasticidin	
293T/NclΔC-myc	pcDNA4/Ncl-ΔC-myc	zeocin	
293T/NclΔTMC	pcDNA4/Ncl-ΔTMC	zeocin	
293T/Ncl-KD	BSENU6-Ncl1531	zeocin	(Haffner et al., 2007)
293T/Nclrescue-myc	BSENU6-Ncl1531 pcDNA6/Ncl-mutmyc	zeocin	(Haffner et al., 2007)
293T/Nclrescue-ΔC	BSENU6-Ncl1531 pcDNA6/Ncl-mutΔC	zeocin	
293T/Nclrescue-ΔTMC	BSENU6-Ncl1531 pcDNA6/Ncl-mutΔTMC	zeocin	
293TR/Ncl-myc	pcDNA4/Ncl-myc	zeocin	(Haffner et al., 2007)
293T/NOMO-myc	pcDNA4/NOMO-myc	zeocin	(Haffner et al., 2007)
293T/NOMO-KD	BSENU6-NOMO2	zeocin	(Haffner et al., 2007)
293T/NOMOrescue	BSENU6-NOMO2 pcDNA6/NOMO-myc	zeocin/ blasticidin	(Haffner et al., 2007)
293T/NOMO-myc/NclΔTMC	pcDNA4/NOMO-myc pcDNA6/Ncl-mutΔTMC	zeocin/ blasticidin	
293T/TMEM147-V5	pcDNA6/T147-V5	blasticidin	
293T/zfTMEM147-myc	pcDNA4/zfT147-myc	zeocin	
293T/NOMO-myc/ TMEM147-V5	pcDNA4/NOMO-myc FUΔZeo-T147mut-V5	zeocin	
293T/NOMO-myc/NclΔTMC/ TMEM147-V5	pcDNA4/NOMO-myc pcDNA6/Ncl-mutΔTMC FUΔZeo-T147mut-V5	zeocin/ blasticidin	
HeLa-pLVTHM	pLVTHM		
HeLa/Ncl-KD	pLVTHM-Ncl		
HeLa/NOMO-KD	pLVTHM-NOMO		
HeLa/T147-KD	pLVTHM-T147		
HeLa/T147-rescue	pLVTHM-T147 FUΔZeo-T147mut-V5		

Tab. 11: List of transgenic cell lines. Stably inegrated DNA constructs, resistances and sources/references are listed.

4.4.2 Cell cultivation

Trypsin-EDTA solution (Invitrogen):
0.05 % Trypsin, 0.53 mM EDTA-4Na

penicillin/streptomycin solution (Invitrogen):
5,000 U/mL penicillin, 5 mg/mL streptomycin

PBS (sterile):
140 mM NaCl, 10 mM Na_2HPO_4,1.75 mM KH_2PO_4, pH 7.4 in H_2O_{dest}, autoclaved at 120 °C and 1.2 bar for 20 min

Standard medium (Gibco Life Sciences):
DMEM (Dulbecco's modified Eagle's Medium + 4500 mg/L Glucose + GlutaMAX™ I - pyruvate) supplemented with 10 % fetal calf serum (FCS; Invitrogen), 5 mL penicillin/streptomycin solution

Selection medium zeocin:
Standard medium + 200 µg/mL zeocin (Invitrogen)

Selection medium blasticidin:
Standard medium + 10 µg/mL blasticidin (Invitrogen)

Cells were cultured in standard or selection medium in the presence of 5 % CO_2 at 37 °C. Selection media contained 200 µg/mL of zeocin or 10 µg/mL of blasticidin. For passaging, the cells were washed once with autoclaved PBS, trypsinized for 5 min and appropriate amounts were seeded in fresh medium after well suspending. The expression of Nicalin in T-Rex-293 cells was induced with 0.1 µg/mL tetracycline.

4.4.3 Stable Isotope Labeling Using Amino acids in Cell Culture (SILAC)

DMEM w/o Arg, Lys (SAFC Biosciences):
Dulbecco's Modified Eagle's Medium (Modified) w/ 4500 mg/L glucose, w/ 4 mM L-alanyl-L-glutamine, w/ 110 mg/L sodium pyruvate, w/o L-arginine, w/o L-glutamine, w/o lysine

SILAC medium 0,0:
DMEM w/o Arg, Lys supplemented with arginine and lysine (Sigma-Aldrich), 10 % dialyzed fetal calf serum (Invitrogen), 5 mL penicillin/streptomycin solution

SILAC medium 6,4:
DMEM w/o arg, lys supplemented with $^{13}C_6$-arginine (Sigma-Aldrich) and 5,5,6,6-D_4-lysine (Sigma-Aldrich) 10 % dialyzed fetal calf serum (Invitrogen), 5 mL penicillin/streptomycin solution.

To stably label all cellular proteins with isotope-labeled lysine and arginine, cells were cultivated in SILAC medium 6,4 (supplemented with $^{13}C_6$-arginine and 5,5,6,6-D_4-lysine) for 5 passages (equivalent to 14 days). Control cells were cultivated in SILAC medium 0,0, containing unlabeled arginine and lysine (see section 2.9, Fig. 35, and section 4.7).

4.4.4 Cell transfection

Cells were cultivated until a confluence of ~90 % was reached. Then transfection was performed using the Lipofectamine 2000 transfection reagent (Invitrogen) following the

manufacturer's manual, except only half of the volumes and DNA amounts recommended were used (Tab. 12). First, DNA and Lipofectamine 2000 were each mixed with OptiMEM (Invitrogen) and incubated for 5 min at RT. Then the solutions were combined, further incubated for 20 min at RT, mixed with the standard medium and added gently to the cells.

Culture vessel	Plating medium	Total cDNA and dilution volume	Lipofectamine 2000 and dilution volume
10 cm	10 mL	12 µg and 0.75 mL OPTMEM	30 µL and 0.75 mL OPTIMEM
6 cm	5 mL	4 µg and 0.25 mL OPTIMEM	15 µL and 0.25 mL OPTIMEM
12 well	1 mL	0.8 µg and 50 µL OPTIMEM	3 µL and 50 µL OPTIMEM

Tab. 12: Tranfection mixtures

For selection of stable single cell clones, 24-48 hrs after transfection the cells were diluted appropriately (e.g., 1:5, 1:10, 1:50, 1:100 and 1:1,000) in selection medium and plated. After growth for ~2 weeks, single cell clones were detached using sterile pipet tips and transferred into 24 well plates. After further expansion steps, clones expressing the target protein were selected based on the expression levels detected by immunoblotting.

4.4.5 Cell transduction, lentiviral

Lentiviral transduction of cells was carried out in cooperation with Drs Peer-Hendrik Kuhn and Stefan F. Lichtenthaler, DZNE (German Center for Neurodegenerative Diseases, Munich) and Adolf Butenandt-Institute, Biochemistry, Ludwig-Maximilians University Munich. Procedures were adapted from protocols described elsewhere (Wiznerowicz and Trono, 2003; Lois et al., 2002).

To generate stable knockdown cells, lentiviral supernatants were produced by transfecting low passage HEK293T cells ('packaging cells') with DNA constructs psPAX2, pcDNA3.1(-)-VSV-G and either pLVTHM-T147, -Ncl or -NOMO (for construct details see Tab. 3-5, and Fig. 45). psPAX2 contains essential genes to generate infectious lentiviral particles, most importantly structural proteins (*gag, group-specific antigen)* and enzymes *(pol, polymerase; pro, protease).* pcDNA3.1(-)-VSV-G encodes fusogenic vesicular stomatitis virus G glycoprotein (VSV-G) to be presented at the viral envelope. pLVTHM-TMEM147, -Nicalin or -NOMO were transcribed by the packaging cells to RNA molecules containing 1) the respective shRNA sequences driven by an H1 promoter, 2) the *gfp (green fluorescent protein*) gene (for selection) driven by an EF1α promoter, 3) lentiviral packaging signals/regulatory elements. Eventually, the packaging cell line released assembled VSV-G pseudotyped lentiviral particles that in their interior contained the respective RNAs as well as viral enzymes, most importantly reverse transcriptase (RT) and integrase. After o/n

incubation, the medium containing the viral particles was filtered through a 0.45-µm sterile filter and added to target cells. VSV-G mediated endocytosis and penetration of the endosome was followed by the release of lentiviral RNA and enzymes into the cytosol. Here, the RNA was reverse transcribed by RT to double-stranded DNA which was stably integrated into the genome by lentiviral integrase. Thus, stable shRNA-producing cell pools were obtained and GFP fluorescence could be used as a marker for transduction efficiency, which generally was close to 100 %. The procedure for the generation of TMEM147 rescue cells was identical except that for the transfection the FUΔZeo-TMEM147mut-V5 construct was used instead of pLVTHM-based shRNA constructs.

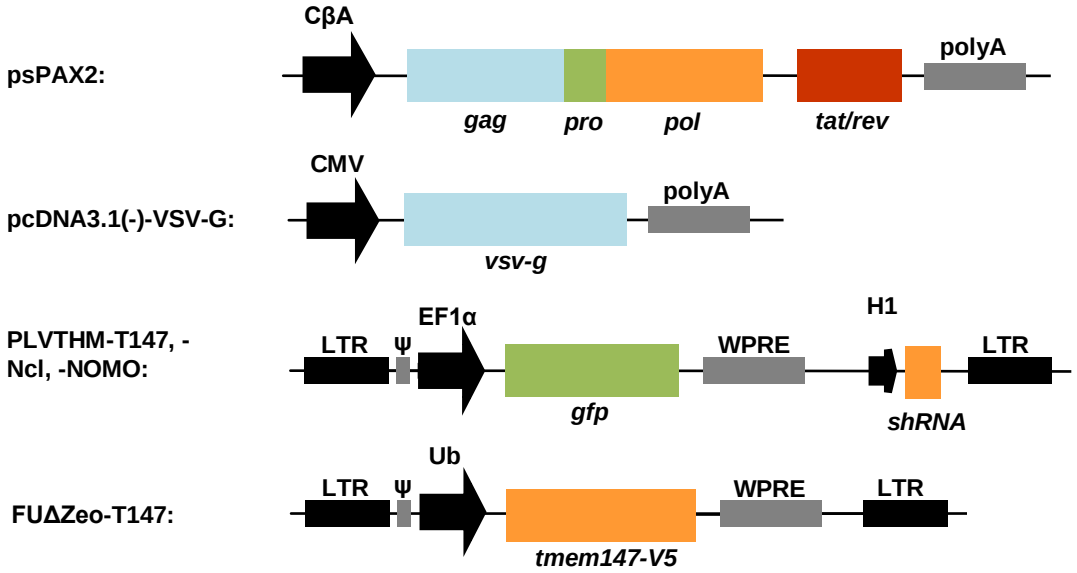

Fig. 45: Vectors for lentiviral transduction - coding and regulatory sequences. Only the most relevant structures are shown. psPAX2 contains essential lentiviral genes to generate infectious particles: *gag (group-specific antigen)* encoding elements of the viral capsid/nucleocapsid; *pol (polymerase)* encoding reverse transcriptase (RT) and integrase (see text); *pro (protease)* encoding the enzyme that cleaves the gag polyprotein precursor into its functional units; *tat (transactivator of transcription); rev (regulator of expression of virion proteins)*, both encoding regulatory lentiviral proteins. pcDNA3.1(-)-VSV-G encodes vesicular stomatitis virus G glycoprotein (VSV-G), which became part of the viral envelope and enhanced infectivity. pLVTHM-T147, -NcI or -NOMO were transcribed by the cellular machinery to larger RNA molecules containing the respective shRNA sequences, the *gfp (green fluorescent protein)* gene, lentiviral packaging signals (ψ), and regulatory elements, among them LTR (long terminal repeat) sequences, which are important for genome integration of the constructs. Upon co-transfection of these plasmids into low confluence 293T cells ('packaging cells'), assembled lentiviral particles were released that presented VSV-G at their surface and in their interior contained the respective PLVTHM-encoded RNA molecules as well as viral enzymes, most importantly reverse transcriptase (RT) and integrase. Promoters, indicated by black arrows, are: CβA, chicken β-actin promoter; CMV, cytomegalovirus promoter; EF1α, elongation factor 1 α promoter; H1 RNA polymerase III promoter; Ub, human ubiquitin promoter. (polyA, poly-adenylation signal; WPRE, Woodchuck hepatitis virus post-transcriptional regulation element, improves the mRNA stability and compensates for the lack of poly-adenylation). Informations on plasmids were retrieved from www.addgene.com.

4.4.6 Cell cryoconservation

Freezing-medium:
FCS containing 5 % (v/v) DMSO

For cryoconservation, ~ 90 % confluent cells in 10 cm-dishes were trypsinized, washed in standard medium and pelleted. Pellets were suspended in 0.5 mL freezing-medium, transferred into a cryotube, frozen o/n at -80 °C and transferred into a liquid-nitrogen tank.

4.5 Protein analysis

4.5.1 Antibodies

Monoclonal Nicalin, NOMO, and TMEM147 antibodies were generated in collaboration with Dr Elisabeth Kremmer, HelmholtzZentrum, Munich, Germany.

The monoclonal α (anti)-Nicalin antibody NiNT-1 was generated by immunizing rats with the peptide containing aa 43-58 of the human sequence and a C-terminal cysteine residue (AHEFTVYRMQQYDLQGC). Hybridoma cell supernatants were used 1:1000 for immunoblotting (1:5 to detect Nicalin in zebrafish lysates) and undiluted for immunofluorescence. The monoclonal α-NOMO antibody NOM4A12 was generated by immunizing rats with a peptide containing aa 923-938 of the human sequence and a N-terminal cysteine residue (CQYYFKPMMKEFRFEPS) and hybridoma cell supernatants were used 1:5 for immunoblotting. The monoclonal α-TMEM147 antibody T147.11 was generated by immunizing mice with a peptide containing aa 124-140 of the human sequence and a C-terminal cysteine residue (RGIEFDWKYIQMSIDSNC) and hybridoma cell supernatants were used 1:7 for immunoblotting. Tab. 13 lists all antibodies that were used.

Antibody	Type	Application	Source/Reference
α-Nicalin (NiNT-1)	rat monoclonal, hybridoma supernatant	IB 1:1000, 1:5 (zf) IP 1:50 IF undiluted	Dr Elisabeth Kremmer, HelmholtzZentrum, Munich, Germany
α-NOMO (NOM4A12)	rat monoclonal, hybridoma supernatant	IB 1:5	Dr Elisabeth Kremmer
α-TMEM147 (T147.11)	mouse monoclonal, hybridoma supernatant	IB 1:7	Dr Elisabeth Kremmer
α-Calnexin	rabbit polyclonal, pur.	IB 1:5000 IF 1:500	Stressgen
α-VCP	mouse monoclonal, pur.	IB 1:1000	Santa Cruz
α-β-Actin	rabbit polyclonal, pur.	IB 1:1000	Sigma
α-β-Catenin	mouse monoclonal, pur.	IB 1:1000	Sigma
α-CD4 (EDU-2)	mouse monoclonal, pur.	IB 1:1000	DIATEC
α-Sec22b	rabbit polyclonal, pur.	IB 1:1000	Dr Mitsuo Tagaya, Tokyo University, Japan; (Hirose et al., 2004)
α-Syntaxin 18	rabbit polyclonal, pur.	IB 1:1000	Dr Mitsuo Tagaya; (Hatsuzawa et al., 2009)
α-p31 (D12)	rabbit polyclonal, pur.	IB 1:1000	Dr Mitsuo Tagaya (Hirose et al., 2004)
α-BNIP1	rabbit polyclonal, pur.	IB 1:1000	Dr Mitsuo Tagaya (Nakajima et al., 2004)
α-V5	mouse monoclonal, pur.	IB 1:1000 IP 1 µL/1 mg ML	Invitrogen
α-myc (9E10)	mouse monoclonal, ascites	IB 1:2,000 IP 0.25 µL/1 mg ML	Developmental Studies Hybridoma Bank, Iowa University, USA
α-flag (M2)	mouse monoclonal, pur.	IB 1:1000 IP 1 µL/1 mg ML	Santa Cruz

Tab. 13: List of primary antibodies. IB: immunoblot, IF: immunofluorescence, IP: immunoprecipitation, ML: membrane lysate, pur.: purified.

4.5.2 Total protein lysates

PBS:
140 mM NaCl, 10 mM Na_2HPO_4 and 1.75 mM KH_2PO4, pH 7.4, in H_2O_{dest}

High citrate buffer, 0.7 % DDM:
50 mM NaCitrat, 1mM EDTA in H_2O_{dest}, 0.7 % (w/v) DDM, 1x PI mix

High citrate buffer, 1 % NP-40:
50 mM NaCitrat, 1mM EDTA in H_2O_{dest}, 1 % (w/v) NP-40, 1x PI mix

PI mix (Protease inhibitors), 500x stock solution in DMSO (Roche)

Cells adherent in culture dishes were washed with chilled PBS. and scraped off in 1 mL of chilled PBS with a cell lifter. The cell solution was transferred to a 1.5 mL disposable tube and centrifuged for 5 minutes at 1000 x g at 4 °C. The supernatant was removed and the pellet was lysed in high citrate buffer, 0.7 % DDM or 1 % NP-40, 1x PI mix and stored on ice for 15 min, followed by centrifugation (10 min, 17,000 rpm x g, 4 °C). The collected supernatant was the sample. Its protein content was detected via Bradford assay (1-2 µL of lysate mixed with 1 mL of BioRad protein assay working solution, incubated 5 min at RT, absorbance measured at 595 nm).

4.5.3 Membrane protein lysates

Low citrate buffer:
15 mM NaCitrate, 1mM EDTA

High citrate buffer, 0.7 % DDM or 1 % NP-40: see section 4.5.2

Cells adherent in the culture vessels were washed with chilled 1x PBS (see section 4.5.2). Then a minimum of 1 mL of chilled PBS was added and cells were scraped off with a cell lifter. The cell solution was pipetted into 1.5 or 2 mL disposable tubes and centrifuged for 5 minutes at 1000 x g and 4 °C. The supernatant was removed. The cell pellet was resuspended in low citrate-buffer + PI mix, 200 µL per 10 cm culture dish and 500 µL per 15 cm dish, respectively, and frozen in liquid nitrogen. The mixture was thawed on ice and the cells disrupted using a syringe with a 0.7 mm diameter needle (10 times). The suspension was centrifuged for 10 min at 1000 x g and 4 °C. The supernatant was centrifuged for 30 min at 17,000 x g and 4 °C. The pellet was resuspended in an adequate volume of lysis buffer (usually High citrate buffer containing 0.7 % DDM) to achieve a protein concentration of ~10 µg/µL (e.g., ~100 µL/ confluent 10 cm dish). Now the samples were incubated for 15 min on ice, centrifuged for 10 min at 13,000 rpm, 4 °C, the supernatant collected and its protein content detemined by a Bradford assay (see section 4.5.2). Typically, one confluent 10 cm culture dish yielded ~1 mg of membrane protein lysate, one confluent 15 cm dish ~3 mg.

4.5.4 Deglycosylation

Deglycosylation experiments were carried out on membrane protein lysates (25 µg) containing 0.1 % SDS using 1 unit of N-glycosidase F (Roche) or 10 milliunits of endoglycosidase H (Roche) for 16 hrs at 37 °C.

4.5.5 Immunoprecipitation (IP)

For immunoprecipitation of myc-tagged Nicalin, V5-tagged TMEM147 or flag-tagged NOMO from stably transfected HEK293T cells, membrane protein lysates (concentration: ~10 µg/µL, but also less for immunoblot analyes) were used, typically containing 1 mg protein for immunoblot analysis, 3-5 mg for silver staining and 10-30 mg for Coomassie staining of SDS gels. The total volume was always more than ~50 % of the tube volume. Large-scale IPs from more than 10 mg starting material were performed in 10 mg aliquots. Preclearing was performed by addition of Protein G Sepharose 4 Fast Flow (Tab. 14) and shaking at 4 °C for a minimum of 2 hrs (also o/n). An appropriate amount of the respective antibody (Tab. 14) was added to the precleared lysates, followed by incubation for a minimum of 2 hrs while shaking at 4 °C (also o/n).

Solution	Application in IP	Source
α-myc 9E10 AB	2 µg/1 mg membrane lysate	Hybridoma bank
α-flag M2 AB	1µg/1 mg membrane lysate	Santa Cruz
α-V5 AB	1µg/1 mg membrane lysate	Invitrogen
PGS beads 1:2 in lysis buffer	5 µL solution/1 mg membrane lysate, but a minimum of 20 µL (double amounts for preclearing)	GE Healthcare

Tab. 14: Solutions used for immunoprecipitation (IP)

Finally, an appropriate amount of PGS beads (Tab. 14) was added, followed by incubation for 2 hrs (but not longer) while shaking at 4 °C. Washing of beads with bound material was performed by three times adding 200 µL of lysis buffer, resuspending the beads and immediate centrifugation for 2 min at 1000 x g. Then ~40 µL 1x sample buffer (see section 4.5.7) were added. The 10 mg aliquots of large-scale IPs were eluted successively in the same sample buffer solution. The suspension was heated for 10 min at only 65 °C to prevent the aggregation of TMEM147. Typically, 30 µL were loaded onto a 14 % 0.75 mm SDS gel.
As a molecular weight standard, 3-5 µL See Blue Plus 2 protein marker (Invitrogen) were used. Electrophoresis was carried out at 99 V and, after migration of the proteins into the separation gel, at 147 V. The separated proteins were either transferred to a PVDF membrane (see section 4.5.8) or SDS gels were stained using either the Silver Stain Plus kit (BioRad) or the Coomassie PageBlue solution (Fermentas) according to the manufacturer's manual.

4.5.6 Density gradient centrifugation

PBS/20 mM EDTA:
140 mM NaCl, 10 mM Na_2HPO_4 and 1.75 mM KH_2PO4, pH 7.4, in H_2O_{dest}, 20 mM EDTA

2x homogenization buffer (stock):
20 mM HEPES pH 7.4, 2 mM EDTA, 0.5 M sucrose

1x homogenization buffer:
10 mM HEPES pH 7.4, 1 mM EDTA, 0.25 M sucrose

Iodixanol solution 60 % (Sigma)

For subcellular fractionation of cell membranes, a discontinuous iodixanol gradient was applied. For sample preparation, cells of 4 confluent 10 cm dishes were washed with chilled PBS (see section 4.5.2) and scraped in PBS/20 mM EDTA (2 mL per dish). Cells were pooled and centrifuged for 10 min at 1000 x g for 10 min at 4 °C. The supernatant was discarded and cells resuspended in 2 mL 1x homogenization buffer + PI mix. To crack cells, the suspension was passed 10 times through a 0.8 mm diameter needle. The suspension was aliquoted in two 1.5 mL disposable tubes and centrifuged for 10 min at 1000 x g for 10 min at 4 °C. The resulting post-nuclear supernatants were transferred into polycarbonate tubes and centrifuged for 1h, 4 °C, at 40,000 rpm (Beckmann Optima, MLA-80 rotor). The resulting pellet was resuspended in 500 µL 1x homogenization buffer + PI mix and stirred o/n at 4 °C. 400 µL were loaded onto the gradient, 100 µL were kept as starting material.
For gradient preparation, a 30 % iodixanol working solution (WS) was prepared by mixing 60 % iodixanol solution and 2x homogenization buffer 1:1. In a next step, 8 solutions of different final iodixanol percentage were prepared by mixing working solution and 1x homogenization buffer as follows (Tab. 15).

Final iodixanol %	WS (mL)	1x homog. buffer (mL)	For 1 gradient
2.5	0.21	2.29	1
5	0.75	3.75	2
7.5	1.125	3.375	2
10	1.5	3	2
12.5	0.625	0.875	0.5
15	2.25	2.25	2
17.5	0.875	0.625	0.5
20	1	0.5	0.5
30 (=WS)	1.5	0	0.3

Tab. 15: Solutions of different final iodixanol percentage

The solutions were underlayed in polyallomer tubes, with the 2.5 % iodixanol solution at the top and 30 % at the bottom. After samples (400 µL) were loaded, the tubes had to be filled up to 2 mm from the top with 2.5 % working solution and balanced to 0.01 g, The gradient was generated by centrifugation for 2 hrs 30 min at 40,000 rpm and 4 °C in a Beckman Optima ultracentrifuge equipped with a Sorval TH-641 rotor. Fractions were collected at 4 °C after placing the tube in a stand and piercing of the tube bottom using a 0.9 mm needle

(Braun). 12 x 1 mL fractions were collected in disposable tubes. For SDS-PAGE analysis, 20 µL 6x sample buffer (see section 4.5.7) were added to 100 µL of each fraction and 25 µL were loaded. As a control, 4 µL of starting material were loaded.

4.5.7 SDS-PAGE

Acrylamide-Bis solution (Serva):
40 % (w/v) Acrylamid/Bisacrylamid 37.5:1 in H_2O_{dest}

Tris buffer 0.5 M:
90.85 g Tris in 500 mL H_2O_{dest}, pH = 8.8 (adjusted using HCl)

Tris buffer 1.5 M:
30.28 g Tris in 500 mL H_2O_{dest}, pH = 6.8 (adjusted using HCl)

Electrophoresis buffer:
25 mM Tris, 192 mM Glycine, 0.1 % (w/v) SDS, pH 8.3

6x sample buffer:
7 mL 0.5 M Tris-HCl with 0.4 % (w/v) SDS, pH 6.8, 3.6 mL glycerol, 1 g SDS, 600 µL 2-mercaptoethanol, 4 mg bromophenol blue, H_2O_{dest} ad 12 mL

Sodium dodecyl sulfate polyacrylamide gel electrophoresis (SDS-PAGE) was performed under denaturing conditions using a discontinuous gel-system including one stacking and one separation gel (BioRad mini-gel system).

Tab. 16 Tab. 16 shows the composition of separating and stacking gels. To protein lysates 6x sample buffer was added. The mixture was heated for 10 min at only 65 °C to prevent the aggregation of TMEM147.

Solution	7.5 % Separating gel	14 % Separating gel	Stacking gel
H_2O_{dest}	5.415 mL	3.8 mL	3.145 mL
Tris buffer 1.5 M (pH 8.8)	2.5 mL	2.5 mL	-
Tris buffer 0.5 M (pH 6.8)	-	-	1.25 mL
10 % SDS	100 µL	100 µL	50 µL
40 % Acrylamide-Bis solution	1.875 mL	3.5 mL	0.5 mL
10 % APS	75 µL	75 µL	50 µL
TEMED	7.5 µL	7.5 µL	5 µL

Tab. 16: Composition of (7.5 % and 14 %) separation and stacking SDS plyacrylamide gels. Amounts indicated are sufficient for 2 mini-gels, 0.75 mm thick or 1 mini-gel, 1.5 mm thick.

As a molecular weight standard, 3-5 µL See Blue Plus 2 protein marker (Invitrogen) were used. Electrophoresis was carried out at 99 V and, after migration of the proteins into the separation gel, at 147 V. For protein staining the the Silver Stain Plus kit (BioRad) or the Coomassie PageBlue solution (Fermentas) was used, for immunoblotting proteins were transferred to a PVDF membrane.

4.5.8 Transfer of proteins to PVDF membranes

Transfer buffer:
25 mM Tris, 192 mM Glycine, pH 8.3

Ponceau-S solution:
0.1 % (w/v) Ponceau-S, 5 % (v/v) acetic acid, H_2O_{dest} ad 100 mL

Blocking solution (I-Bloc): 0,2 % I-Bloc (w/v) in TBST

For the transfer of proteins to polyviylidene difluoride (PVDF) Immobilon-P membranes (Millipore) the Mini Trans-Blot Cell system (Bio-Rad) was used. PVDF membranes were soaked with 80 % (v/v) ethanol, washed with H_2O_{dest}, and incubated in transfer buffer for several minutes. The protein transfer was performed in transfer buffer for 1 h at 400 mA on a magnetic stirrer at 4 °C. After transfer, membranes were dried at RT and then again soaked with 80 % (v/v) ethanol. Membranes were stained using Ponceau-S solution. The stain was partially removed by washing in H_2O_{dest}, and membranes were blocked for 1 h at RT or over night at 4 °C in blocking solution.

4.5.9 Immunological detection of proteins

Tris-buffered saline/0.05 % Tween (TBST):
10mM Tris pH 8.0, 150mM NaCl, 0.05 % Tween 20

horseradish peroxidase (HRP)-coupled IgGs: α-rabbit (Promega), α-mouse (Promega), α-rat IgG (Santa Cruz)

ECL Plus Western Blotting Reagents (GE Healthcare):
Chemiluminiscence reagent A and B, mixed 40:1

Blocked membranes were incubated with primary antibodies (see section 4.5.1) for 1 h at RT or o/n at 4 °C, washed 3 times for 10 min in TBST, incubated for 1 h at RT with horseradish peroxidase (HRP)-conjugated secondary antibodies, diluted 1:10,000 in blocking solution and washed again 3 times for 10 min in TBST. Signals were generated by ECL Plus Western Blotting Reagents (GE Healthcare) and were exposed on X-ray films (Super RX, Fuji) for an appropriate time span.

4.6 Immunocytochemistry

poly-L-lysine solution:
100 µg/mL poly-L-lysine in H_2O_{dest}

Mowiol:
24 g glycerol, 9,6 g Mowiol 4-88, 24 mL dH20, 48 mL 0.2 M Tris, pH8.5

Cells were grown on poly-L-lysine-coated (30 min poly-L-lysine solution, 3 washes with PBS) coverslips. Cells were fixed for 20 min with PBS/3.7 % paraformaldehyde, permeabilized 20

min with PBS/0.2 % Triton X-100, and blocked 1 h with PBS/1 % bovine serum albumine. Antibody incubations were performed for 1 h at room temperature in PBS using a humid chamber (for antibody details, see section 4.5.1). After washes with PBS, Alexa 488- and 555-coupled secondary antibodies (Molecular Probes) were used for detection. After washing (3 times PBS, once H_2O_{dest}, once 80 % ethanol) and mounting in Mowiol, samples were analyzed with a Zeiss Axioplan) fluorescence microscope.

4.7 Mass spectrometry

Mass spectrometry (MS) analyses were performed in collaboration with Dr Marcus Krüger, Max-Planck-Institute for Heart and Lung Research, Bad Nauheim, Germany.

Enhanced liquid chromatography-mass spectrometry (GeLC-MS) was essentially carried out as described (Kruger et al., 2008). Briefly, proteins were separated on a NuPAGE 4 %-12 % Bis-Tris gel (Invitrogen), stained with Coomassie Blue (PageBlue, Fermentas) and bands of interest were cut out. Proteins within gel pieces were subjected to alkylation and reduction, followed by trypsin cleavage. Then peptides were extracted as described (Shevchenko et al., 2006) and both desalted and concentrated by Stage Tips (Thermo). Reverse-phase nano-LC-MS/MS was performed using an Agilent 1200 nanoflow LC system (Agilent Technologies). The LC system was online coupled to a LTQ-Orbitrap (Thermo Scientific) which was equipped with a nanoelectrospray source (Proxeon). To identify proteins, the MASCOT database was searched using the following parameters: maximum of two missed trypsin cleavages, cysteine carbamidomethylation, methionine oxidation, and N-terminal protein acetylation (and SILAC labels Lys-D4 and Arg-6, for the SILAC experiment).
For the analysis of the Nicalin interactom, MS was combined with SILAC (see section 4.4.3) and Nicalin-immunoprecipitation (Ncl-IP, see section 4.5.5). Fig. 35 in section 2.9 illustrates the workflow of the SILAC/Ncl-IP/MS experiment.

4.8 Zebrafish techniques

4.8.1 General

E3 embryo medium:
5 mM NaCl, 0,17 mM KCl, 0,33 mM $CaCl_2$, 0,33 mM $MgSO_4$, 0.1 % (w/v) methylene blue

Experiments were carried out using the *Danio rerio* wild-type line AB (George Streisinger, Institute of Neuroscience, University of Oregon, USA) in compliance with the guidelines of

the Bavarian Council on Animal care. Zebrafish were maintained, raised, and mated as described (Mullins et al., 1994). Embryos were kept at 28 °C in E3 embryo medium and staged as described (Kimmel et al., 1995).

4.8.2 *In situ* hybridization

20x SSC:
3M NaCl, 0.3 M sodium citrate, pH 7.0

hybridization (hyb) mix:
50 % (v/v) formamide, 5x SSC, 50 µg/mL heparin, 500 µg/mL tRNA, 9 mM citric acid, 0.1 % (v/v) Tween 20

PBT:
0.1 % Tween-20 in PBS (see section 4.5.2)

Pi buffer:
PBT containing 2 % (v/v) sheep serum and 0.2 % (w/v) BSA)

AP (alkaline phosphatase) buffer:
5 mL 1 M Tris pH 9.5, 2.5 mL 1 M MgCl2, 1 mL 5 M NaCl, 250 µL 20 % Tween-20

NBT/BCIP stock solution (Roche):
18.75 mg/mL NBT (Nitro blue tetrazolium chloride) and 9.4 mg/mL BCIP (5-Bromo-4-chloro-3-indolyl phosphate, toluidine salt) in 67 % DMSO (v/v).

Digoxigenin-labeled RNA probes were synthesized using DIG RNA Labeling Mix, 10 × conc. (Roche) with the NotI-linearized construct PCS2+/zfTMEM as template for antisense probe synthesis using T7 polymerase, and EcoRI-linearized PCS2+/zfTMEM as template for sense probe (control) synthesis using SP6 polymerase. RNA *in situ* hybridization was carried out as previously described (Hammerschmidt et al., 1996). Day 2 embryos were bleached prior to *in situ* hybridization by incubation in 3 % H_2O_2/0.5 % KOH. Embryos were fixed for ~ 24 hrs in PBS/4 % PFA, manually dechorionated and dehydrated o/n in methanol at -20 °C. Then the embryos were rehydrated stepwise in methanol/PBT (90 %, 75 %, 50 %, 25 %, 10 % methanol) and finally put back in 100 % PBT (0.1 % Tween-20 in PBS). Embryos older than the beginning of somitogenesis were treated for 10 minutes with 10 µg/mL proteinase K (Roche) in PBT at RT, post-fixed in 4 % PFA for 20 minutes and then rinsed in PBT 5 times for 5 minutes each. Then they were prehybridized for 3 hrs at 70 °C in hybridization (hyb) mix, post-fixed in 4 % PFA and washed extensively followed by incubation in hyb mix for 3 hrs at 70 °C. Probe hybridization was carried out o/n at 70 °C in hyb mix containing 50 ng to 100 ng of probe. Unbound probe was removed in a series of washes at 70 °C: 10 minutes in 75 % hyb mix/25 % 2x SSC, 10 minutes in 50 % hyb mix/50 % 2x SSC, 10 minutes in 25 % hyb mix, 75 % 2x SSC, 10 minutes in 2x SSC, 2 times 30 minutes in 0.2x SSC. Further washes were performed at RT for 5 minutes in 75 % 0.2x SSC/25 % PBT, 5 minutes in 50 % 0.2x SSC/50 % PBT, 5 minutes in 25 % 0.2x SSC/75 % PBT and 5 minutes in PBT. In the

next step, embryos were blocked for 1 h in Pi buffer and incubated o/n at 4 °C with pre-adsorbed alkaline phosphatase-coupled anti-digoxigenin Fab fragments (Roche) at a 1:5000 dilution in Pi buffer. Finally the embryos were washed 6 times for 15 minutes each in PBT at room temperature and once in AP buffer. Detection was performed using NBT/BCIP stock solution diluted 1:50 in AP buffer. When the color was developed, the reaction was stopped by several washes with PBT. Embryos were transferred to glycerol and photographed using a Zeiss Axioplan 2 imaging compound microscope.

4.8.3 Zebrafish total protein lysates

10 embryos or larvae were frozen in 300 µL of 1x sample buffer (see section 4.5.7). After thawing, samples were heated for 5 min at 60 °C and homogenized by sonification (5 strokes), followed by 5 min at 60 °C. 10 % of the lysate were subjected to an SDS-PAGE.

4.9 Bioinformatical methods

Tab. 17 lists the databases and bioinformatical programs that were used, applications are characterized and web addresses are shown.

Application	Database/Program	Web address
mRNA, genomic DNA and protein database	NCBI	http://www.ncbi.nlm.nih.gov/
protein database	Uniprot	http://www.uniprot.org
RNA expression (expressed sequence tag, EST) database	GeneNote	http://bioinfo2.weizmann.ac.il/cgi-bin/genenote/home_page.pl
search of orthologous proteins and identity calculation	FASTA	http://www.ebi.ac.uk/Tools/fasta33/
interspecies multiple protein alignment	clustalw2	http://www.ebi.ac.uk/Tools/clustalw2/
interspecies multiple protein alignment visualization	Jalview	http://www.jalview.org
overall protein hydrophobicity calculation	ProtParam	http://expasy.org/cgi-bin/protparam
global protein alignment	EMBOSS by the Needleman/Wunsch algorithm	http://www.ebi.ac.uk/Tools/emboss/align/
local protein alignment	EMBOSS by the Smith/Waterman algorithm	http://www.ebi.ac.uk/Tools/emboss/align/
membrane protein topology prediction	PRODIV-TMHMM	http://topcons.cbr.su.se
signal peptide determination	Signal P 3.0	http://www.cbs.dtu.dk/services/SignalP/
N-linked glycosylation prediction	NetNGlyc 1.0	http://www.cbs.dtu.dk/services/NetNGlyc/
global protein analysis	SMART	http://smart.embl-heidelberg.de/
protein domain analysis	Pfam	http://pfam.sanger.ac.uk
generation of protein hydrophobicity plots	Protscale by the Kyte-Dolittle method	http://www.expasy.ch/tools/protscale.html
transcription factor binding site prediction	PROMO 8.3	http://alggen.lsi.upc.es/cgi-bin/promo_v3/promo/promoinit.cgi?dirDB=TF_8.3
identification of proteins from mass spectrometry data	MASCOT database	http://www.matrixscience.com

Tab. 17: Databases and bioinformatical programs

5. List of references

Albuquerque, E. X., E. F. Pereira, M. Alkondon and S. W. Rogers (2009). "Mammalian nicotinic acetylcholine receptors: from structure to function." Physiol Rev **89**(1): 73-120.

Almedom, R. B., J. F. Liewald, G. Hernando, C. Schultheis, D. Rayes, J. Pan, T. Schedletzky, H. Hutter, C. Bouzat and A. Gottschalk (2009). "An ER-resident membrane protein complex regulates nicotinic acetylcholine receptor subunit composition at the synapse." EMBO J **28**(17): 2636-2649.

Aoki, T., M. Kojima, K. Tani and M. Tagaya (2008). "Sec22b-dependent assembly of endoplasmic reticulum Q-SNARE proteins." Biochem J **410**(1): 93-100.

Bell, E., I. Munoz-Sanjuan, C. R. Altmann, A. Vonica and A. H. Brivanlou (2003). "Cell fate specification and competence by Coco, a maternal BMP, TGFbeta and Wnt inhibitor." Development **130**(7): 1381-1389.

Blader, P. and U. Strahle (1998). "Casting an eye over cyclopia." Nature **395**(6698): 112-113.

Branford, W. W. and H. J. Yost (2002). "Lefty-dependent inhibition of Nodal- and Wnt-responsive organizer gene expression is essential for normal gastrulation." Curr Biol **12**(24): 2136-2141.

Capell, A., D. Beher, S. Prokop, H. Steiner, C. Kaether, M. S. Shearman and C. Haass (2005). "Gamma-secretase complex assembly within the early secretory pathway." J Biol Chem **280**(8): 6471-6478.

Capell, A., J. Grunberg, B. Pesold, A. Diehlmann, M. Citron, R. Nixon, K. Beyreuther, D. J. Selkoe and C. Haass (1998). "The proteolytic fragments of the Alzheimer's disease-associated presenilin-1 form heterodimers and occur as a 100-150-kDa molecular mass complex." J Biol Chem **273**(6): 3205-3211.

Capell, A., C. Kaether, D. Edbauer, K. Shirotani, S. Merkl, H. Steiner and C. Haass (2003). "Nicastrin interacts with gamma-secretase complex components via the N-terminal part of its transmembrane domain." J Biol Chem **278**(52): 52519-52523.

Chavez-Gutierrez, L., A. Tolia, E. Maes, T. Li, P. C. Wong and B. de Strooper (2008). "Glu(332) in the Nicastrin ectodomain is essential for gamma-secretase complex maturation but not for its activity." J Biol Chem **283**(29): 20096-20105.

Chen, F., G. Yu, S. Arawaka, M. Nishimura, T. Kawarai, H. Yu, A. Tandon, A. Supala, Y. Q. Song, E. Rogaeva, P. Milman, C. Sato, C. Yu, C. Janus, J. Lee, L. Song, L. Zhang, P. E. Fraser and P. H. St George-Hyslop (2001). "Nicastrin binds to membrane-tethered Notch." Nat Cell Biol **3**(8): 751-754.

Chen, Y. and A. F. Schier (2002). "Lefty proteins are long-range inhibitors of squint-mediated nodal signaling." Curr Biol **12**(24): 2124-2128.

Cheng, S. K., F. Olale, A. H. Brivanlou and A. F. Schier (2004). "Lefty Blocks a Subset of TGFbeta Signals by Antagonizing EGF-CFC Coreceptors." PLoS Biol **2**(2): E30.

Chiara, D. C. and J. B. Cohen (1997). "Identification of amino acids contributing to high and low affinity d-tubocurarine sites in the Torpedo nicotinic acetylcholine receptor." J Biol Chem **272**(52): 32940-32950.

Chyung, J. H., D. M. Raper and D. J. Selkoe (2005). "Gamma-secretase exists on the plasma membrane as an intact complex that accepts substrates and effects intramembrane cleavage." J Biol Chem **280**(6): 4383-4392.

Cleary, J. P., D. M. Walsh, J. J. Hofmeister, G. M. Shankar, M. A. Kuskowski, D. J. Selkoe and K. H. Ashe (2005). "Natural oligomers of the amyloid-beta protein specifically disrupt cognitive function." Nat Neurosci **8**(1): 79-84.

De Strooper, B., P. Saftig, K. Craessaerts, H. Vanderstichele, G. Guhde, W. Annaert, K. Von Figura and F. Van Leuven (1998). "Deficiency of presenilin-1 inhibits the normal cleavage of amyloid precursor protein." Nature **391**(6665): 387-390.

Deivanayagam, C. C., R. L. Rich, M. Carson, R. T. Owens, S. Danthuluri, T. Bice, M. Hook and S. V. Narayana (2000). "Novel fold and assembly of the repetitive B region of the Staphylococcus aureus collagen-binding surface protein." Structure **8**(1): 67-78.

Doolittle, M. H., O. Ben-Zeev, S. Bassilian, J. P. Whitelegge, M. Peterfy and H. Wong (2009). "Hepatic lipase maturation: a partial proteome of interacting factors." J Lipid Res **50**(6): 1173-1184.

Dries, D. R., S. Shah, Y. H. Han, C. Yu, S. Yu, M. S. Shearman and G. Yu (2009). "Glu-333 of nicastrin directly participates in gamma-secretase activity." J Biol Chem **284**(43): 29714-29724.

Edbauer, D., E. Winkler, C. Haass and H. Steiner (2002). "Presenilin and nicastrin regulate each other and determine amyloid beta-peptide production via complex formation." Proc Natl Acad Sci U S A **99**(13): 8666-8671.

Edbauer, D., E. Winkler, J. T. Regula, B. Pesold, H. Steiner and C. Haass (2003). "Reconstitution of gamma-secretase activity." Nat Cell Biol **5**(5): 486-488.

Eichinger, L., J. A. Pachebat, G. Glockner, M. A. Rajandream, R. Sucgang, M. Berriman, J. Song, R. Olsen, K. Szafranski, Q. Xu, B. Tunggal, S. Kummerfeld, M. Madera, B. A. Konfortov, F. Rivero, A. T. Bankier, R. Lehmann, N. Hamlin, R. Davies, P. Gaudet, P. Fey, K. Pilcher, G. Chen, D. Saunders, E. Sodergren, P. Davis, A. Kerhornou, X. Nie, N. Hall, C. Anjard, L. Hemphill, N. Bason, P. Farbrother, B. Desany, E. Just, T. Morio, R. Rost, C. Churcher, J. Cooper, S. Haydock, N. van Driessche, A. Cronin, I. Goodhead, D. Muzny, T. Mourier, A. Pain, M. Lu, D. Harper, R. Lindsay, H. Hauser, K. James, M. Quiles, M. Madan Babu, T. Saito, C. Buchrieser, A. Wardroper, M. Felder, M. Thangavelu, D. Johnson, A. Knights, H. Loulseged, K. Mungall, K. Oliver, C. Price, M. A. Quail, H. Urushihara, J. Hernandez, E. Rabbinowitsch, D. Steffen, M. Sanders, J. Ma, Y. Kohara, S. Sharp, M. Simmonds, S. Spiegler, A. Tivey, S. Sugano, B. White, D. Walker, J. Woodward, T. Winckler, Y. Tanaka, G. Shaulsky, M. Schleicher, G. Weinstock, A. Rosenthal, E. C. Cox, R. L. Chisholm, R. Gibbs, W. F. Loomis, M. Platzer, R. R. Kay, J. Williams, P. H. Dear, A. A. Noegel, B. Barrell and A. Kuspa (2005). "The genome of the social amoeba Dictyostelium discoideum." Nature **435**(7038): 43-57.

Fagan, R., M. Swindells, J. Overington and M. Weir (2001). "Nicastrin, a presenilin-interacting protein, contains an aminopeptidase/transferrin receptor superfamily domain." Trends Biochem Sci **26**(4): 213-214.

Fassler, M., M. Zocher, S. Klare, A. G. de la Fuente, J. Scheuermann, A. Capell, C. Haass, C. Valkova, A. Veerappan, D. Schneider and C. Kaether (2010). "Masking of transmembrane-based retention signals controls ER export of gamma-secretase." Traffic **11**(2): 250-258.

Fortini, M. E. (2002). "g-Secretase-mediated proteolysis in cell-surface-receptor signalling." Nat. Rev. Mol. Cell Biol. **3**(9): 673-684.

Fortna, R. R., A. S. Crystal, V. A. Morais, D. S. Pijak, V. M. Lee and R. W. Doms (2004). "Membrane topology and nicastrin-enhanced endoproteolysis of APH-1, a component of the gamma-secretase complex." J Biol Chem **279**(5): 3685-3693.

Fraering, P. C., M. J. LaVoie, W. Ye, B. L. Ostaszewski, W. T. Kimberly, D. J. Selkoe and M. S. Wolfe (2004). "Detergent-dependent dissociation of active gamma-secretase reveals an interaction between Pen-2 and PS1-NTF and offers a model for subunit organization within the complex." Biochemistry **43**(2): 323-333.

Francis, R., G. McGrath, J. Zhang, D. A. Ruddy, M. Sym, J. Apfeld, M. Nicoll, M. Maxwell, B. Hai, M. C. Ellis, A. L. Parks, W. Xu, J. Li, M. Gurney, R. L. Myers, C. S. Himes, R. Hiebsch, C. Ruble, J. S. Nye and D. Curtis (2002). "aph-1 and pen-2 are required for Notch pathway signaling, gamma-secretase cleavage of betaAPP, and presenilin protein accumulation." Dev Cell **3**(1): 85-97.

Fukumori, A., R. Fluhrer, H. Steiner and C. Haass (2010). "Three-amino acid spacing of presenilin endoproteolysis suggests a general stepwise cleavage of gamma-secretase-mediated intramembrane proteolysis." J Neurosci **in press**.

Geling, A., H. Steiner, M. Willem, L. Bally-Cuif and C. Haass (2002). "A g-secretase inhibitor blocks Notch signaling *in vivo* and causes a severe neurogenic phenotype in zebrafish." EMBO Rep. **3**(7): 688-694.

Gilchrist, A., C. E. Au, J. Hiding, A. W. Bell, J. Fernandez-Rodriguez, S. Lesimple, H. Nagaya, L. Roy, S. J. Gosline, M. Hallett, J. Paiement, R. E. Kearney, T. Nilsson and J. J. Bergeron (2006). "Quantitative proteomics analysis of the secretory pathway." Cell **127**(6): 1265-1281.

Gottschalk, A., R. B. Almedom, T. Schedletzky, S. D. Anderson, J. R. Yates, 3rd and W. R. Schafer (2005). "Identification and characterization of novel nicotinic receptor-associated proteins in Caenorhabditis elegans." EMBO J **24**(14): 2566-2578.

Goutte, C., M. Tsunozaki, V. A. Hale and J. R. Priess (2002). "APH-1 is a multipass membrane protein essential for the Notch signaling pathway in Caenorhabditis elegans embryos." Proc Natl Acad Sci U S A **99**(2): 775-779.

Gu, Y., F. Chen, N. Sanjo, T. Kawarai, H. Hasegawa, M. Duthie, W. Li, X. Ruan, A. Luthra, H. T. Mount, A. Tandon, P. E. Fraser and P. St George-Hyslop (2003). "APH-1 interacts with mature and immature forms of presenilins and nicastrin and may play a role in maturation of presenilin-nicastrin complexes." J. Biol. Chem. **278**: 7374-7380.

Haass, C. (2004). "Take five-BACE and the gamma-secretase quartet conduct Alzheimer's amyloid beta-peptide generation." EMBO J **23**(3): 483-488.

Haass, C. and H. Steiner (2002). "Alzheimer disease g-secretase: a complex story of GxGD-type presenilin proteases." Trends Cell Biol. **12**: 556-562.

Haffner, C., U. Dettmer, T. Weiler and C. Haass (2007). "The Nicastrin-like protein Nicalin regulates assembly and stability of the Nicalin-nodal modulator (NOMO) membrane protein complex." J Biol Chem **282**(14): 10632-10638.

Haffner, C., M. Frauli, S. Topp, M. Irmler, K. Hofmann, J. T. Regula, L. Bally-Cuif and C. Haass (2004). "Nicalin and its binding partner Nomo are novel Nodal signaling antagonists." EMBO J **23**(15): 3041-3050.

Haffner, C. and C. Haass (2004). "The biochemical and genetic odyssey to the function of a nicastrin-like protein." Neurodegener Dis **1**(4-5): 192-195.

Haffner, C. and C. Haass (2006). "Cellular functions of gamma-secretase-related proteins." Neurodegener Dis **3**(4-5): 284-289.

Hammerschmidt, M., F. Pelegri, M. C. Mullins, D. A. Kane, M. Brand, F. J. van Eeden, M. Furutani-Seiki, M. Granato, P. Haffter, C. P. Heisenberg, Y. J. Jiang, R. N. Kelsh, J. Odenthal, R. M. Warga and C. Nusslein-Volhard (1996). "Mutations affecting morphogenesis during gastrulation and tail formation in the zebrafish, Danio rerio." Development **123**: 143-151.

Hardy, J. (1997). "Amyloid, the presenilins and Alzheimer's disease [see comments]." Trends Neurosci **20**(4): 154-159.

Hardy, J. and D. J. Selkoe (2002). "The amyloid hypothesis of Alzheimer's disease: progress and problems on the road to therapeutics." Science **297**(5580): 353-356.

Harms, P. W. and C. Chang (2003). "Tomoregulin-1 (TMEFF1) inhibits nodal signaling through direct binding to the nodal coreceptor Cripto." Genes Dev **17**(21): 2624-2629.

Hasegawa, H., N. Sanjo, F. Chen, Y. J. Gu, C. Shier, A. Petit, T. Kawarai, T. Katayama, S. D. Schmidt, P. M. Mathews, G. Schmitt-Ulms, P. E. Fraser and P. St George-Hyslop (2004). "Both the

sequence and length of the C terminus of PEN-2 are critical for intermolecular interactions and function of presenilin complexes." J Biol Chem **279**(45): 46455-46463.

Hashimoto, H., M. Rebagliati, N. Ahmad, O. Muraoka, T. Kurokawa, M. Hibi and T. Suzuki (2004). "The Cerberus/Dan-family protein Charon is a negative regulator of Nodal signaling during left-right patterning in zebrafish." Development **131**(8): 1741-1753.

Hatsuzawa, K., H. Hashimoto, S. Arai, T. Tamura, A. Higa-Nishiyama and I. Wada (2009). "Sec22b is a negative regulator of phagocytosis in macrophages." Mol Biol Cell **20**(20): 4435-4443.

Hatsuzawa, K., H. Hirose, K. Tani, A. Yamamoto, R. H. Scheller and M. Tagaya (2000). "Syntaxin 18, a SNAP receptor that functions in the endoplasmic reticulum, intermediate compartment, and cis-Golgi vesicle trafficking." J Biol Chem **275**(18): 13713-13720.

He, G., H. Qing, Y. Tong, F. Cai, S. Ishiura and W. Song (2007). "Degradation of nicastrin involves both proteasome and lysosome." J Neurochem **101**(4): 982-992.

Helenius, J. and M. Aebi (2002). "Transmembrane movement of dolichol linked carbohydrates during N-glycoprotein biosynthesis in the endoplasmic reticulum." Semin Cell Dev Biol **13**(3): 171-178.

Herreman, A., G. Van Gassen, M. Bentahir, O. Nyabi, K. Craessaerts, U. Mueller, W. Annaert and B. De Strooper (2003). "gamma-Secretase activity requires the presenilin-dependent trafficking of nicastrin through the Golgi apparatus but not its complex glycosylation." J Cell Sci **116**(Pt 6): 1127-1136.

Hirose, H., K. Arasaki, N. Dohmae, K. Takio, K. Hatsuzawa, M. Nagahama, K. Tani, A. Yamamoto, M. Tohyama and M. Tagaya (2004). "Implication of ZW10 in membrane trafficking between the endoplasmic reticulum and Golgi." EMBO J **23**(6): 1267-1278.

Hu, Y. and M. E. Fortini (2003). "Different cofactor activities in gamma-secretase assembly: evidence for a nicastrin-Aph-1 subcomplex." J Cell Biol **161**(4): 685-690.

Iinuma, T., T. Aoki, K. Arasaki, H. Hirose, A. Yamamoto, R. Samata, H. P. Hauri, N. Arimitsu, M. Tagaya and K. Tani (2009). "Role of syntaxin 18 in the organization of endoplasmic reticulum subdomains." J Cell Sci **122**(Pt 10): 1680-1690.

Iratni, R., Y. T. Yan, C. Chen, J. Ding, Y. Zhang, S. M. Price, D. Reinberg and M. M. Shen (2002). "Inhibition of excess nodal signaling during mouse gastrulation by the transcriptional corepressor DRAP1." Science **298**(5600): 1996-1999.

Jackson, M. R., T. Nilsson and P. A. Peterson (1990). "Identification of a consensus motif for retention of transmembrane proteins in the endoplasmic reticulum." EMBO J **9**(10): 3153-3162.

Jiang, Y. J., B. L. Aerne, L. Smithers, C. Haddon, D. Ish-Horowicz and J. Lewis (2000). "Notch signalling and the synchronization of the somite segmentation clock." Nature **408**(6811): 475-479.

Jones, A. K., P. Davis, J. Hodgkin and D. B. Sattelle (2007). "The nicotinic acetylcholine receptor gene family of the nematode Caenorhabditis elegans: an update on nomenclature." Invert Neurosci **7**(2): 129-131.

Kaether, C., A. Capell, D. Edbauer, E. Winkler, B. Novak, H. Steiner and C. Haass (2004). "The presenilin C-terminus is required for ER-retention, nicastrin-binding and gamma-secretase activity." EMBO J **23**(24): 4738-4748.

Kaether, C., C. Haass and H. Steiner (2006). "Assembly, trafficking and function of gamma-secretase." Neurodegener Dis **3**(4-5): 275-283.

Kaether, C., S. Lammich, D. Edbauer, M. Ertl, J. Rietdorf, A. Capell, H. Steiner and C. Haass (2002). "Presenilin-1 affects trafficking and processing of betaAPP and is targeted in a complex with nicastrin to the plasma membrane." J Cell Biol **158**(3): 551-561.

Karlin, A. (2002). "Emerging structure of the nicotinic acetylcholine receptors." Nat Rev Neurosci **3**(2): 102-114.

Kim, S. H. and S. S. Sisodia (2005). "Evidence that the "NF" motif in transmembrane domain 4 of presenilin 1 is critical for binding with PEN-2." J Biol Chem **280**(51): 41953-41966.

Kim, S. H., Y. I. Yin, Y. M. Li and S. S. Sisodia (2004). "Evidence that assembly of an active gamma-secretase complex occurs in the early compartments of the secretory pathway." J Biol Chem **279**(47): 48615-48619.

Kimberly, W. T., M. J. LaVoie, B. L. Ostaszewski, W. Ye, M. S. Wolfe and D. J. Selkoe (2002). "Complex N-linked glycosylated nicastrin associates with active gamma-secretase and undergoes tight cellular regulation." J Biol Chem **277**(38): 35113-35117.

Kimberly, W. T., M. J. LaVoie, B. L. Ostaszewski, W. Ye, M. S. Wolfe and D. J. Selkoe (2003). "g-Secretase is a membrane protein complex comprised of presenilin, nicastrin, Aph-1, and Pen-2." Proc. Natl. Acad. Sci. USA **100**(11): 6382-6387.

Kimberly, W. T., W. Xia, T. Rahmati, M. S. Wolfe and D. J. Selkoe (2000). "The transmembrane aspartates in presenilin 1 and 2 are obligatory for gamma-secretase activity and amyloid beta-protein generation." J Biol Chem **275**(5): 3173-3178.

Kimmel, C. B., W. W. Ballard, S. R. Kimmel, B. Ullmann and T. F. Schilling (1995). "Stages of embryonic development of the zebrafish." Dev Dyn **203**(3): 253-310.

Kruger, M., I. Kratchmarova, B. Blagoev, Y. H. Tseng, C. R. Kahn and M. Mann (2008). "Dissection of the insulin signaling pathway via quantitative phosphoproteomics." Proc Natl Acad Sci U S A **105**(7): 2451-2456.

Laudon, H., E. M. Hansson, K. Melen, A. Bergman, M. R. Farmery, B. Winblad, U. Lendahl, G. von Heijne and J. Naslund (2005). "A nine-transmembrane domain topology for presenilin 1." J Biol Chem **280**(42): 35352-35360.

LaVoie, M. J., P. C. Fraering, B. L. Ostaszewski, W. Ye, W. T. Kimberly, M. S. Wolfe and D. J. Selkoe (2003). "Assembly of the gamma-secretase complex involves early formation of an intermediate subcomplex of Aph-1 and nicastrin." J Biol Chem **278**(39): 37213-37222.

Lee, S. F., S. Shah, H. Li, C. Yu, W. Han and G. Yu (2002). "Mammalian APH-1 interacts with presenilin and nicastrin and is required for intramembrane proteolysis of amyloid-beta precursor protein and Notch." J Biol Chem **277**(47): 45013-45019.

Leem, J. Y., S. Vijayan, P. Han, D. Cai, M. Machura, K. O. Lopes, M. L. Veselits, H. Xu and G. Thinakaran (2002). "Presenilin 1 is required for maturation and cell surface accumulation of nicastrin." J Biol Chem **277**(21): 19236-19240.

Livak, K. J. and T. D. Schmittgen (2001). "Analysis of relative gene expression data using real-time quantitative PCR and the 2(-Delta Delta C(T)) Method." Methods **25**(4): 402-408.

Loftus, B. J., U. J. Kim, V. P. Sneddon, F. Kalush, R. Brandon, J. Fuhrmann, T. Mason, M. L. Crosby, M. Barnstead, L. Cronin, A. Deslattes Mays, Y. Cao, R. X. Xu, H. L. Kang, S. Mitchell, E. E. Eichler, P. C. Harris, J. C. Venter and M. D. Adams (1999). "Genome duplications and other features in 12 Mb of DNA sequence from human chromosome 16p and 16q." Genomics **60**(3): 295-308.

Lois, C., E. J. Hong, S. Pease, E. J. Brown and D. Baltimore (2002). "Germline transmission and tissue-specific expression of transgenes delivered by lentiviral vectors." Science **295**(5556): 868-872.

Martin, J., C. Han, L. A. Gordon, A. Terry, S. Prabhakar, X. She, G. Xie, U. Hellsten, Y. M. Chan, M. Altherr, O. Couronne, A. Aerts, E. Bajorek, S. Black, H. Blumer, E. Branscomb, N. C. Brown, W. J. Bruno, J. M. Buckingham, D. F. Callen, C. S. Campbell, M. L. Campbell, E. W. Campbell, C. Caoile, J. F. Challacombe, L. A. Chasteen, O. Chertkov, H. C. Chi, M. Christensen, L. M. Clark, J. D. Cohn, M. Denys, J. C. Detter, M. Dickson, M. Dimitrijevic-Bussod, J. Escobar, J. J. Fawcett, D. Flowers, D. Fotopulos, T. Glavina, M. Gomez, E. Gonzales, D. Goodstein, L. A. Goodwin, D. L. Grady, I. Grigoriev,

M. Groza, N. Hammon, T. Hawkins, L. Haydu, C. E. Hildebrand, W. Huang, S. Israni, J. Jett, P. B. Jewett, K. Kadner, H. Kimball, A. Kobayashi, M. C. Krawczyk, T. Leyba, J. L. Longmire, F. Lopez, Y. Lou, S. Lowry, T. Ludeman, C. F. Manohar, G. A. Mark, K. L. McMurray, L. J. Meincke, J. Morgan, R. K. Moyzis, M. O. Mundt, A. C. Munk, R. D. Nandkeshwar, S. Pitluck, M. Pollard, P. Predki, B. Parson-Quintana, L. Ramirez, S. Rash, J. Retterer, D. O. Ricke, D. L. Robinson, A. Rodriguez, A. Salamov, E. H. Saunders, D. Scott, T. Shough, R. L. Stallings, M. Stalvey, R. D. Sutherland, R. Tapia, J. G. Tesmer, N. Thayer, L. S. Thompson, H. Tice, D. C. Torney, M. Tran-Gyamfi, M. Tsai, L. E. Ulanovsky, A. Ustaszewska, N. Vo, P. S. White, A. L. Williams, P. L. Wills, J. R. Wu, K. Wu, J. Yang, P. Dejong, D. Bruce, N. A. Doggett, L. Deaven, J. Schmutz, J. Grimwood, P. Richardson, D. S. Rokhsar, E. E. Eichler, P. Gilna, S. M. Lucas, R. M. Myers, E. M. Rubin and L. A. Pennacchio (2004). "The sequence and analysis of duplication-rich human chromosome 16." Nature **432**(7020): 988-994.

Massague, J. (1998). "TGF-beta signal transduction." Annu Rev Biochem **67**: 753-791.

Mishina, M. (1986). "[Structure and function of the nicotinic acetylcholine receptor]." Seikagaku **58**(10): 1275-1291.

Mullins, M. C., M. Hammerschmidt, P. Haffter and C. Nusslein-Volhard (1994). "Large-scale mutagenesis in the zebrafish: in search of genes controlling development in a vertebrate." Curr Biol **4**(3): 189-202.

Mumm, J. S. and R. Kopan (2000). "Notch signaling: from the outside in." Dev. Biol. **228**(2): 151-165.

Myslinski, E., M. A. Gerard, A. Krol and P. Carbon (2006). "A genome scale location analysis of human Staf/ZNF143-binding sites suggests a widespread role for human Staf/ZNF143 in mammalian promoters." J Biol Chem **281**(52): 39953-39962.

Nakajima, K., H. Hirose, M. Taniguchi, H. Kurashina, K. Arasaki, M. Nagahama, K. Tani, A. Yamamoto and M. Tagaya (2004). "Involvement of BNIP1 in apoptosis and endoplasmic reticulum membrane fusion." EMBO J **23**(16): 3216-3226.

Naruse, S., G. Thinakaran, J. J. Luo, J. W. Kusiak, T. Tomita, T. Iwatsubo, X. Qian, D. D. Ginty, D. L. Price, D. R. Borchelt, P. C. Wong and S. S. Sisodia (1998). "Effects of PS1 deficiency on membrane protein trafficking in neurons." Neuron **21**(5): 1213-1221.

Needleman, S. B. and C. D. Wunsch (1970). "A general method applicable to the search for similarities in the amino acid sequence of two proteins." J Mol Biol **48**(3): 443-453.

Nilsson, T., M. Jackson and P. A. Peterson (1989). "Short cytoplasmic sequences serve as retention signals for transmembrane proteins in the endoplasmic reticulum." Cell **58**(4): 707-718.

Oh, Y. S. and R. J. Turner (2005). "Topology of the C-terminal fragment of human presenilin 1." Biochemistry **44**(35): 11821-11828.

Okumura, A. J., K. Hatsuzawa, T. Tamura, H. Nagaya, K. Saeki, F. Okumura, K. Nagao, M. Nishikawa, A. Yoshimura and I. Wada (2006). "Involvement of a novel Q-SNARE, D12, in quality control of the endomembrane system." J Biol Chem **281**(7): 4495-4506.

Ong, S. E., B. Blagoev, I. Kratchmarova, D. B. Kristensen, H. Steen, A. Pandey and M. Mann (2002). "Stable isotope labeling by amino acids in cell culture, SILAC, as a simple and accurate approach to expression proteomics." Mol Cell Proteomics **1**(5): 376-386.

Prokop, S., K. Shirotani, D. Edbauer, C. Haass and H. Steiner (2004). "Requirement of PEN-2 for stabilization of the presenilin N-/C-terminal fragment heterodimer within the gamma-secretase complex." J Biol Chem **279**(22): 23255-23261.

Rayes, D., M. Flamini, G. Hernando and C. Bouzat (2007). "Activation of single nicotinic receptor channels from Caenorhabditis elegans muscle." Mol Pharmacol **71**(5): 1407-1415.

Rupp, R. A., L. Snider and H. Weintraub (1994). "Xenopus embryos regulate the nuclear localization of XMyoD." Genes Dev **8**(11): 1311-1323.

Sakuma, R., Y. Ohnishi Yi, C. Meno, H. Fujii, H. Juan, J. Takeuchi, T. Ogura, E. Li, K. Miyazono and H. Hamada (2002). "Inhibition of Nodal signalling by Lefty mediated through interaction with common receptors and efficient diffusion." Genes Cells **7**(4): 401-412.

Sato, T., T. S. Diehl, S. Narayanan, S. Funamoto, Y. Ihara, B. De Strooper, H. Steiner, C. Haass and M. S. Wolfe (2007). "Active gamma-secretase complexes contain only one of each component." J Biol Chem **282**(47): 33985-33993.

Saura, C. A., T. Tomita, F. Davenport, C. L. Harris, T. Iwatsubo and G. Thinakaran (1999). "Evidence that intramolecular associations between presenilin domains are obligatory for endoproteolytic processing." J Biol Chem **274**(20): 13818-13823.

Schier, A. F. (2003). "Nodal signaling in vertebrate development." Annu Rev Cell Dev Biol **19**: 589-621.

Schier, A. F. and M. M. Shen (2000). "Nodal signalling in vertebrate development." Nature **403**(6768): 385-389.

Selkoe, D. and R. Kopan (2003). "Notch and Presenilin: regulated intramembrane proteolysis links development and degeneration." Annu Rev Neurosci **26**: 565-597.

Selkoe, D. J. (2001). "Alzheimer's disease: genes, proteins, and therapy." Physiol. Rev. **81**(2): 741-766.

Shah, S., S. F. Lee, K. Tabuchi, Y. H. Hao, C. Yu, Q. LaPlant, H. Ball, C. E. Dann, 3rd, T. Sudhof and G. Yu (2005). "Nicastrin functions as a gamma-secretase-substrate receptor." Cell **122**(3): 435-447.

Shankar, G. M., B. L. Bloodgood, M. Townsend, D. M. Walsh, D. J. Selkoe and B. L. Sabatini (2007). "Natural oligomers of the Alzheimer amyloid-beta protein induce reversible synapse loss by modulating an NMDA-type glutamate receptor-dependent signaling pathway." J Neurosci **27**(11): 2866-2875.

Shearman, M. S., D. Beher, E. E. Clarke, H. D. Lewis, T. Harrison, P. Hunt, A. Nadin, A. L. Smith, G. Stevenson and J. L. Castro (2000). "L-685,458, an aspartyl protease transition state mimic, is a potent inhibitor of amyloid beta-protein precursor gamma-secretase activity." Biochemistry **39**(30): 8698-8704.

Shen, M. M. (2007). "Nodal signaling: developmental roles and regulation." Development **134**(6): 1023-1034.

Shevchenko, A., H. Tomas, J. Havlis, J. V. Olsen and M. Mann (2006). "In-gel digestion for mass spectrometric characterization of proteins and proteomes." Nat Protoc **1**(6): 2856-2860.

Shi, Y. and J. Massague (2003). "Mechanisms of TGF-beta signaling from cell membrane to the nucleus." Cell **113**(6): 685-700.

Shirotani, K., D. Edbauer, M. Kostka, H. Steiner and C. Haass (2004). "Immature nicastrin stabilizes APH-1 independent of PEN-2 and presenilin: identification of nicastrin mutants that selectively interact with APH-1." J Neurochem **89**(6): 1520-1527.

Sisodia, S. S. and P. H. St George-Hyslop (2002). "gamma-Secretase, Notch, Abeta and Alzheimer's disease: where do the presenilins fit in?" Nat Rev Neurosci **3**(4): 281-290.

Smith, T. F. and M. S. Waterman (1981). "Identification of common molecular subsequences." J Mol Biol **147**(1): 195-197.

Sobhanifar, S., B. Schneider, F. Lohr, D. Gottstein, T. Ikeya, K. Mlynarczyk, W. Pulawski, U. Ghoshdastider, M. Kolinski, S. Filipek, P. Guntert, F. Bernhard and V. Dotsch (2010). "Structural investigation of the C-terminal catalytic fragment of presenilin 1." Proc Natl Acad Sci U S A **107**(21): 9644-9649.

Spasic, D. and W. Annaert (2008). "Building gamma-secretase: the bits and pieces." J Cell Sci **121**(Pt 4): 413-420.
Steiner, H., K. Duff, A. Capell, H. Romig, M. G. Grim, S. Lincoln, J. Hardy, X. Yu, M. Picciano, K. Fechteler, M. Citron, R. Kopan, B. Pesold, S. Keck, M. Baader, T. Tomita, T. Iwatsubo, R. Baumeister and C. Haass (1999). "A loss of function mutation of presenilin-2 interferes with amyloid beta-peptide production and notch signaling." J Biol Chem **274**(40): 28669-28673.

Steiner, H. and C. Haass (2000). "Intramembrane proteolysis by presenilins." Nat. Rev. Mol. Cell Biol. **1**: 217-224.

Steiner, H., M. Kostka, H. Romig, G. Basset, B. Pesold, J. Hardy, A. Capell, L. Meyn, M. L. Grim, R. Baumeister, K. Fechteler and C. Haass (2000). "Glycine 384 is required for presenilin-1 function and is conserved in bacterial polytopic aspartyl proteases." Nat Cell Biol **2**(11): 848-851.

Steiner, H., E. Winkler, D. Edbauer, S. Prokop, G. Basset, A. Yamasaki, M. Kostka and C. Haass (2002). "PEN-2 is an integral component of the gamma-secretase complex required for coordinated expression of presenilin and nicastrin." J Biol Chem **277**(42): 39062-39065.

Strizzi, L., K. M. Hardy, E. A. Seftor, F. F. Costa, D. A. Kirschmann, R. E. Seftor, L. M. Postovit and M. J. Hendrix (2009). "Development and cancer: at the crossroads of Nodal and Notch signaling." Cancer Res **69**(18): 7131-7134.

Takasugi, N., T. Tomita, I. Hayashi, M. Tsuruoka, M. Niimura, Y. Takahashi, G. Thinakaran and T. Iwatsubo (2003). "The role of presenilin cofactors in the gamma-secretase complex." Nature **422**(6930): 438-441.

Templeton, N. S., L. A. Rodgers, A. T. Levy, K. L. Ting, H. C. Krutzsch, L. A. Liotta and W. G. Stetler-Stevenson (1992). "Cloning and characterization of a novel human cDNA that has DNA similarity to the conserved region of the collagenase gene family." Genomics **12**(1): 175-176.

Thinakaran, G., D. R. Borchelt, M. K. Lee, H. H. Slunt, L. Spitzer, G. Kim, T. Ratovitsky, F. Davenport, C. Nordstedt, M. Seeger, J. Hardy, A. I. Levey, S. E. Gandy, N. A. Jenkins, N. G. Copeland, D. L. Price and S. S. Sisodia (1996). "Endoproteolysis of presenilin 1 and accumulation of processed derivatives in vivo." Neuron **17**(1): 181-190.

Thinakaran, G., C. L. Harris, T. Ratovitski, F. Davenport, H. H. Slunt, D. L. Price, D. R. Borchelt and S. S. Sisodia (1997). "Evidence that levels of presenilins (PS1 and PS2) are coordinately regulated by competition for limiting cellular factors." J Biol Chem **272**(45): 28415-28422.

Tian, T. and A. M. Meng (2006). "Nodal signals pattern vertebrate embryos." Cell Mol Life Sci.

Topczewska, J. M., L. M. Postovit, N. V. Margaryan, A. Sam, A. R. Hess, W. W. Wheaton, B. J. Nickoloff, J. Topczewski and M. J. Hendrix (2006). "Embryonic and tumorigenic pathways converge via Nodal signaling: role in melanoma aggressiveness." Nat Med **12**(8): 925-932.

Tsai, J., J. Grutzendler, K. Duff and W. B. Gan (2004). "Fibrillar amyloid deposition leads to local synaptic abnormalities and breakage of neuronal branches." Nat Neurosci **7**(11): 1181-1183.

van Eeden, F. J., M. Granato, U. Schach, M. Brand, M. Furutani-Seiki, P. Haffter, M. Hammerschmidt, C. P. Heisenberg, Y. J. Jiang, D. A. Kane, R. N. Kelsh, M. C. Mullins, J. Odenthal, R. M. Warga, M. L. Allende, E. S. Weinberg and C. Nusslein-Volhard (1996). "Mutations affecting somite formation and patterning in the zebrafish, Danio rerio." Development **123**: 153-164.

Vassar, R. (2004). "BACE1: the beta-secretase enzyme in Alzheimer's disease." J Mol Neurosci **23**(1-2): 105-114.

Viklund, H. and A. Elofsson (2004). "Best alpha-helical transmembrane protein topology predictions are achieved using hidden Markov models and evolutionary information." Protein Sci **13**(7): 1908-1917.

Wakabayashi, T., K. Craessaerts, L. Bammens, M. Bentahir, F. Borgions, P. Herdewijn, A. Staes, E. Timmerman, J. Vandekerckhove, E. Rubinstein, C. Boucheix, K. Gevaert and B. De Strooper (2009).

"Analysis of the gamma-secretase interactome and validation of its association with tetraspanin-enriched microdomains." Nat Cell Biol **11**(11): 1340-1346.
Walsh, D. M., I. Klyubin, J. V. Fadeeva, W. K. Cullen, R. Anwyl, M. S. Wolfe, M. J. Rowan and D. J. Selkoe (2002). "Naturally secreted oligomers of amyloid beta protein potently inhibit hippocampal long-term potentiation in vivo." Nature **416**(6880): 535-539.

Watanabe, N., T. Tomita, C. Sato, T. Kitamura, Y. Morohashi and T. Iwatsubo (2005). "Pen-2 is incorporated into the gamma-secretase complex through binding to transmembrane domain 4 of presenilin 1." J Biol Chem **280**(51): 41967-41975.

Wegele, H., L. Muller and J. Buchner (2004). "Hsp70 and Hsp90--a relay team for protein folding." Rev Physiol Biochem Pharmacol **151**: 1-44.

Wickner, W. and R. Schekman (2008). "Membrane fusion." Nat Struct Mol Biol **15**(7): 658-664.

Wiltfang, J., H. Esselmann, M. Bibl, A. Smirnov, M. Otto, S. Paul, B. Schmidt, H. W. Klafki, M. Maler, T. Dyrks, M. Bienert, M. Beyermann, E. Ruther and J. Kornhuber (2002). "Highly conserved and disease-specific patterns of carboxyterminally truncated Abeta peptides 1-37/38/39 in addition to 1-40/42 in Alzheimer's disease and in patients with chronic neuroinflammation." J Neurochem **81**(3): 481-496.

Winkler, E., S. Hobson, A. Fukumori, B. Dumpelfeld, T. Luebbers, K. Baumann, C. Haass, C. Hopf and H. Steiner (2009). "Purification, pharmacological modulation, and biochemical characterization of interactors of endogenous human gamma-secretase." Biochemistry **48**(6): 1183-1197.

Wiznerowicz, M. and D. Trono (2003). "Conditional suppression of cellular genes: lentivirus vector-mediated drug-inducible RNA interference." J Virol **77**(16): 8957-8961.

Wolfe, M. S., W. Xia, C. L. Moore, D. D. Leatherwood, B. Ostaszewski, T. Rahmati, I. O. Donkor and D. J. Selkoe (1999). "Peptidomimetic probes and molecular modeling suggest that Alzheimer's gamma-secretase is an intramembrane-cleaving aspartyl protease." Biochemistry **38**(15): 4720-4727.

Ye, J. and C. Koumenis (2009). "ATF4, an ER stress and hypoxia-inducible transcription factor and its potential role in hypoxia tolerance and tumorigenesis." Curr Mol Med **9**(4): 411-416.

Yeo, C. and M. Whitman (2001). "Nodal signals to Smads through Cripto-dependent and Cripto-independent mechanisms." Mol Cell **7**(5): 949-957.

Yu, G., F. Chen, G. Levesque, M. Nishimura, D. M. Zhang, L. Levesque, E. Rogaeva, D. Xu, Y. Liang, M. Duthie, P. H. St George-Hyslop and P. E. Fraser (1998). "The presenilin 1 protein is a component of a high molecular weight intracellular complex that contains beta-catenin." J Biol Chem **273**(26): 16470-16475.

Yu, G., M. Nishimura, S. Arawaka, D. Levitan, L. Zhang, A. Tandon, Y. Q. Song, E. Rogaeva, F. Chen, T. Kawarai, A. Supala, L. Levesque, H. Yu, D. S. Yang, E. Holmes, P. Milman, Y. Liang, D. M. Zhang, D. H. Xu, C. Sato, E. Rogaev, M. Smith, C. Janus, Y. Zhang, R. Aebersold, L. S. Farrer, S. Sorbi, A. Bruni, P. Fraser and P. St George-Hyslop (2000). "Nicastrin modulates presenilin-mediated notch/glp-1 signal transduction and betaAPP processing." Nature **407**(6800): 48-54.

Zhang, L., J. Lee, L. Song, X. Sun, J. Shen, G. Terracina and E. M. Parker (2005). "Characterization of the reconstituted gamma-secretase complex from Sf9 cells co-expressing presenilin 1, nicastrin [correction of nacastrin], aph-1a, and pen-2." Biochemistry **44**(11): 4450-4457.

Zhang, L., H. Zhou, Y. Su, Z. Sun, H. Zhang, Y. Zhang, Y. Ning, Y. G. Chen and A. Meng (2004). "Zebrafish Dpr2 inhibits mesoderm induction by promoting degradation of nodal receptors." Science **306**(5693): 114-117.

Zhang, Y. W., W. J. Luo, H. Wang, P. Lin, K. S. Vetrivel, F. Liao, F. Li, P. C. Wong, M. G. Farquhar, G. Thinakaran and H. Xu (2005). "Nicastrin is critical for stability and trafficking but not association of other presenilin/gamma-secretase components." J Biol Chem **280**(17): 17020-17026.

6. List of abbreviations

(Abbreviations are also explained in the text by their first appearance. Therefore, only abbreviations that were used more than once are listed.)

α-	anti-
aa	amino acid
Aβ	amyloid β- (Aβ-) peptide
AB	antibody
AD	Alzheimer's disease
APH-1 (aL, aS, b)	Anterior Pharynx-Defective 1(a long isoform, a short isoform, b)
AP	aminopeptidase
APP	β-amyloid precursor protein
AU	arbitrary units
bp	base pairs
°C	centigrade
CO_2	carbon dioxide
C-terminus	carboxy-terminus (of a protein)
cDNA	coding desoxyribonucleic acid
ce	*Caenorhabditis elegans*
co-IP	co-immunoprecipitation
DAP	DYIGS and peptidase hydrophobic region
dest	distilled
DMEM	Dulbecco's Modified Eagle Medium
dNTP	desoxyribonuceic acid triphosphate
DNA	desoxyribonucleic acid
E. coli	*Escherichia coli*
ER	endoplasmic reticulum
et al.	et alii (and others)
FAD	familial AD
FCS	fetal calf serum
Fig.	figure
g	gram or Earth's gravity
h, hrs	hour, hours
H_2O	water
HEK	human embryonic kidney
HeLa	Henrietta Lacks human epithelial cervical cancer cells
Ig	immunoglobulin
IgG	immunoglobulin, class G
IP	immunoprecipitation
KD	knockdown
kDa	kilo-Dalton
L	liter
M	molar
mM	millimolar
µM	micromolar

µg	microgram
mg	milligram
min	minute
µL	microliter
mL	milliliter
mRNA	messenger ribonucleic acid
N-terminus	amino-terminus (of a protein)
Ncl, Nicalin	Nicastrin-like protein
ng	nanogram
nM	nanomolar
NCT	Nicastrin
Nicalin	Nicastrin-like protein
NOMO	Nodal modulator
NOMO-L	Nodal modulator, long isoform
o/n	over night
OD	optical density
PAGE	polyacrylamide gel electrophoresis
PBS	phosphate-buffered saline
PCR	polymerase chain reaction
PEN-2	Presenilin-Enhancer 2
PI	protease inhibitor(s)
PS	Presenilin
PS1	Presenilin 1
PS2	Presenilin 2
RNA	ribonucleic acid
RNAi	RNA interference
rpm	revolutions per minute
RT	room temperature
SDS	sodiumdodecylsulfate
SDS-PAGE	sodiumdodecylsulfate polyacrylamide gel electrophoresis
sec	second(s)
SP	signal peptide
T147, TMEM147	Transmembrane Protein 147
Tab.	table
TBST	tris-buffered saline +Tween
TGFβ	transforming growth factor β
TM	transmembrane
TMD	transmembrane domain
U	unit (enzyme unit)
UV	ultraviolet
v/v	volume/volume
w/v	mass/volume
wt	wild-type
zf	zebrafish

Amino acids:

A	alanine
C	cysteine
D	aspartate
E	glutamate
F	phenylalanine
G	glycine
H	histidine
I	isoleucine
K	lysine
L	leucine
M	methionine
N	asparagine
P	proline
Q	glutamine
R	arginine
S	serine
T	threonine
V	valine
W	tryptophane
Y	tyrosine

Nucleosides:

A	adenosine, deoxyadenosine
C	cytidine, deoxycytidine
G	guanosine, deoxyguanosine
T	thymidine (= deoxythymidine)

7. List of companies

Agfa, Cologne, Germany (www.agfa.de)
Applichem, Darmstadt, Germany (www.applichem.de)
Applied Biosystems, Rotkreutz, Switzerland (www.appliedbiosystems.com)
B. Braun Biotech International/Sartorius, Göttingen, Germany (www.sartorius.de)
Baker Phillipsburg, NJ, USA (www.jtbaker.com)
Beckman, Krefeld, Germany (www.beckmancoulter.de)
Becton Dickinson, Franklin Lakes, NJ, USA (www.bd.com)
Biorad, Munich, Germany (www.bio-rad.com)
Bosch, Stuttgart, Germany (www.bosch.de)
Brand, Wertheim, Germany (www.brand.de)
Clontech, Mountain View, CA, USA (www.clontech.com)
Costar/Corning, Lowell, MA, USA (www.corning.com)
DIATEC, Oslo, Norway (www.diatec.com)
Developmental Studies Hybridoma Bank, Iowa University, USA
Edmund Bühler, Hechingen, Germany (www.edmund-buehler.de)
Electrolux, Nuremberg, Germany (www.electrolux.de)
Eppendorf Hamburg, Germany (www.eppendorf.com)
Fermentas, Helsinki, Finland (www.fermentas.com)
Fuji Film, Kiel, Germany (www.fujifilm.de)
GATC, Konstanz, Germany (www.gatc.de)
General Electric Lifescience, Chalfon St. Giles, Great Britain (www4.gelifesciences.com)
Gilson, Den Haag, Netherlands (www.gilson.com)
Heraeus/Thermo Scientific, Waltham, MA, USA (www.thermo.com)
Invitrogen (and Gibco Life Sciences), Carlsbad, CA, USA (www.invitrogen.com)
IKA Labortechnik, Staufen, Germany (www.ika.de)
J. T. Baker, Philipsburg, NJ, USA (www.jtbaker.com)
Liebisch, Bielefeld, Germany (www.liebisch.com)
Macherey-Nagel, Düren, Germany (www.macherey-nagel.com)
Menzel Gläser, Braunschweig, Germany (www.menzel.de)
Merck, Darmstadt, Germany (www.merck.de)
Messer, Sulzbach, Germany (www.messergroup.com)
Millipore, Schwalbach, Germany (www.millipore.com)
MS Laborgeräte, Wiesloch, Germany (www.ms-l.de)
New England Biolabs (NEB), Frankfurt a. M., Germany (www.neb-online.de)
Nunc, Wiesbaden, Germany (www.nunc.de)
Ohaus, Frankfurt, Germany (www.ohaus.com)
Owl Separation Systems, Rochester, NY, USA (www.owlsci.com)
PEQLAB, Erlangen, Germany (www.peqlab.de)
Perkin-Elmer, Waltham, MA, USA (www.perkinelmer.com)
Promega, Mannheim, Germany (www.promega.com)
Qualilab, Olivet, France (www.qualilab.dom)
Roche, Basel, Switzerland (www.roche.de)
Roth, Karlsruhe, Germany (www.carl.roth.de)
SAFC Biosciences, Lenexa, KA, USA (www.safcglobal.com)
Sarstedt, Nümbrecht, Germany (www.sarstedt.com)
Santa Cruz, Santa Cruz, CA, USA (www.scbt.com)
Schleicher und Schuell, Dassel, Germany (www.schleicher-schuell.de)
Schott, Mainz, Germany (www.schott.com)
Scientific Industries, Bohemia, NY, USA (www.scientificindustries.com)
SERVA, Heidelberg, Germany (www.serva.de)
Sigma (Sigma-Aldrich), Taufkirchen, Germany (www.sigmaaldrich.com)
Stressgen, Ann Arbor, MI, USA (www.stressgen.com)
Systec, Wettenberg, Germany (www.systec-lab.com)
Terumo, Tokyo, Japan (www.terumo.com)
Thermo Electron, Ulm, Germany (www.thermo.de)
UVP, Upland, CA, USA (www.uvp.com)
WTW, Weilheim, Germany (www.wtw.de)
Zeiss, Jena, Germany (www.zeiss.com)

8. Curriculum vitae

Personal Data

Name	Ulf Holger Wilhelm Dettmer
Degree	Master of Science Molecular Biotechnology (TU Munich)
Born	January 19th 1981 in Nuremberg, Germany
Nationality	German
E-mail Address	ulf.dettmer@gmx.de

University

Oct. 2006 - Jun. 2010	PhD thesis at the Adolf-Butenandt-Institute of the Ludwig-Maximilians-University (LMU) Munich, Dept. of Biochemistry, chair: Prof. C. Haass
	Speaker of the Graduate Program Neurodegenerative Disease Research of the LMU Munich 2007 - 2008
Oct. 2004 - Jul. 2006	Master studies of Molecular Biotechnology at the Technical University of Munich, Germany
	Degree: Master of Science
	Title of Master's thesis: Domain analysis of the Nicalin-NOMO protein complex (same laboratory as PhD thesis)
Oct. 2001 - Sep. 2004	Bachelor studies of Biochemistry and Molecular Biotechnology at the Technical University Munich, Germany
	Title of Bachelor's thesis: Analysis of nut proteins using chromatographic and immunochemical methods (Institute of Hydrochemistry of the TU Munich, chair: Prof. R. Nießner)

Alternative Service

Oct. 2000 - Aug. 2001	Klinikum Großhadern, hospital of the LMU Munich Department of Urology (IT service, patient care, diagnostics)

School Education

1992 - 2000	Secondary school:	Wilhelmsgymnasium Munich
	Degree:	General qualification for university entrance
1988 - 1992	Elementary school:	Schule an der Gebelestraße Munich

Scholarships

PhD Scholarship	Stiftung Stipendien-Fonds des Verbandes der chemischen Industrie
2007 - 2009	(Funds of the German Chemical Industry)

9. Publications and meetings

Peer-reviewed Articles

Dettmer U, Kuhn PH, Abou-Ajram C, Lichtenthaler SF, Krüger M, Haass C, Haffner C (2010): "The transmembrane protein 147 (TMEM147) is a novel component of the Nicalin-NOMO protein complex", Journal of Biological Chemistry: in press

Haffner C, **Dettmer U**, Weiler T, Haass C (2007): The Nicastrin-like protein Nicalin regulates assembly and stability of the Nicalin-Nodal Modulator (NOMO) membrane protein complex; Journal of Biological Chemistry **282** (14): 10632-10638

Poster Presentations at International Meetings

EMBO Meeting 2009 in Amsterdam, Netherlands:
Dettmer U, Krüger M, Haffner C: The transmembrane protein 147 (TMEM147) is a component of the Nicalin-NOMO protein complex

Golgi Meeting 2008 in Pavia, Italy:
Dettmer U, Abou-Ajram C., Krüger M, Haass C, Haffner C: The Nicalin-NOMO complex interacts with endoplasmic reticulum SNAREs

Textbooks

Dettmer U, Folkerts M, Kächler E, Sönnichsen A: Intensivkurs Biochemie, *Urban und Fischer Verlag* Munich (2005) - a textbook about biochemistry for medical students

Buchta M, Sönnichsen A: Das Physikum, *Urban und Fischer Verlag* Munich (2009) (contributing author: chemistry and biochemistry) - a compendium for medical students

10. Acknowledgments

I want to thank all the people who contributed to my PhD years at the Adolf-Butenandt-Institute being a unique and unforgettable time. Especially I want to thank:

Dr Christof Haffner, who was the direct scientific supervisor of this thesis, for his constant support and advice throughout the last years, for always finding time for very stimulating discussions as well as for his reliability and thorough way of solving any kinds of problems,

Prof Dr Christian Haass for giving me the opportunity to join his laboratory and to work on this great project, for advice, generous support and mentoring as well as for his big contribution to a stimulating scientific environment and nice atmosphere in the lab,

PD Dr Konstanze Winklhofer for her helpfulness and kind support, for supervision of this thesis and for fruitful discussions in my thesis advisory committee,

Prof Dr Martin Biel, Prof. Dr Klaus Förstemann, Prof Dr Dietmar Martin, and Prof Dr Christian Wahl-Schott for evaluation of this thesis and participating in my PhD examination,

Dr Christian Brösamle for introducing me to the zebrafish model system and fruitful discussions in my thesis advisory committee,

Prof Dr Axel Imhof, Dr Ignasi Forné, Dr Peer-Hendrik Kuhn, Dr Elisabeth Kremmer, Dr Marcus Krüger, and Dr Stefan Lichtenthaler for their help and contributions to this work,

Claudia Abou-Ajram, Timo Weiler, Hartmut Kaiser, Katrin Fellerer, Ann-Kathrin Ludwig, Gabi Basset, and my friend Božidar Novak for technical and non-technical support,

Dr Lena Bouman for establishing the graduate program together with me, and Anna Münch and Anja Krauss following up the organization of this program,

Dr Ayako Yamamoto, Dr Karin Görner, Eve Holtorf, Dr Dorothee Dormann, Ramona Rodde and Eva Bentmann for sharing lab 817, years, months, weeks, days and hours,

Anna Pilsl, Bettina Brunner, Dr Iris Henn, Dr Julia Schlehe, Kathrin Lutz, Dr Nicole Exner, and Veronika Müller for good neighborship and friendly door-to-door atmosphere,

Dr Tim Bartels, Dr Richard Page, Dr Lucas Martin, Amelie Gutsmiedl, Dr Anita Schlierf, Benedikt Kretner, Dr Blanca Perez-Revuelta, Daniel Fleck, Manuel Lehm, Mara Taverna, Matthias Voss, Natalie Pfeiffer, Sebastian Hogl, Sonja Zilow, Dr Stefan Mitterreiter, and Ulrike Resenberger for fruitful and fruitless scientific and para-scientific discussions,

Dr Karin Schaefer, Katharina Stahl, Dr Frauke van Bebber, Dr Dominik Paquet, Alex Hruscha, Matthias Teucke and Dr Bettina Schmid for their help in the zebrafish facility,

Sabine Odoy for perfect lab organization,

Dr Regina Fluhrer for the organization of our lab seminars,

Prof Dr Harald Steiner and Edith Winkler for their help and sharing knowledge on protein complexes,

Prof Dr Jörg Tatzelt for his support and sharing knowledge on ER import,

Dr Anja Capell, Dr Sven Lammich, Dr Michael Willem, and Alice Sülzen for their friendly scientific and non-scientific support,

Ina Haass for making every invitation of the PhD students to Icking a very special event,

Annette Schell and Barbara Kassner for their excellent work in the (γ-)secretariat,

Benno Fredmüller, Andreas Kräutler, and Alexander Kräutler for IT solutions,

Dr Melanie Meyer-Luehmann and Dr Dieter Edbauer for Boston consulting,

my parents and my sister for their constant support during the last 29.5 years,

Alexandra Lantermann, Felix Halbach, Frieder Schroff, and all my friends for making life worthwhile.

In addition, I want to thank the ‘Stiftung Stipendien-Fonds des Verbandes der chemischen Industrie’ for supporting this work with a PhD scholarship.